CUMULATIVE DISSERTATION

FLOOD DYNAMICS IN THE VIETNAMESE MEKONG DELTA
current state and future projections

for the degree of
doctor rerum naturalium
(Dr. rer. nat.)
in Natural Hazards Research

Submitted to the Faculty of Science
at the University of Potsdam

prepared at the Section Hydrology
of the German Research Centre for Geosciences (GFZ)

by
Nguyen Van Khanh Triet

Potsdam, December 21, 2020

First supervisor: Prof. Dr. Bruno Merz
Second supervisor: Ass. Prof. Dr. Matti Kummu
Mentor: Dr. Heiko Apel

First reviewer: Prof. Dr. Bruno Merz
Second reviewer: Ass. Prof. Dr. Matti Kummu
Third reviewer: Prof. Stephen Darby

Examination board members:
Prof. Dr. Bruno Merz
Ass. Prof. Dr. Matti Kummu
Prof. Stephen Darby
PD. Dr. Maik Heistermann
Prof. Dr. Annegret Thieken
Prof. Oliver Korup

Published online on the
Publication Server of the University of Potsdam:
https://doi.org/10.25932/publishup-51283
https://nbn-resolving.org/urn:nbn:de:kobv:517-opus4-512830

Declaration of originality

I hereby declare that I have not submitted this dissertation in its current or similar version to any university or other institution for a degree, diploma or other qualifications.

I officially ensure, that this work has been written solely on my own. I herewith officially ensure, that I have not used any other sources but those stated by me. Any and every parts of the text which constitute quotes in original wording or in its essence have been explicitly referred by me by using official marking and proper quotation. This is also valid for used graphs, pictures and similar formats.

I also officially ensure, that the printed version as submitted by me fully confirms with my digital version. I agree that the digital version will be used to subject the dissertation to plagiarism examination

Potsdam, December 21, 2020

Nguyen Van Khanh Triet

Acknowledgement

I am deeply grateful to many people who help me on this journey. This thesis would not be possible without their valuable support and advice.

This PhD work is carried out at the Section Hydrology at the German Research Center for Geosciences Potsdam. My acknowledgement to the German Academic Exchange Service (DAAD) with the financial support for my PhD work. My appreciation goes to the GFZ Potsdam for covering the cost of my three publications, and the CATCH-MEKONG project for funding the last year of my PhD study.

First of all, I would like to express my deepest thanks to my supervisors, Dr. Heiko Apel, Prof. Bruno Merz, Ass. Prof. Matti Kummu for the patient guidance, constant support, advice and encouragement throughout my PhD work. I am grateful to Dr. Nguyen Viet Dung for his advice and support in modelling as well as constructive comments and feedbacks on my research topic.

My deep acknowledgement to my first mentor on hydrodynamic modelling. Thank you for guiding me through the complex of hydraulic modelling for the Mekong and numerous valuable tips in handling the model issues.

I would like to thank you all the member of the Hydrology section for the wonderful research environment. My special thanks toHeiko Thoss, Knut Günther, Astrid Krahn and Romianna Zimmerfor their endless supports whenever I have technical issues, fieldwork, and the German paper works.

I would like to acknowledge Dr. Nguyen Nghia Hung, Dr. To Quang Toan, Dr. Pham The Vinh and many colleagues at the Southern Institute of Water Resources Research, Dr. Akihiko Kotera and Mr. Kimseng Choeun for the cooperation, and support in the fieldwork, providing important data for this work, together with valuable comments, suggestions for the model setup. and many colleagues at the Southern Institute of Water Resources Research.

My special thanks to my fellow PhDs, Nguyen Le Duy and Tran Tuan Anh for their cooperation, support and countless good memories.

Finally, to my parents, thank you so much for your continuous support, encouragement and empathy. To my sister in law and my brother, thank you very much for taking care of our parents. To my wife, Ngoc Lan thank you for your patience, accompanying me through the ups and downs in my journey, and taking care of our little angel.

To Cherry, ba xin lỗi vì những hôm cuối tuần không thể cùng con đi công viên, đi khu vui chơi. Thương con rất rất nhiều!

Abstract

Today, the Mekong Delta in the southern of Vietnam is home for 18 million people. The delta also accounts for more than half of the country's food production and 80% of the exported rice. Due to the low elevation, it is highly susceptible to the risk of fluvial and coastal flooding. Although extreme floods often result in excessive damages and economic losses, the annual flood pulse from the Mekong is vital to sustain agricultural cultivation and livelihoods of million delta inhabitants.

Delta-wise risk management and adaptation strategies are required to mitigate the adverse impacts from extreme events while capitalising benefits from floods. However, a proper flood risk management has not been implemented in the VMD, because the quantification of flood damage is often overlooked and the risks are thus not quantified. So far, flood management has been exclusively focused on engineering measures, i.e. high- and low-dyke systems, aiming at flood-free or partial inundation control without any consideration of the actual risks or a cost-benefit analysis. Therefore, an analysis of future delta flood dynamics driven these stressors is valuable to facilitate the transition from sole hazard control towards a risk management approach, which is more cost-effective and also robust against future changes in risk.

Built on these research gaps, this thesis investigates the current state and future projections of flood hazard, damage and risk to rice cultivation, the most important economic activity in the VMD. The study quantifies the changes in risk and hazard brought by the development of delta-based flood control measures in the last decades, and analyses the expected changes in risk driven by the changing climate, rising sea-level and deltaic land subsidence, and finally the development of hydropower projects in the Mekong Basin. For this purpose, flood trend analyses and comprehensive hydraulic modelling were performed, together with the development of a concept to quantify flood damage and risk to rice plantation.

The analysis of observed flood levels revealed strong and robust increasing trends of peak and duration downstream of the high-dyke areas with a step change in 2000/2001, i.e. after the disastrous flood which initiated the high-dyke development. These changes were in contrast to the negative trends detected upstream, suggested that high-dyke development has shifted flood hazard downstream. Findings of the trend's analysis were later confirmed by hydraulic simulations of the two recent extreme floods in 2000 and 2011, where the hydrological boundaries and dyke system settings were interchanged.

However, the high-dyke system was not the only and often not the main cause for a shift of

flood hazard, as a comparative analysis of these two extreme floods proved. The high-dyke development was responsible for 20–90% of the observed changes in flood level between 2000 and 2011, with large spatial variances. The particular flood hydrograph of the two events had the highest contribution in the northern part of the delta, while the tidal level had 2–3 times higher influence than the high-dyke in the lower-central and coastal areas downstream of high-dyke areas. The impact of the high-dyke development was highest in the areas closely downstream of the high-dyke area just south of the Cambodia-Vietnam border. The hydraulic simulations also validated that the concurrence of the flood peak with spring tides, i.e. high sea level along the coast, amplified the flood level and inundation in the central and coastal regions substantially.

The risk assessment quantified the economic losses of rice cultivation to USD 25.0 and 115 *million* (0.02–0.1% of the total GDP of Vietnam in 2011) corresponding to the 10-year and the 100-year floods, with an expected annual damage of about USD 4.5 *million*. A particular finding is that the flood damage was highly sensitive to flood timing. Here, a 10-year event with an early peak, i.e. late August-September, could cause as much damage as a 100-year event that peaked in October. This finding underlines the importance of a reliable early flood warning, which could substantially reduce the damage to rice crops and thus the risk.

The developed risk assessment concept was furthermore applied to investigate two high-dyke development alternatives, which are currently under discussion among the administrative bodies in Vietnam, but also in the public. The first option favouring the utilization of the current high-dyke compartments as flood retention areas instead for rice cropping during the flood season could reduce flood hazard and expected losses by 5–40%, depending on the region of the delta. On the contrary, the second option promoting the further extension of the areas protected by high-dyke to facilitate third rice crop planting on a larger area, tripled the current expected annual flood damage. This finding challenges the expected economic benefit of triple rice cultivation, in addition to the already known reducing of nutrient supply by floodplain sedimentation and thus higher costs for fertilizers.

The economic benefits of the high-dyke and triple rice cropping system is further challenged by the changes in the flood dynamics to be expected in future. For the middle of the 21st century (2036-2065) the effective sea-level rise an increase of the inundation extent by 20–27% was projected. This corresponds to an increase of flood damage to rice crops in dry, normal and wet year by USD 26.0, 40.0 and 82.0 *million* in dry, normal and wet year compared to the baseline period 1971-2000.

Hydraulic simulations indicated that the planned massive development of hydropower dams in the Mekong Basin could potentially compensate the increase in flood hazard and agriculture losses stemming from climate change. However, the benefits of dams as miti-

gation of flood losses are highly uncertain, because a) the actual development of the dams is highly disputed, b) the operation of the dams is primarily targeted at power generation, not flood control, and c) this would require international agreements and cooperation, which is difficult to achieve in South-East Asia. The theoretical flood mitigation benefit is additionally challenged by a number of negative impacts of the dam development, e.g. disruption of floodplain inundation in normal, non-extreme flood years. Adding to the certain reduction of sediment and nutrient load to the floodplains, hydropower dams will drastically impair rice and agriculture production, the basis livelihoods of million delta inhabitants.

In conclusion, the VMD is expected to face increasing threats of tidal induced floods in the coming decades. Protection of the entire delta coastline solely with "hard" engineering flood protection structures is neither technically nor economically feasible, adaptation and mitigation actions are urgently required. Better control and reduction of groundwater abstraction is thus strongly recommended as an immediate and high priority action to reduce the land subsidence and thus tidal flooding and salinity intrusion in the delta. Hydropower development in the Mekong basin might offer some theoretical flood protection for the Mekong delta, but due to uncertainties in the operation of the dams and a number of negative effects, the dam development cannot be recommended as a strategy for flood management. For the Vietnamese authorities, it is advisable to properly maintain the existing flood protection structures and to develop flexible risk-based flood management plans. In this context the study showed that the high-dyke compartments can be utilized for emergency flood management in extreme events. For this purpose, a reliable flood forecast is essential, and the action plan should be materialised in official documents and legislation to assure commitment and consistency in the implementation and operation.

Zusammenfassung

Das Mekong-Delta im Süden Vietnams ist die Heimat von 18 Millionen Menschen. Im Delta werden mehr als die Hälfte der Nahrungsmittel des Landes und 80% des exportierten Reises produziert. Aufgrund der geringen Höhen und Topographie ist das Delta sehr anfällig für Überflutungen, sowohl durch Fußhochwasser als auch durch gezeitenbedingte Rückstauüberflutungen. Obwohl extreme Überschwemmungen oft zu hohen Schäden und wirtschaftlichen Verlusten führen, ist der jährliche Hochwasserimpuls des Mekong lebenswichtig für die Aufrechterhaltung des landwirtschaftlichen Anbaus und des Lebensunterhalts von Millionen Deltabewohnern.

Ein deltaweites Risikomanagement bestehend aus Hochwasserschutzmaßnahmen und Anpassungsstrategien ist erforderlich, um die negativen Auswirkungen von Extremereignissen zu mindern, zeitgleich aber auch die positiven Aspekte der Hochwasser beizubehalten. Ein Hochwasserrisikomanagement ist im VMD jedoch nicht implementiert, da die Quantifizierung von Hochwasserschäden typischerweise nicht vorgenommen wird. Bisher konzentriert sich das Hochwassermanagement ausschließlich auf ingenieurtechnische Maßnahmen zur Eindämmung der Gefährdung. Dies geschieht entweder durch Hoch- oder Niederdeichung, die auf eine hochwasserfreie oder teilweise Überflutungssteuerung abzielen. Eine risikobasierte Bewertung der Vor- und Nachteile zwischen Hoch- und Niederdeichansatz sowie Kosten-Nutzen-Rechnungen fehlen allerdings ebenfalls. Zudem ist zu erwarten, dass sich die Überschwemmungen Dynamik und das Hochwasserrisiko im Mekong Delta als Folge des Klimawandels und menschlicher Eingriffe in das Delta und das Mekong-Einzugsgebiet verändern werden. Die Analyse der zukünftigen Hochwasserdynamik in Abhängigkeit von diesen Stressoren ist notwendig, um den Übergang von einer alleinigen Gefahrenabwehr zu einem zukunftssicheren, probabilistischen Risikomanagement zu erleichtern.

Ausgehend von diesen Forschungslücken untersucht diese Arbeit den aktuelle Hochwassergefährdung und die zu erwartenden zukünftigen Änderungen, sowie der damit einhergehenden Schäden und Risiken für den Reisanbau im Mekong Delta unter Berücksichtigung existierender und möglicher Hochwasserschutzmaßnahmen, des sich ändernden Klimas, des steigenden Meeresspiegels in Kombination mit der Landabsenkung des Deltas und der geplanten Staudämme im Mekong Einzugsgebiet.

Eine Analyse der jährlichen Hochwasserpegel zeigte starke und robuste steigende Trends in den maximalen Wasserständen der Hochwasser und der Hochwasserdauer flussabwärts der Hochdeichgebiete, wobei eine sprunghafte Veränderung in den Jahren 2000/2001 nach. dem katastrophalen Hochwasser, das die Hochdeichentwicklung einleitete, festgestellt wurde. Diese Veränderungen stehen im Gegensatz zu den negativen Trends, oberstrom der

Hocdeichgebiete, was darauf schließen lässt, dass die Hochdeichentwicklung die Hochwassergefahr flussabwärts verlagert hat. Die Ergebnisse der Trendanalyse wurden weiterhin durch hydraulische Simulationen der Überflutungsdynamiken der Hochwasser von 2000 und 2011 bestätigt. Allerdings waren die Hochdeiche nicht die Haupt- und einzige Ursache für den höheren Hochwasserpegel im Jahr 2011 im Vergleich zum Hochwasser im Jahr 2000. Die Hochwasserganglinie des Mekongs hatte den höchsten Beitrag im nördlichen Teil des Deltas oberstrom der Hochdeichgebiete, während der Tidenhub in den zentralen und küstennahen Gebieten stromabwärts des Hochdeichs einen 2–3 mal höheren Einfluss hatte als die Hochdeiche.

Die wirtschaftlichen Verluste des Reisanbaus wurden rezent auf 25,0–115 Mio. USD geschätzt, für jeweils das 10- und 100-jährliche Hochwasser. Die Schäden sind hierbei sehr sensitiv gegenüber der Hochwasserganglinie, insbesondere dem Zeitpunkt des Auftretens des Hochwasserscheitels. Ein frühes 10-jährliches Hochwasser kann aufgrund des Zusammentreffens des Hochwassers mit der Ernte der Frühjahrsaussaat oder der Aussaat der Sommerfrucht ähnliche Verluste verursachen wie ein 100-jährliches Ereignis, das im Oktober seinen Höhepunkt erreicht. Neben dem Anbau einer dritten Frucht im Jahr könnten die existierenden Hochdeichabschnitte als Hochwasserrückhalteräume genutzt werden und so die Hochwassergefahr und die zu erwartenden Schäden um 5–40% reduzieren. Umgekehrt würde ein weiterer Ausbau der Hochdeiche die derzeit erwarteten jährlichen Hochwasserschäden verdreifachen.

Die Zukunftsprojektionen des Hochwasserrisikos ergaben, dass das Mekong Delta in den nächsten Jahrzehnten zunehmend von tidebedingten Überschwemmungen bedroht sein wird. Der Anstieg des Meeresspiegels in Kombination mit der Landabsenkung erhöht das Ausmaß der Überflutung des Deltas um 20% und den Schaden an der Reisernte um 40–85 Mio. USD. Technische Hochwasserschutzmaßnahmen können diesen Anstieg des Risikos nicht verhindern, da der Schutz des gesamten Deltas allein durch harte Hochwasserschutzbauten technisch und wirtschaftlich nicht realisierbar ist. Daher sind Maßnahmen zur Schadensminderung und zur Anpassung an das veränderte Risiko dringend erforderlich. Als erster und wichtiger Schritt wird hier eine bessere Kontrolle und Reduzierung der Grundwasserentnahme im Delta dringend empfohlen, um die Landabsenkung und dadurch die tidenbedingten Überflutungen sowie die Salzwasserintrusion zu verringern.

Der Klimawandel und die daraus resultierenden Veränderungen im Hochwasserregime des Mekong verursachen eine weitere, aber geringere Erhöhung des Hochwasserrisikos. Die geplanten Staudämme im Mekong Einzugsgebiet könnten die Zunahme der Hochwassergefahr und der landwirtschaftlichen Verluste aufgrund des Klimawandels in extremen Hochwasserjahren zumindest theoretisch abmildern. Der Nutzen von Dämmen zur Minderung des Hochwasserrisikos ist jedoch ungewiss, da die Realisierung der geplanten Dämme sehr umstritten und damit unsicher ist. Weiterhin spielt das Management der Staudämme eine

wichtige Rolle für die Hochwasserregulierung. Da die Dämme in erste Linie zur Stromerzeugung gebaut werden, ist der Hochwasserschutz der unterliegenden Anrainerstaaten eher von untergeordneter Bedeutung. Für Vietnam bedeutet das, dass eine ordnungsgemäße Instandhaltung von Deichen und Hochwasserschutzbauten eine hohe Priorität haben sollte, um Abhängigkeiten von den Nachbarstaaten zu vermeiden. Weiterhin ist die Entwicklung von „weichen“ Hochwasserschutzmaßnahmen und -plänen dringend notwendig, da ein alleiniger Schutz durch technische Maßnahmen unmöglich ist. Aufgrund der in dieser Arbeit erzielten Ergebnisse wird daher empfohlen, die Hochdeichkompartimente für das Notfall-Hochwassermanagement bei Extremereignissen zu nutzen. Zu diesem Zweck ist eine verlässliche Hochwasservorhersage unerlässlich, und der Aktionsplan sollte in offiziellen Dokumenten und Gesetzen festgehalten werden, um die Verbindlichkeit und konsequente Umsetzung sicherzustellen.

Contents

List of Figures

List of Tables

Chapter 1 Motivation and objectives

1.1 Flood in the Vietnamese Mekong Delta

World river deltas comprise less than 1% of the Earth's landmass, they are home for 340 *million* inhabitants, 4.5% of world population in 2017 [Edmonds et al., 2020]. Edmonds et al. [2020] estimated about 70% of the delta inhabitants live in the low elevation coastal zone (below 10 m), therefore expose to the risk of fluvial and coastal floods. Nevertheless, many deltas become major hubs of urban development (e.g. Yangtze and Yellow deltas), fishery (e.g. Mississippi delta), industry and commerce; some deltas are the key source of regional and even global nutrition due to their rich ecological systems and fertile soils supporting agriculture and aquaculture production (e.g. Ganges-Brahmaputra-Meghna and Mekong deltas) [Loucks, 2019].

Floods are highly visible natural disasters, and among the most damaging events in term of both fatalities and economic losses. According to MunichRE [2020] floods account for 40% of all losses related to natural disasters worldwide between 1980 and 2019, aggregated at USD 1.1 *trillion*.

Floods in the Vietnamese Mekong Delta (VMD) are recurrent events in response to the tropical monsoon, with average economic losses estimated at USD 40–50 *million* [MRC, 2012]. The inundation dynamics in the delta is a complex hydraulic interaction of (i) high Mekong river flow triggered by the monsoon in the Mekong basin, (ii) flood buffering of the Tonle Sap Lake and its system, (iii) overland flow from Cambodia to the VMD, (iv) rainfall in the VMD and (v) the two tidal regimes of Biển Đông (the South China Sea) and Biển Tây (the Gulf of Thailand).

During the months June-October, on average 335 km^3 of the Mekong flow route to the VMD, submerge a land area 12,000–19,000 km^2 in the northern and center part of the VMD (30–47% delta land area) by 0.5–4.0 m for 2–4 *months* [Toan, 2014, SIWRP, 2015]. This part is commonly defined as delta flood-prone region. Floods in the VMD are categorized as low rising floods, with the rising rate of 5–10 $cm\ day^{-1}$ on average, and 15–25 $cm\ day^{-1}$ measured in extreme floods [Tri, 2012]. Apart from inundation driven by the Mekong flow, tidal induced inundation occurs in many delta cities/ towns in the vicinity of rivers/canals in the coastal areas, characterized by short but repeated durations following the high tides [Apel et al., 2016].

It is to notice that not all floods in the VMD are damaging events. Statistical data reveal that there are 12 damaging floods (bad floods) in the VMD between 1960-2020 (Table 1.1). These damaging floods are often characterised by one or more of the following: early

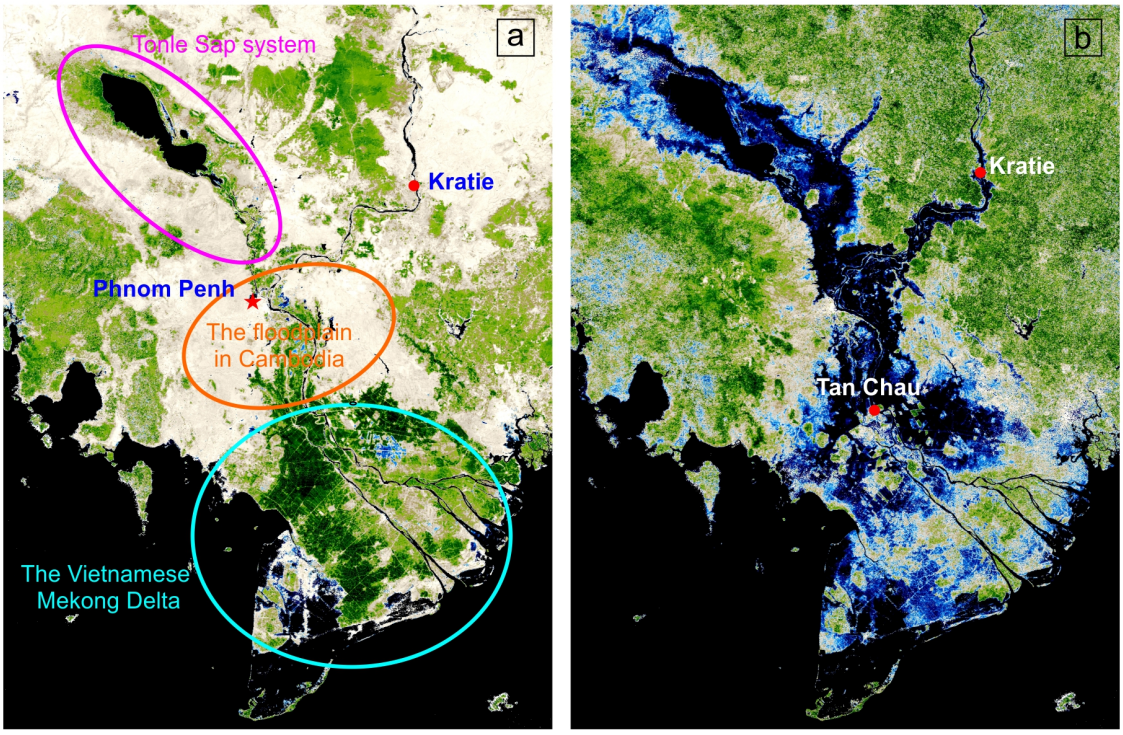

Figure 1.1: The Mekong Delta and its systems from remote sensing in the dry season (a) and in the wet/flood season (b). Data from Kotera et al. [2015].

Table 1.1: Important flood events and damages in the Vietnamese Mekong Delta. Data source: MRC [2012] and SIWRP [2015].

Year of the flood event	Flood peak at Kratie		Flood peak at Tan Chau		Flood damages	
	Q_{max} (m^3s^{-1})	Flood volume (km^3)	H_{max} (m)	Duration [a] (day)	Economic losses (USD *million*)	Fatalities
1961[b]	62,400	417	5.12	88	-[c]	-
1966	58,600	380	5.11	83	-	-
1978	68,000	421	4.78	88	-	-
1981	62,600	411	4.52	59	-	-
1984	47,400	392	4.81	85	-	-
1991	59,800	376	4.64	75	-	-
1994	53,100	355	4.51	85	-	-
1996	63,600	416	4.87	67	113	-
2000	61,200	475	5.06	118	250	453
2001	62,700	435	4.78	95	99	393
2002	59,300	429	4.82	81	0.3	71
2011	62,400	452	4.86	90	53	43

[a] *number of day which flood level at Tan Chau exceeds the 1st flood alarm level (3.5 m)*
[b] *the years in bold mark extreme flood events*
[c] *no data*

onset, high peaks, extended duration of high water level and/or delayed recession [MRC, 2012]. Within these events, special attention has to be given to the extreme flood in 2000; the event resulted in over 450 fatalities and economic losses of USD 250 *million* in the

VMD [MRC, 2012]. The flood in 2000 with the aggregated flood volume at Kratie of 475 km^3, is considered as the 50-year flood [Dung et al., 2015], and the flood level in 2000 is chosen as reference benchmark in designing flood control structures in the VMD.

Despite the adverse effects from floods, e.g. disruption of agriculture cultivation, damages to infrastructures, and even fatalities, millions of people continue to live in the VMD due to its fertile soils. Gradually, they have adapted their livelihoods to the annual flood pulse of the Mekong (i.e. "living with floods"). From the first human settlements in the VMD in the 1600s [Huu Nguyen et al., 2016], presently the delta is home for over 18 million people. The VMD is known the "rice-bowl" of Vietnam, contributing over 50% the country's rice production and 80% of the exported rice [GSO, 2015]. Fruits, vegetables, shrimp and fresh water fish are among the most recognized agricultural products of the region.

1.2 Flood management in the VMD

Traditionally, flood management in the VMD focussed mainly on engineering solutions to control floodwater. Structural measures, i.e. dyke systems, sluice gates and man-made canals have been implemented across the delta since 1980s seeking to increase rice production. The total length of the dyke system is about 14,000 km [SIWRP, 2011], providing flood protection to most of the farm lands in the flood-prone region.

Initially the dyke system aims at protecting rice fields against the early flood peak arriving in mid-July to mid-August, ensuring farmers to grow two rice crops each year. Post-harvesting the second crop, floodwater overflows the dykes and submerges rice paddies during the high flood phase (September-October). The dyke system is referred as "low-dyke" or "đê chống lũ tháng tám". The farmers sustain their livings in these months by temporal migrating and working in major cities (e.g. Can Tho, Ho Chi Minh) or by fish trapping.

Nowadays, many farmlands are protected with the so-called "high-dyke" system or "đê chống lũ cả năm". The high-dyke together with pumps and sluice gates completely protect rice paddies against floods as high as the historical flood in 2000, allowing farmers to plant an additional rice crop during the high flood months. The numbers of farmlands protected by high-dyke rapidly increased between 2000-2011. By 2011, the length of high-dyke system in the VMD aggregated at 6,000 km [SIWRP, 2011]. The majority of the high-dyke protected rice paddies are located in the two delta northern provinces: An Giang and Dong Thap [SIWRR, 2010]. Figure 1.3 schematizes the two dyke systems in the VMD.

Figure 1.2: Natural landscape in the Vietnamese Mekong Delta. (a) rice paddies in An Giang during high-flood phase of 2019. (b) Shrimp farms in Soc Trang, a coastal province. (c) Residential settlements along canal in Bac Lieu. (d) An example of a farm house in the VMD.

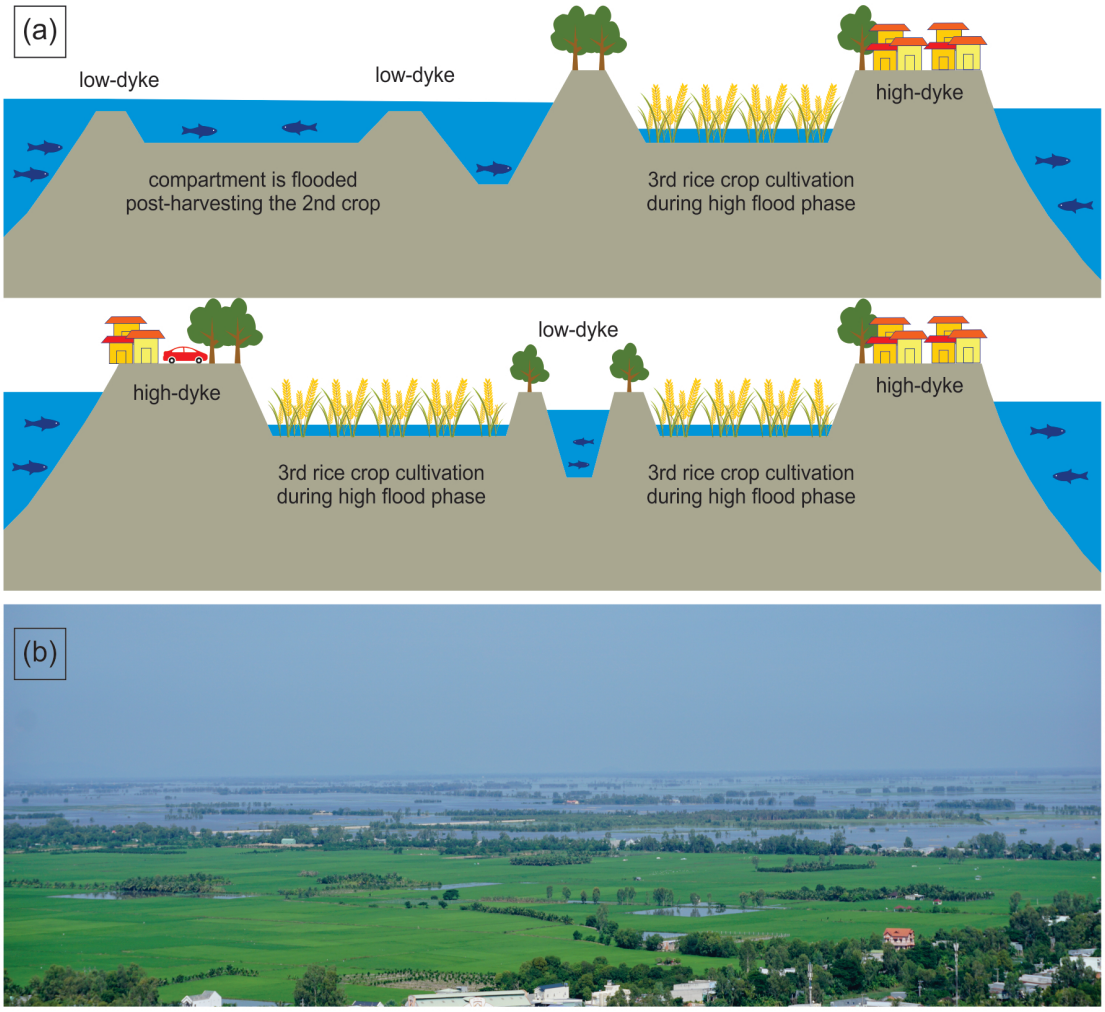

Figure 1.3: (a) Schematization of rice paddies protected with high- and low-dykes. (b) A demonstration high-dyke and low-dyke compartments during high flood phase, captured in in September 2019.

1.3 Motivation, objectives and research questions

The **motivation** of this work stems from the lack of quantitative analyses on impacts of the above-mentioned *delta-based flood control approaches* and *possible future changes* on delta flood hazard and damage to paddy rice cultivation.

Regarding the delta-based flood control approaches, the benefits of having an additional harvest in high-dyke protected compartments versus disadvantages of impeding inundation is an ongoing debate in academics, policy makers and public platforms since high-dyke was initiated in 2000/2001. Another damaging flood, with the recurrence between 15–20 year, hits the VMD in 2011, and again questions the impacts of high-dyke system. High-dyke systems are criticized as the main drivers of the observed higher and longer inundation in the centre of the VMD in 2011 compared to 2000. However, there is missing quantitative information to support the discussion; historical studies often measure high-dyke against

the "no-dyke" scenario [Le et al., 2007, Tran et al., 2018b].

Besides, the flood dynamics in the VMD is projected to be altered under the impacts of climate change, sea level rise, and hundreds of hydropower projects in the Mekong mainstream and its tributaries. The VMD with its extreme low mean elevation below 1.0 m [Minderhoud et al., 2019] is one of the globally most vulnerable deltas to climate change and sea-level rise [Tessler et al., 2015]. Recent climate impact projections reveal an intensification in magnitude [Lauri et al., 2012, Hoang et al., 2018] and frequency of extreme floods (i.e. the 100-year flood) in the Mekong River basin [Hirabayashi et al., 2013]. The Fifth Assessment Report of the Intergovernmental Panel on Climate Change predicts an increase of 17–38 cm in tidal level along the coast of the VMD by mid-century [IPCC, 2014a].

Similar to many world river deltas, the VMD is rapidly sinking at rate 1.0–2.5 $cm\ year^{-1}$, and is expected to continue in the future [Erban et al., 2014, Minderhoud et al., 2017]. This is the result of natural compaction processes and accelerated by anthropogenic interventions, e.g. sand mining, disruption of floodplain inundation, and over abstraction of groundwater. All increase the risk in both fluvial and tidal induced floods [Erban et al., 2014, Minderhoud et al., 2017].

On basin scale, the Mekong river and its tributaries have been and will be heavily dams to meet the energy demands of the fast-growing riparian countries. The Mekong River Commission estimates the basin's active reservoir storage in 2025, excluding the installed and planned dams in China, would reach 86.8 km^3, about 19% of the mean annual flow of the Mekong [MRC, 2015b]. Räsänen et al. [2017] suggests existing dams in the Mekong Basin increase the river discharges at Kratie 40–74% in March-May and reduce 0–6% in July-August. These changes in the Mekong flow subsequently disrupt the annual flood dynamics in the VMD.

Although many analyses highlighted the impacts of individual driver [e.g. Le et al., 2007, Van, 2009, Van et al., 2012, Toan, 2014, Dang et al., 2018, Tran et al., 2018b], the compound impacts of all drivers have not been explicitly quantified. Besides, large scale flood damage and risk analyses to paddy rice cultivation, the dominant land-use in the VMD, are missing in the literature. This study aims to fill in these knowledge and research gaps. The results will provide materials to facilitate the new master plan for the Vietnamese Mekong Delta, which flood management and triple rice cultivation are one of the key components [GOV, 2017]. Besides, the flood risk indicator (to rice paddies) calculated in this research is expected to provide the basis input for the agriculture insurance programme in Vietnam.

The general objective of this study is the numerical quantification of the current state and future projections on flood hazard and rice crop damage in the VMD driven by natural

changes and anthropogenic stressors. This results in the five research questions, resolved in the main chapters marked in brackets:

1. Has high-dyke development in the VMD shifted flood hazard downstream? (Chapter 2)
2. What explains the flood level observed in many gauges in 2011 compared to the flood in 2000? (Chapter 2)
3. What is the expected annual flood damage to rice cultivation in the VMD with the current dyke system? (Chapter 3)
4. How does expansion of high-dyke area, or conversion of high- to low-dyke affect the flood damage and risk? (Chapter 3)
5. What are the future projections of delta flood hazard and agricultural damage? (Chapter 4)

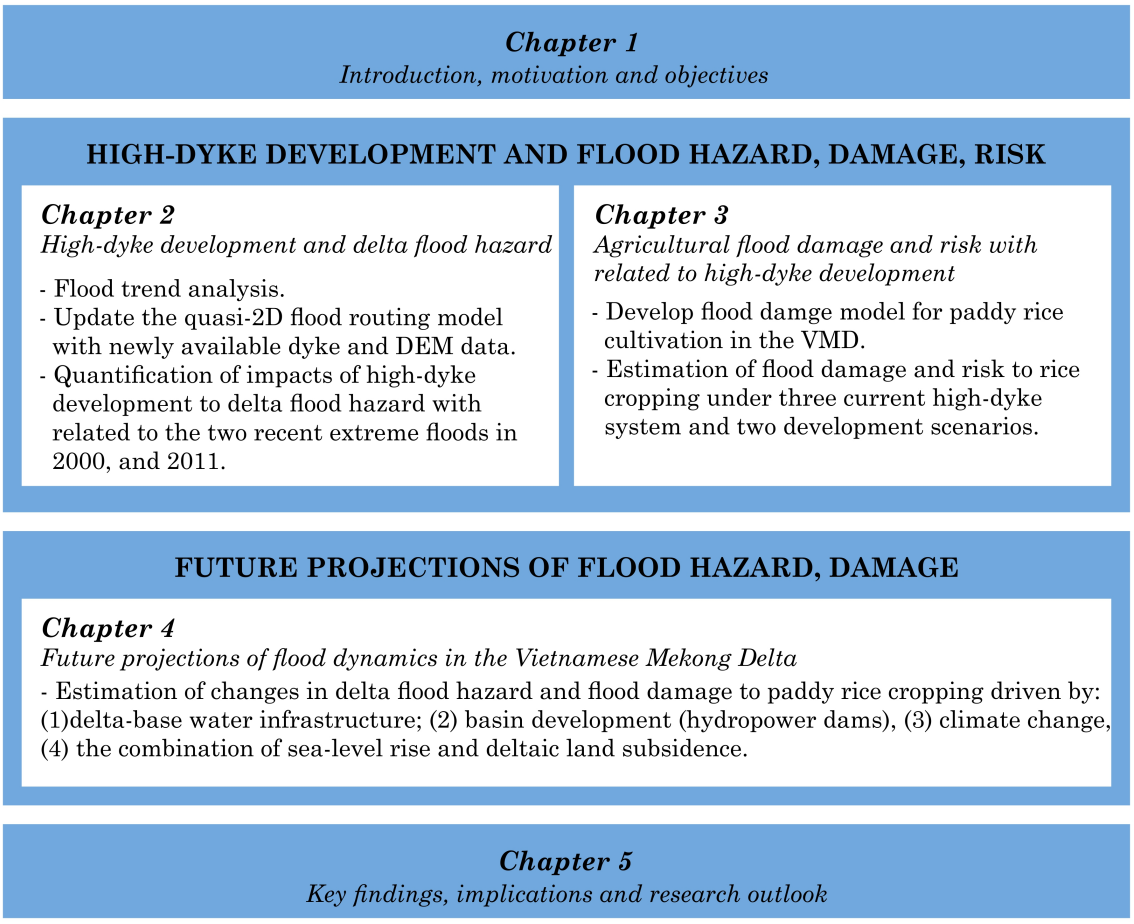

Figure 1.4: Structure of the dissertation

1.4 Structure of the dissertation

This cumulative thesis consists of an introductory chapter, three main chapters addressing the main research questions, and a concluding chapter highlighting key findings and future

research outlooks (see Fig. 1.4). Chapter 2 to 4 of the dissertation are arranged following the widely used procedure of natural disaster risk assessment, i.e. hazard, expose and vulnerability, and flood risk, and on the temporal projection, i.e. current stage (Chapter 2 and 3) and the future projections (Chapter 4).

The three main chapters take the form of three manuscripts that have been published in peer-reviews journals. Chapter 2 analyses trends in flood characteristics (peak and duration) at different monitoring gauges in the Mekong Delta. The second part of this chapter quantifies and attributes the detected trends to high-dyke development and other important drivers, e.g. tidal level, flood hydrograph by a detailed hydraulic modelling approach. Chapter 3 provides an estimation of flood damages and risks to rice cultivation in the VMD, quantified as expected annual damage. The calculation explicitly takes plant phenomenology and timing of floods in a probabilistic modelling framework into account. Chapter 4 highlights future projections of flood hazard and damage in the VMD driven by (1) delta-base water infrastructure (high-dyke), (2) basin development (hydropower dams), (3) climate change and (4) the effective sea-level rise (the combination of sea-level rise and deltaic land subsidence) in a set of eight modelling scenarios. The scenarios model possible changes driven by individual drivers, follow by their cumulative impacts.

1.5 Author contributions

The manuscripts in the three main chapters are the result of the collaboration between the author of this thesis (N.V.K.T.) and several co-authors. The following paragraphs summary the contribution of N.V.K.T. and other co-authors (initials) in each manuscript:

Chapter 2: Has dyke development in the Vietnamese Mekong Delta shifted flood hazard downstream?

N.V.K.T. designed the research with contribution from N.V.D. and H.A.; N.V.K.T. collected the data, updated the hydrodynamic model, performed the trend analysis, interpreted the results, generated all figures and table; N.V.D. supported with generating inundation raster from modelled results. N.V.K.T. wrote the paper with contributions from H.A., M.K., B.M. and H.F.

Chapter 3: Towards risk-based flood management in highly productive paddy rice cultivation – concept development and application to the Mekong Delta

N.V.K.T. designed the research with contribution from H.A.; N.V.D. provided data for Section 3.1 and supported with Figure 3.4. N.V.K.T. developed the rice crop flood damage and risk estimation, performed the calculation, interpreted results, generated all tables and figures, and compiled results in a draft manuscript. All authors (H.A., B.M., N.V.D. and

N.V.K.T.) discussed the results and contributed to finalize the paper.

Chapter 4: Future projections of flood dynamics in the Vietnamese Mekong Delta

N.V.K.T. and L.P.H. designed the research with contribution from N.V.D. and D.D.T.; L.P.H. provided data and supported writing Section 4.1.1; D.D.T. contributed to writing Section 3.1.1. N.V.K.T. prepared the scenarios, performed the simulations, interpreted results, generated all tables and figures; and wrote the manuscript with discussions and supports from H.A., B.M., N.V.D., M.K., N.L.D. and T.T.A.

Chapter 2 Flood hazards in the Mekong Delta - impacts of local flood control measures

Abstract

In the Vietnamese part of the Mekong Delta (VMD) the areas with three rice crops per year have been expanded rapidly during the last 15 years. Paddy-rice cultivation during the flood season has been made possible by implementing high-dyke flood defences and flood control structures. However, there are widespread claims that the high-dyke system has increased water levels in downstream areas. Our study aims at resolving this issue by attributing observed changes in flood characteristics to high-dyke construction and other possible causes. Maximum water levels and duration above the flood alarm level are analysed for gradual trends and step changes at different discharge gauges. Strong and robust increasing trends of peak water levels and duration downstream of the high-dyke areas are found with a step change in 2000/2001, i.e. immediately after the disastrous flood which initiated the high-dyke development. These changes are in contrast to the negative trends detected at stations upstream of the high-dyke areas. This spatially different behaviour of changes in flood characteristics seems to support the public claims. To separate the impact of the high-dyke development from the impact of the other drivers, i.e. changes in the flood hydrograph entering the Mekong Delta, and changes in the tidal dynamics, hydraulic model simulations of the two recent large flood events in 2000 and 2011 are performed. The hydraulic model is run for a set of scenarios whereas the different drivers are interchanged. The simulations reveal that for the central VMD an increase of 9–13 *cm* in flood peak and 15 *days* in duration can be attributed to high-dyke development. However, for this area the tidal dynamics have an even larger effect in the range of 19–32 *cm*. However, the relative contributions of the three drivers of change vary in space across the delta. In summary, our study confirms the claims that the high-dyke development has raised the flood hazard downstream. However, it is not the only and not the most important driver of the observed changes. It has to be noted that changes in tidal levels caused by sea level rise in combination with the widely observed land subsidence and the temporal coincidence of high water levels and spring tides have even larger impacts. It is recommended to develop flood risk management strategies using the high-dyke areas as retention zones to mitigate the flood hazard downstream.

Published as: Triet, N. V. K., Dung, N. V., Fujii, H., Kummu, M., Merz, B., and Apel, H.: Has dyke development in the Vietnamese Mekong Delta shifted flood hazard downstream?, Hydrol. Earth Syst. Sci., 21, 3991-4010, 10.5194/hess-21-3991-2017, 2017.

2.1 Introduction

The Vietnamese Mekong Delta (VMD), the so-called rice bowl of Vietnam, encompasses an area of 4.0 *million ha*, of which over 2.6 *million ha* are used for agriculture. It accounts for more than 52% of the national food production and more than 85% of the annual rice export [GSO, 2015]. Being a low-lying coastal region, the VMD is susceptible to both riverine and tidal floods, threatening agricultural production and the safety of people [Le et al., 2007, Schumann et al., 2008, Dung et al., 2009, 2011, Van et al., 2012, Kuenzer et al., 2013]. Climate change and sea level rise are expected to increase the risk, not only due to flooding but also due to droughts and salinity intrusion [Wassmann et al., 2004, Khang et al., 2008, Toan, 2014, Hak et al., 2016]. Further, the region faces severe sediment starvation as a consequence of massive hydropower development [Fu and He, 2007, Kummu and Varis, 2007, Fu et al., 2008, Kummu et al., 2010, Xue et al., 2011, Gupta et al., 2012, Manh et al., 2015]. In a recent study, Manh et al. [2015] estimated the delta sedimentation and the amount of sediment reaching the South China Sea to be diminished by 40–95% considering hydropower development scenarios, climate change, sea level rise and the deltaic land subsidence. Land subsidence becomes a notable problem in many cities in the delta, with an estimated rate of 1–4 $cm\ year^{-1}$ [Erban et al., 2014, Anthony et al., 2015].

The population in the VMD has extensive experience in living with floods. The first major human interventions were the construction of the Thoai Ha and Vinh Te canals in the 1820s, followed by several water works before and during the colonial period as well as after the reunification in 1975. However, large-scale flood control systems had not been implemented until the late 1990s [Käkönen, 2008]. Starting from 1996, the government of Vietnam constructed a series of waterways to divert part of the overland flood flow from Cambodia towards the Gulf of Thailand, followed by the development of comprehensive dyke systems and hydraulic structures according to the Five-Year Development Plan 1996-2000 for the region [GOV, 1996]. The majority of dykes constructed within this period were so-called low dykes. Low dykes provide protection against the early flood peak arriving around mid-July to mid-August, ensuring the farmers can grow two rice crops per year by keeping floodwater in the paddy fields after the summer crop. The so-called high dykes were mainly built after the disastrous flood in 2000. They were designed according to farmers' needs and the demand of the provinces to protect the floodplains against a flood as high as in 2000. This protection standard along with the full control of the flow into the floodplains nowadays allows the cultivation of three crops per year in the provinces An Giang and Dong Thap in the upper part of the delta.

The implementation of high dykes was claimed to benefit the population by providing safety and additional income for the farmers. However, Howie [2005] and Käkönen [2008]

questioned this claim, because impeding floodplain inundation reduces the input of sediments and thus of natural fertilizers to the paddy fields. This leads to reduced crop yields [Manh et al., 2014] and consequently, intensified use of agrochemicals and higher costs. Howie [2005] and Käkönen [2008] also pointed to other social and environmental adverse consequences, e.g. water pollution, stress and exhaustion because of missing "resting time" for the farmers, and higher damages in the case of an extreme event causing dyke breaches and flooding of the third summer crops. One important aspect in this discussion is the question regarding to what extent upstream flood control has increased flood risk downstream.

Recently, Dang et al. [2016] and Fujihara et al. [2016] attempted to quantify the impacts of the high-dyke development on downstream water levels. Both studies derived high-dyke areas from Moderate Resolution Imaging Spectroradiometer (MODIS) satellite images and analysed historical records to detect trends in water levels and to attribute these trends to the dyke development. Fujihara et al. [2016] investigated the period 1987-2006 at 24 stations in the VMD, while flooded areas were identified for 2000-2007. Dang et al. [2016]) reduced the number of stations to 10, but included four stations in the Cambodian floodplains (CFP) and expanded the hydrological and satellite data to 2013/2014. Both studies concluded that high-dyke development in the northern part of the VMD and the increasing water levels downstream are linked. Dang et al. [2016] also stated that the hydraulic alterations in the VMD had the largest influence on water level changes, compared to dam construction in the Mekong Basin, sea level rise and deltaic land subsidence. However, both studies were not able to quantify the contribution of the hydraulic alterations to the observed changes. Moreover, Dang et al. [2016] noted that the findings were prone to considerable uncertainties, notably the uncertainty of the water level data. Possible sources of these uncertainties are land subsidence, change in reference datum, and instrument or observer errors. Building on these findings, our study has two objectives: (1) to re-analyse the water level trends found in the previous studies under explicit consideration of uncertainty, and (2) to quantify the changes caused by the development of the dyke system on water levels in the VMD by a detailed hydraulic modelling approach, as recommended by Dang et al. [2016].

The first objective is achieved by comparing flood trends at the two major gauging stations downstream of the high-dyke development areas with flood trends at stations upstream of the development areas. This comparison includes an analysis of the robustness against data errors. To obtain a better understanding of the trends, changes in flood peak and flood duration are analysed, which in combination define the severity of floods in the Mekong Delta [Dung et al., 2015]. To quantify the relative contribution of high-dyke development, we update the quasi-2-D flood model developed by Dung et al. [2011] and Manh et al. [2014] using the latest comprehensive dyke survey data and high-resolution

topographical data from the newly available 5×5 m resolution lidar-based DEM for the VMD. Changes in delta inundation dynamics for the pre- and post- high-dyke development are investigated in different model setups, simulating the two recent, most severe flood events in 2000 and 2011.

2.2 Study area, data and methodology

2.2.1 Study area

Originating from the Tibetan Plateau, the Mekong River runs through the territories of China, Myanmar, Laos, Thailand, Cambodia and Vietnam before it discharges into the South China Sea (termed the East Sea in Vietnam). With a mainstream length of almost 4,100 km, drainage area of about 795,000 km^2 and annual mean discharge of 475 km^3, the Mekong is ranked 10^{th} in the list of the world's largest rivers. The basin is subjected to a monsoonal regime, in which the wet season lasts from June to November accounting for 80–90% of the total annual flow. During this period a huge amount of water is routed to the lowland areas, causing extensive inundation in the MD. The MD encompasses the Cambodian floodplains (CFP) downstream of Kratie (Fig. 2.1) and the VMD, which differs considerably from the CFP due its enormous amount of man-made hydraulic structures like channels, dykes, sluice gates and pumps. Although large floods, such as in 2000 or 2011, result in considerable economic and social damages [MRC, 2012, 2015a], flooding is the backbone of the agricultural production in the region. Moderate floods, commonly perceived as "good floods" by the local population, bring various benefits, e.g. reduction in soil acidity; removal of residual pesticides and other pollutants in paddy fields; an immense wealth of wild fish in the rivers, channels and inundated floodplains; and provision of nutrients through deposited sediments on the floodplains [Hashimoto, 2001, Sakamoto et al., 2007, Hung et al., 2012, Manh et al., 2013, 2014].

Floodwater enters the VMD via three main routes, i.e. the mainstream flow through the Mekong River (named Tien River in Vietnam) and Bassac River (named Hau River in Vietnam), and transboundary overland flow to the Plain of Reeds (PoR) east of the Mekong River and to Long Xuyen Quadrangle (LXQ) west of the Bassac River (Fig.2.1). The mainstream flow accounts for 90% of the total flood volume entering the VMD (Tri, 2012). The flood-prone areas cover a territory of approximately 2.0 $million\ ha$ in the northern part of the VMD (Fig. 2.1). The average inundation depth varies from 0.5 to 4.0 m and lasts for 3 to 6 $month$ [Toan, 2014, SIWRP, 2015]. The floodplains are protected by extensive dyke systems, both low dykes and high dykes, with a total length of over 13,000 km, of which 8,000 km comprises low dykes with crest levels vary from 1.5 to 4.0 $m\ a.m.s.l$. High-dyke areas are mainly concentrated in the provinces An Giang and Dong

Thap in the upper part of the delta (green areas in Fig. 2.1). About 65% of the cultivation area in An Giang and 40% in Dong Thap are protected by high dykes with crest levels of 4.0–6.0 *m a.m.s.l.* [SIWRR, 2010]. The area of triple cropping in 2014 was 175,000 *ha* in An Giang and 120,000 *ha* in Dong Thap, respectively [GSO, 2015].

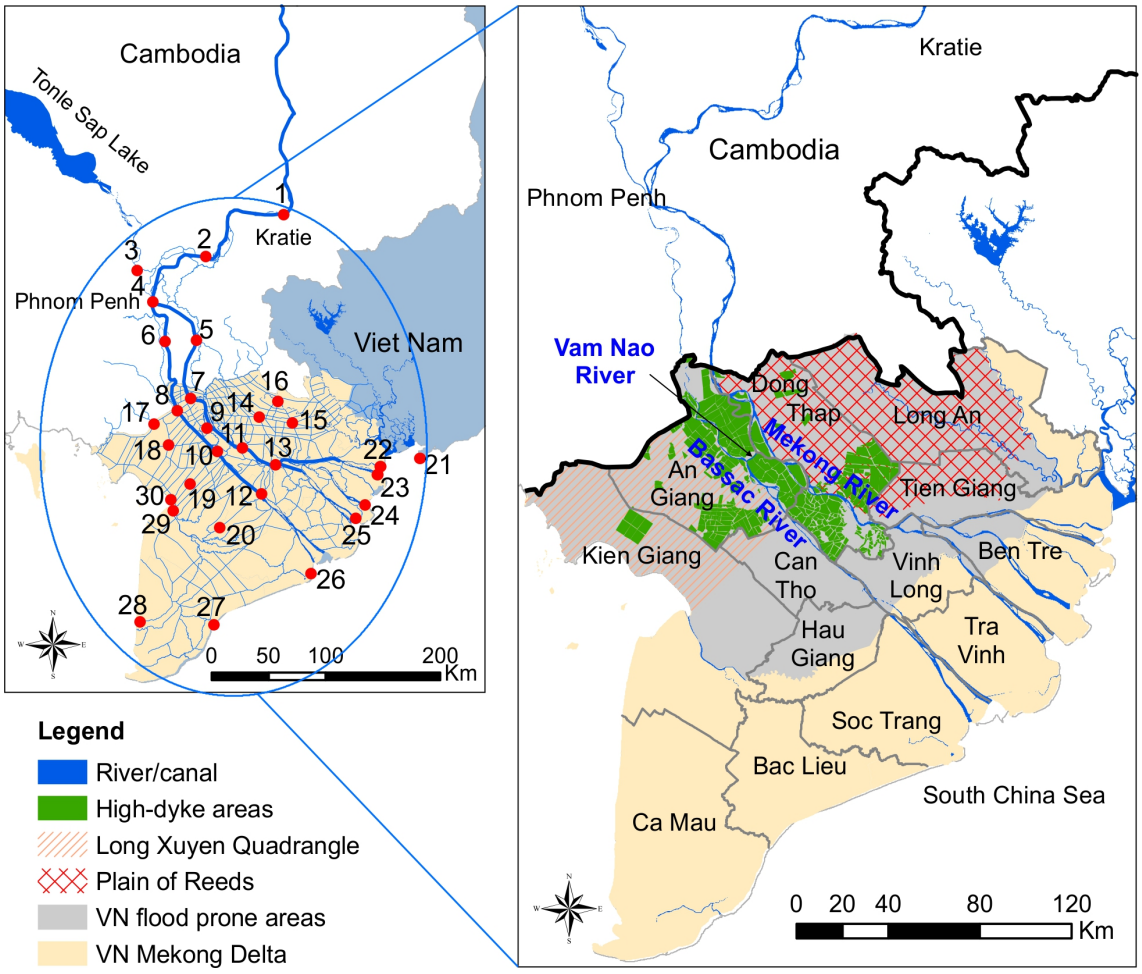

Figure 2.1: The Vietnamese Mekong Delta, its flood-prone areas and the location of measuring stations (red dots). The names in black indicate the provinces in the VMD.

2.2.2 Data

Gauge data

Gauge data were used as boundaries for the hydraulic model, for model calibration and validation and for detection of flood trends. Daily and hourly water level and discharge data were collected at 30 stations. They include 13 stations along the rivers Mekong and Bassac, of which 6 stations are located in Cambodia, along with 10 tidal gauge stations and 7 stations located in secondary rivers/canals (Fig. 2.1). The location and name of each station are given in Table A1 of Appendix A. These data were provided by the

Mekong River Commission (MRC) and the Southern Regional Hydro-Meteorology Centre of Vietnam (SRHMC). The MRC database contains daily readings from 1960s to present, with some stations having data back to the 1930s. However, the data often have gaps due to the past political conflicts in the region. SRHMC data are measured in hourly intervals and are relatively complete, but cover only the period from the late 1970s to present. To obtain a common period for the trend analyses for the Vietnamese and Cambodian stations, time series of 38 years of daily water level/discharge data (1978-2015) at five key stations, i.e. Kratie, Tan Chau, Chau Doc, Can Tho and My Thuan, were chosen. These two databases use different vertical reference points, i.e. Hatien1960 in MRC data, and Hondau72 in SRHMC data. To ensure consistency, the MRC data were converted to the Hondau72 datum.

For the calibration and verification of the hydraulic model, hourly data of all VMD gauging stations (Fig. 2.1 and Table A1) and inundation maps derived from MODIS satellite images were used. Cloud cover of the MODIS images was removed by Kotera et al. [2014, 2016]. The calibration considered the rainy season (June to November) of the years 2000 and 2011.

Dyke and topography data

To evaluate the impact of the high-dyke development, two benchmark states were selected: the year 2000, which marked the start of the large-scale high-dyke development, and the status in 2011 with large-scale high-dyke protection in place. These two years are among the most severe floods in the MD, second only to the flood in 1978. The dyke system in 2000 was taken from Hoi [2005]. Details of the dyke system of 2011 were based on a survey undertaken by the Southern Institute of Water Resources Research (SIWRR) from 2009 to 2010; the dataset included all the dykes constructed before the 2011 flood, except those possibly built in the dry season of 2011. The survey was conducted in four flood-prone provinces in the VMD, i.e. An Giang, Dong Thap, Kien Giang and Long An, and included maps of compartments protected by dykes, and their classification as either low dykes or high dykes. In addition, dyke height, width at crest, slopes and sluice gate locations and further specifications were provided in the survey.

The high-resolution lidar-based DEM surveyed during 2008-2010 for all provinces in the VMD was obtained from the Ministry of Natural Resources and Environment of Vietnam (MONRE). Floodplain compartments with dyke lines and elevation, which were not detectable in the Shuttle Radar Topography Mission (SRTM) DEM used in the previous version of the hydraulic model, are represented in the high resolution DEM, as the widths of dyke crests are in the range of 3.0–5.0 m. The final dyke heights of the updated hydraulic model were determined by combining information from these two sources of topographical

information. The new DEM was also applied to extract updated cross sections for the representation of floodplain compartments and to derive simulated inundation extent and duration maps from the hydraulic model results.

2.2.3 Trend analysis

Long-term trend detection

The Mann-Kendall (MK) non-parametric trend test [Mann, 1945, Kendall, 1975] was applied to detect changes in flood characteristics. The trend magnitude was estimated by the non-parametric method of Sen [1968]. The annual maximum water level ($AMWL$) and the flood volume and duration were selected as flood characteristics, as the flood severity is not fully represented by the maximum discharge/water level alone [Dung et al., 2015]. For example, the maximum water level in 2014 at Kratie was 19 cm higher than the peak of the disastrous flood in 2000. However, in 2014 the duration of flow above which overbank flow and floodplain inundation starts and the volume of the flood hydrograph were about 55 and 65% of 2000, respectively. This explains the large difference in losses for these two floods.

The annual flood volume (FV), defined as the sum of daily discharge during the flood season June-November, at Kratie was selected as second important factor describing the severity of the floods entering the MD. At all downstream gauges, the number of days with maximum water level equal or higher than a certain threshold value (DOT) was selected. This indicates the severity of floods in terms of the duration of critical water levels and was chosen, instead of the annual flood volume, because discharge data are less complete, and because river flow is influenced by the tidal magnitude at the stations in the VMD. For the coastal stations and those directly downstream of the high-dyke areas (e.g. Can Tho, My Thuan), the tidal signal is clearly visible even during the high-flood period [Hung et al., 2012]. This means that under high-tide conditions overbank flow and inundation can occur even during comparatively low river discharge.

The critical threshold values were selected on the basis of the three flood alarm levels, as indicated in the national standards of Vietnam. When the water stage exceeds alarm *level* 3, flooding reaches an unusual and hazardous state. Although *level* 3 is a good indicator for damaging floods, it is not suitable as threshold to calculate flood duration, as only in a few years of the study period did the water level exceed this highest alarm level. For instance, at Tan Chau and Chau Doc, *level* 3 was reached in only 11 years. Using this level would not yield robust results for the trend tests. Hence, alarm *level* 1 was used, i.e. 3.50 m at Tan Chau, 3.0 m at Chau Doc and 1.5 m at Can Tho and My Thuan.

Step-change detection

Past studies agreed on the direction and magnitude of flood trends at key locations in the VMD, specifically for Can Tho and My Thuan [Le et al., 2007, Dang et al., 2016, Fujihara et al., 2016]. They disagreed, however, on the timing of the changes and, consequently, on the reasons for changes. Le et al. [2007] found rising water levels at some stations in the VMD and linked these changes to infrastructure development during the period 1996-2002. Similarly, Toan [2014] reported an unprecedented change in tidal levels at Can Tho after 2000. On the other hand, Fujihara et al. [2016] concluded that infrastructure development until 2006 had minor impacts. Therefore, to analyse if and when changes in water levels can be linked to infrastructure development, the non-parametric approach by Pettitt [1979] for detecting step changes was applied in addition to the MK test. This method has not been applied by the previous studies.

Uncertainty analysis of the detected trend

Gauged data are subject to errors, stemming from either human operation or instrument failures including subsidence of the gauge reference. These errors might influence the trend analysis. Therefore, the trend analysis was tested against hypothetical measurement errors in a Monte Carlo (MC) experiment by randomly disturbing the observation data with uniformly distributed errors. The error ranges were ± 5, ± 10 and ± 20 cm, from which randomly drawn errors were added to every gauged water level data point. The lowest error range is derived from the accuracy range of instruments applied to monitor water stage, e.g. staff level gauges, automatic measurement using sonar or pressure probes, which is in the range of ± 2 cm for the current modern instruments in place. In order to account for lower precision of earlier instruments and the unknown error range of manual staff readings this range was extended to ± 5 cm. The higher error ranges are meant for testing the trends against hypothetical higher errors not caused by instrument errors alone. For Kratie, these error ranges in water level correspond to an alteration of 1, 3 and 6% in discharge based on a rating curve derived from contemporaneous records of water level and discharge. $AMWL$, DOT and FV were calculated from the disturbed time series, and the MK trend test, Sen's slope estimation and Pettitt's test were performed again. By repeating this procedure 1000 times, the robustness of the detected trends against data errors was tested.

2.2.4 Hydrodynamic modelling

To quantify the contribution of high-dyke development, a hydrodynamic model for the simulation of the flood propagation in the MD was used. The model is a quasi-2-D model

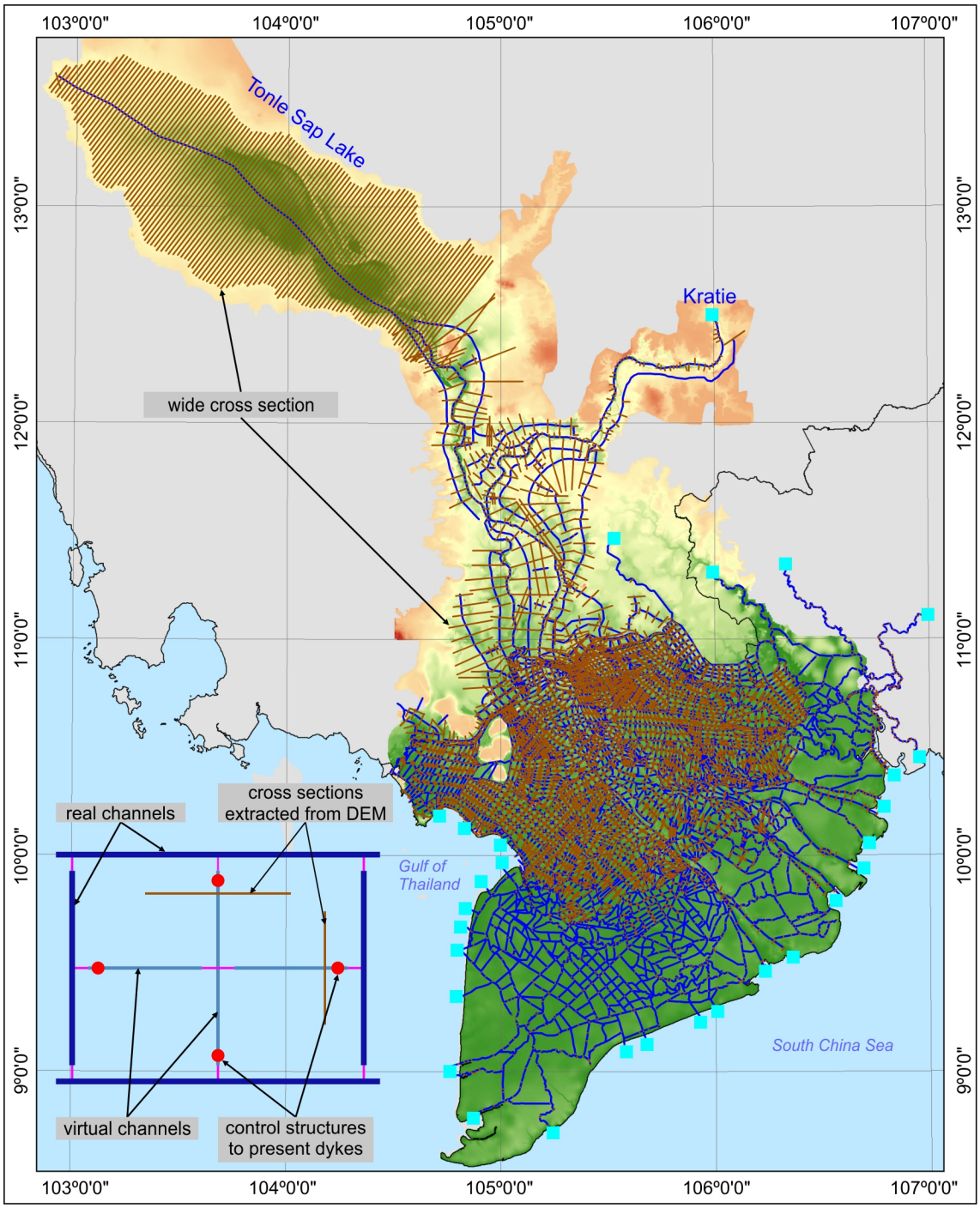

Figure 2.2: The channel network of the quasi-2-D flood model for the MD, and the simulation concept for flood compartments in the model.

based on the 1-D hydrodynamic modelling suite MIKE11. The MIKE 11 hydrodynamic (HD) module solves the vertically integrated equations of conservation of continuity and momentum (the "Saint Venant" equations). The solution of the equations of continuity (Eq. 2.1) and momentum (Eq. 2.2) is based on an implicit finite difference scheme developed by Abbott and Ionescu [1967]. The model domain includes the CFP, the Tonle Sap Lake and the majority of the channels and hydraulic structures in the VMD. The model was initially developed by Dung et al. [2011] and refined by Manh et al. [2014]. It is

a quasi-2-D model, and takes the complex hydraulic system of the VMD into account. A typical flood compartment, i.e. part of the floodplain encircled by channels, is described by "virtual" channels with wide cross sections connected to the channels by sluice gate model structures.These cross sections were originally extracted from the SRTM DEM. The cross section width is defined in such a way to preserve the flood compartment area. Dyke lines of each flood compartment are described by four control structures right after the points where virtual and real channels are linked. These structures are introduced in the model as broad crest weirs. The crest levels of dyke lines are presented as sill levels of these control structures (see Fig. 2.2).

$$\frac{\partial Q}{\partial x} + \frac{\partial A}{\partial t} = q \tag{2.1}$$

$$\frac{\partial Q}{\partial t} + \frac{\partial \left(\alpha \frac{Q^2}{A}\right)}{\partial x} + gA\frac{\partial h}{\partial x} + \frac{gQ|Q|}{C^2 AR} = 0 \tag{2.2}$$

where Q is discharge, A flow area, $|Q|$ lateral inflow, H stage above datum, C Chezy resistance coefficient, R hydraulic or resistance radius, and α the momentum distribution coefficient.

A comprehensive description of how floodplain compartments are introduced by the "virtual" channels and wide cross sections can be found in Dung et al. [2011]. The model has been calibrated by Dung et al. [2011] and Manh et al. [2014] with recent flood events in the VMD, encompassing the high floods of 2011, the medium floods in 2008 and 2009, and the extraordinarily low flood in 2010.

The multi-objective calibration by Dung et al. [2011] showed that the model could satisfyingly simulate the inundation extent only, if the model dyke levels were lowered by 20%. This indicated that the dyke level data were not accurate. Therefore, in this study the model was updated with the latest DEM and dyke survey data as follows: first, dyke survey maps and river networks of the flood model were loaded into ArcGIS in order to identify which and where updates in the model setup were necessary. These were typically single big flood compartments in the current model setting, which can only be set as either low dykes or high dykes. However, based on the up-to-date survey data, they consist of multiple smaller flood compartments composed of low dykes and high dykes. Thus, the river network model for these areas needed to be updated. Figure 2.3 demonstrates an example. The compartment is located at Binh Phu commune in An Giang Province. It includes four small flood compartments with both dyke types: high dykes (number 25 and 26) and low dykes (number 55 and 57). In the original model setup it was represented as a single and semi-protected flood compartment (Fig. 2.3b). Figure 2.3c shows the compartment in the new model representing high- and low-dyke areas.

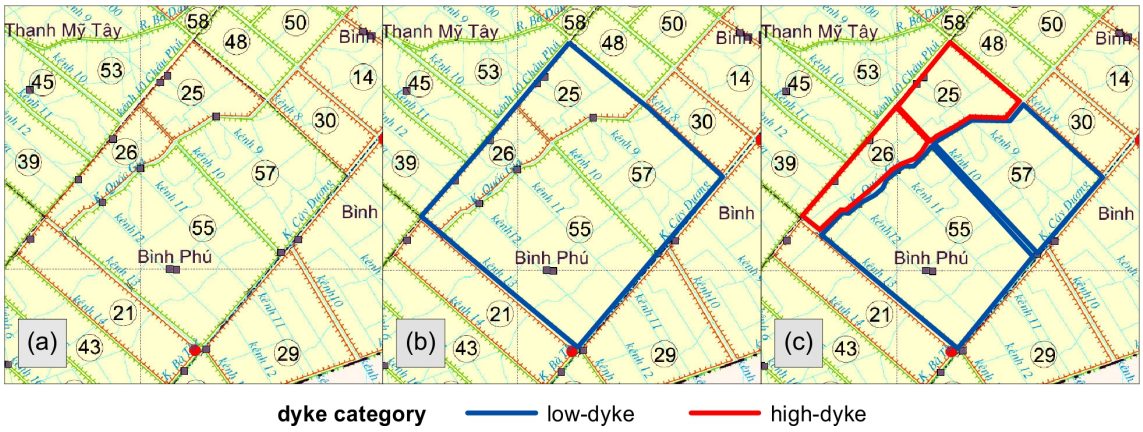

Figure 2.3: An example of a flood compartment updated in the presented model:(a) dyke survey map: orange lines mean high dykes, green lines represent low dykes, (b) presented as a single compartment in the original model, and (c) updated model river network and dyke system.

In total, approximately 150 flood compartments were updated. In a second step the wide cross sections representing floodplains, which were previously extracted from the SRTM DEM, were derived from the higher-resolution lidar DEM. The hydrodynamic model was then calibrated against observed water levels and discharge, and inundation extents derived from MODIS satellite images. The Nash-Sutcliffe efficiency (NSE) and the flood area index (FAI) were used to quantify model performance. Results are presented in Fig. 2.4 and Table 2.1.

The majority of stations used for model calibration have NSE values in the range of 0.85 to 0.98: for the years 2000 and 2011, 11 and 14 out of 19 locations, respectively, have NSE values greater than 0.85 with a maximum value of 0.98 (Table 2.1). At other locations, NSE values are lower, but still higher than 0.7. These are mainly stations with tidal influence, e.g. Can Tho, My Thuan. Generally, the model captures the water levels at high water stages well (see Fig. 2.4a). Its performance deteriorates for low water stages because of a tendency to overestimate low water levels. As the focus of this study is flooding, the model performance for simulating water levels is very acceptable. The model calibration against discharge is also good, with NSE in the range 0.68–0.96. In addition, inundation extents generated from the model results are very similar to water masks derived from remotely sensing data (see Fig. 2.4c and d). The good agreement is expressed by the relatively high FAI, which improved from 0.46 of the original model to 0.64 (Table 2.2). One possible explanation for the mismatch of simulated and observed inundation extend for the areas in Ca Mau peninsula (the south-western part of the VMD) is the land-use type. In this area shrimp farming or a mixture of shrimp farming and paddy rice dominates throughout the year. Thus, the areas detected as wet from satellite data could very likely be the water surface of shrimp ponds. As these farming schemes are not considered in the model setup, they are simulated as dry areas. In fact, this area is not known to be flooded regularly; thus, this explanation is plausible. Overall, and despite this mismatch

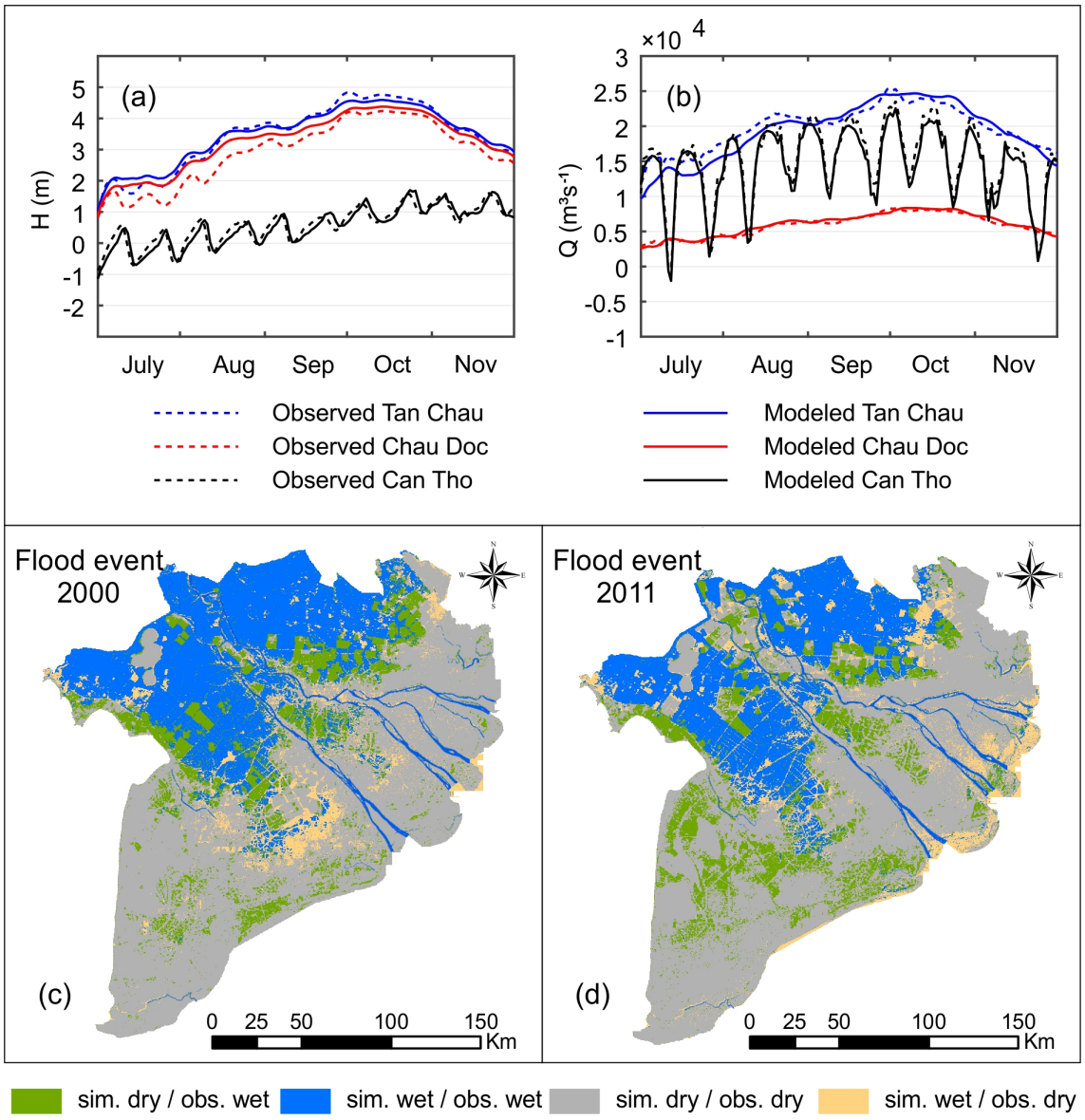

Figure 2.4: Model performance: comparison of gauged and simulated water level (a) and discharge (b) at stations Tan Chau, Chau Doc and Can Tho for the 2011 flood; comparison of observed data, i.e. derived from satellite, and simulated maximum inundation extent for the floods in 2000 (c) and 2011 (d). Grey and blue indicate agreement, green means observed inundation but no inundation simulated, and yellow implies simulated inundation but no inundation observed.

of simulated inundation areas in Ca Mau the FAI values are comparable with other flood inundation modelling studies [e.g. Aronica et al., 2002]. Therefore, it can be concluded that the updated model is reliable and produces realistic inundation dynamics and can thus be used to evaluate the impacts of high-dyke development on flood characteristics.

Table 2.1: Model performance: location, parameter and results for the two flood events in 2000 and 2011. Model performance is quatified by the Nash-Sutcliffe Efficiency (NSE).

No.	Station	Location	Flood event in 2000		Flood event in 2011	
			H	*Q*	*H*	*Q*
1	Kampong Cham	CFP	0.88		0.84	
2	Prekdam	CFP	0.95		0.96	
3	Phnom Penh port	CFP	0.93		0.96	
4	Neakluong	CFP	0.98		0.98	
5	Khokhel	CFP	*N/A**		0.86	
6	Tan Chau	VMD	0.96	*N/A*	0.97	0.80
7	Chau Doc	VMD	0.97	0.76	0.87	0.96
8	Vam Nao	VMD	0.98	0.74	0.96	0.74
9	Long Xuyen	VMD	0.97		0.96	
10	Cao Lanh	VMD	0.96		0.96	
11	Can Tho	VMD	0.76	0.73	0.86	0.74
12	My Thuan	VMD	0.72	0.68	0.80	0.73
13	Hung Thanh	VMD	0.74		0.92	
14	Moc Hoa	VMD	0.78		0.94	
15	Kien Binh	VMD	0.91		0.80	
16	Xuan To	VMD	0.88		0.89	
17	Tri Ton	VMD	0.89		0.94	
18	Tan Hiep	VMD	*N/A*		0.80	
19	Vi Thanh	VMD	*N/A*		0.78	

**N/A means no data for model performance evaluation*

2.2.5 Quantifying the contributions of dyke development and of other drivers

An inspection of the hydrographs at the tidal stations in 2000 and 2011 revealed an increase in the tidal level. At tidal gauge My Thanh, approximately 80 *km* downstream of Can Tho, an increase of 22 *cm* in the water level averaged across the flood season was observed. Because a tidal signal can still be found at gauge stations at the Vietnam–Cambodia border [Hung et al., 2012], changes in the lower boundary might have a notable contribution to water level changes in the VMD. Also, the flood hydrograph entering the Mekong Delta at Kratie showed some notable differences between 2000 and 2011. To separate

Table 2.2: Comparison of model performance for the flood event of 2011 between the pre- and post-updated versions. Values show the mean of all stations, resp. satellite images used for the model performance evaluation.

Objectives	Pre-updated version*		Post-updated version	
	NSE	*FAI*	*NSE*	*FAI*
Water level *(m)*	0.84		0.90	
Discharge m^3s^{-1}	0.63		0.79	
Inundation (flood area index *FAI*)		0.46		0.64

** from Manh et al. [2014]*

Table 2.3: Scenarios used to separate the impacts of high-dyke development, and changes in upstream and lower boundary conditions to the alteration of inundation dynamics in the VMD. Scenarios 1 and 3 are the baseline scenarios.

Scenario name	Upper boundaries	Dyke development	Downstream boundaries
S1:u00-nHD-d00	2000	no high-dyke	2000
S2:u00-yHD-d00	2000	with high-dyke	2000
S3:u11-yHD-d11	2011	with high-dyke	2011
S4:u11-nHD-d11	2011	no high-dyke	2011
S5:u11-nHD-d00	2011	no high-dyke	2000
S6:u00-yHD-d11	2000	with high-dyke	2011
S7:u00-nHD-d11	2000	no high-dyke	2011
S8:u11-yHD-d00	2011	with high-dyke	2000
S2 – S1	impacts of high-dyke development (setup1–flood event 2000)		
S3 – S4	impacts of high-dyke development (setup2–flood event 2011)		
S5 – S1	impacts of upper boundaries (setup1–flood event 2000)		
S3 – S6	impacts of upper boundaries (setup2–flood event 2011)		
S7 – S1	impacts of lower boundaries (setup1–flood event 2000)		
S3 – S8	impacts of lower boundaries (setup2–flood event 2011)		

the contributions of the three drivers, i.e. changes in the upper boundary, in the lower boundary, and in the dyke system, on the flood dynamics in the VMD, the study design shown in Table 2.3 was developed. For each driver, the flood dynamics, i.e. inundation extent, depth and timing, were simulated for two virtual scenarios and compared to the historical situation (called the baseline scenario), i.e. the floods in 2000 and 2011. For example, to separate the impact of the dyke development, the dyke situation in 2000 (mainly low dykes) and in 2011 (many high-dyke areas in An Giang and Dong Thap) were interchanged, whereas the other two drivers were taken from the historical situation. In other words, we simulated how the flood in 2000 would have propagated, if the high-dyke system of 2011 was already in place, and how the flood in 2011 would have propagated, if the dyke system of 2000 was still be in place. The same procedure was applied for the other two drivers.

2.3 Results and discussion

2.3.1 Long-term flood trends and uncertainty analysis

A summary of the trend analysis of the five selected stations for the period 1978-2015 is presented in Figure 2.5. Figure 2.5a presents the results for $AMWL$ (annual maximum water level), while Figure 2.5b shows the results for FV (annual flood volume) at Kratie and DOT (flow duration over threshold) at the other locations. Our findings reveal highly

significant upward trends in both flood peak and flood duration downstream of high-dyke areas, i.e. in Can Tho and My Thuan. However, negative trends are detected at upstream locations, but at lower significance levels. The slopes of the downward trends in $AMWL$ at the upstream stations Chau Doc and Tan Chau are larger than the upward trends at Can Tho and My Thuan. For DOT the upward and downward trend slopes are in the range of 1.0–1.5 $day\ year^{-1}$. The results of the uncertainty analysis presented in Table 2.4 indicate that the upward trends at the downstream stations Can Tho and My Thuan are robust against data errors, as similar flood trends are detected at these stations for all assumed error magnitudes with high significance (p value; hereafter termed as $p \leq 0.001$). For $AMWL$, the median slope and even the minimum and maximum detected slopes remain similar to those of the original data set. Interestingly, the increasing detected slopes on DOT at these two stations are even higher than those of the original data. The downward trends at the upstream stations are, however, not robust against data errors, as indicated by the range of slopes, the MK test statistic and the low to non-existent overall significance in Table 2.4. In the following, the results of the trend analysis are discussed in detail for the different regions of the MD from upstream to downstream.

Trends of floods entering the Mekong Delta

The station Kratie on the Mekong mainstream represents the characteristics of the floods entering the MD. For Kratie, positive trends are obtained for $AMWL$ and negative trends for FV. However, these trends are very small, not statistically significant and not robust against data errors. The positive trend of $AMWL$, although not statistically significant, is in line with Delgado et al. [2010], who investigated the flood variability for the Mekong and found, through non-stationary extreme value statistics, increasing probabilities for annual maximum discharges exceeding the 2-year flood at Kratie after 1975. Prior to 1975 the trends were, however, decreasing. Using the MK test on annual maximum discharge from 1924 to 2007, they reported an overall negative trend. Because discharge is calculated from water level data using a rating curve, performing the MK test on either discharge or water level should yield similar results. The difference between our study and Delgado et al. [2010] can be explained by the different time periods used. The small increasing trend detected for 1978-2015 is cancelled out in the longer time series (1924-2004) by the declining trends prior to 1975.

Trends of flood entering the Vietnamese Mekong Delta

The stations Tan Chau and Chau Doc, where the Mekong and Bassac rivers enter the VMD, are located just upstream of the high-dyke areas. These stations exhibit decreasing trends in both $AMWL$ and DOT ($p > 0.1$ to $p \leq 0.05$). $AMWL$ at Tan Chau and Chau

Table 2.4: Uncertainty analysis of detected trends obtained from Mann-Kendall's test and Sen's slope to evaluate the trend robustness against data error (Cv denotes the Coefficient of Variation)

Station	test parameter	Error scale	Mann-Kendall test statistic Z value				Significance level of 1000 disturbed time-series*						Sen's slope estimation			
			2.5% quantile	*97.5% quantile*	*median*	*Cv*	*no trend*	*p > 0.1*	*p ≤ 0.1*	*p ≤ 0.05*	*p ≤ 0.01*	*p ≤ 0.001*	*2.5% quantile*	*97.5% quantile*	*median*	*Cv*
Kratie	AMWL	± 5 cm	-0.03	0.18	0.08	0.71	129	871					-0.6	3.4	1.3	0.77
		± 10 cm	-0.03	0.23	0.08	0.95	118	882					-1.0	5.4	2.2	0.74
		± 20 cm	-0.13	0.35	0.10	1.22	107	893					-2.6	7.4	2.3	1.11
	AFV	± 1 %	-0.45	-0.23	-0.33	0.19		1000					-0.6	-0.3	-0.4	0.14
		± 3 %	-0.68	-0.18	-0.43	0.30		1000					-0.7	-0.2	-0.5	0.26
		± 6 %	-0.93	-0.08	-0.50	0.43	8	992					-0.9	-0.1	-0.5	0.41
Tan Chau	AMWL	± 5 cm	-2.11	-1.73	-1.94	0.05		3	565	432			-18.4	-15.2	-16.8	0.05
		± 10 cm	-2.19	-1.56	-1.89	0.08		68	574	358			-19.2	-14.2	-16.9	0.07
		± 20 cm	-2.34	-1.38	-1.84	0.14		214	444	342			-21.2	-12.8	-16.9	0.13
	DOT	± 5 cm	-2.58	-2.36	-2.48	0.02				961	39		-2.6	-2.4	-2.5	0.02
		± 10 cm	-2.54	-2.26	-2.40	0.03				993	7		-2.5	-2.3	-2.4	0.03
		± 20 cm	-2.51	-2.20	-2.36	0.03				995	5		-2.5	-2.2	-2.4	0.03
Chau Doc	AMWL	± 5 cm	-1.73	-1.41	-1.58	0.05		816	184				-16.4	-13.4	-15.0	0.05
		± 10 cm	-1.81	-1.31	-1.58	0.08		721	287	1			-17.4	-12.5	-14.9	0.09
		± 20 cm	-1.91	-1.11	-1.52	0.14		707	272	21			-19.2	-10.8	-14.9	0.14
	DOT	± 5 cm	-1.65	-1.43	-1.53	0.03		971	29				-1.6	-1.4	-1.5	0.03
		± 10 cm	-1.65	-1.38	-1.52	0.04		963	37				-1.6	-1.4	-1.5	0.04
		± 20 cm	-1.62	-1.27	-1.46	0.06		984	16				-1.6	-1.3	-1.5	0.06
Can Tho	AMWL	± 5 cm	5.18	6.03	5.61	0.04						1000	11.9	13.8	12.8	0.04
		± 10 cm	4.73	6.06	5.36	0.06						1000	10.9	14.7	12.9	0.08
		± 20 cm	3.49	5.48	4.50	0.11					11	989	9.2	16.4	12.8	0.15
	DOT	± 5 cm	4.84	5.32	5.09	0.02						1000	4.8	5.3	5.1	0.02
		± 10 cm	4.76	5.42	5.09	0.03						1000	4.8	5.4	5.1	0.03
		± 20 cm	4.74	5.71	5.23	0.05						1000	4.7	5.7	5.2	0.05
My Thuan	AMWL	± 5 cm	4.45	5.56	5.03	0.05						1000	8.0	10.2	9.1	0.06
		± 10 cm	3.87	5.41	4.63	0.09					1	999	7.3	11.2	9.1	0.11
		± 20 cm	2.21	4.78	3.58	0.18			5	52	271	672	5.4	12.8	9.2	0.20
	DOT	± 5 cm	4.20	4.71	4.46	0.03						1000	4.2	4.7	4.5	0.03
		± 10 cm	4.04	4.75	4.39	0.04						1000	4.0	4.8	4.4	0.04
		± 20 cm	3.68	4.66	4.17	0.06						1000	3.7	4.7	4.2	0.06

** number of cases when detected trend is significant at certain level within 1000 disturbed time series*

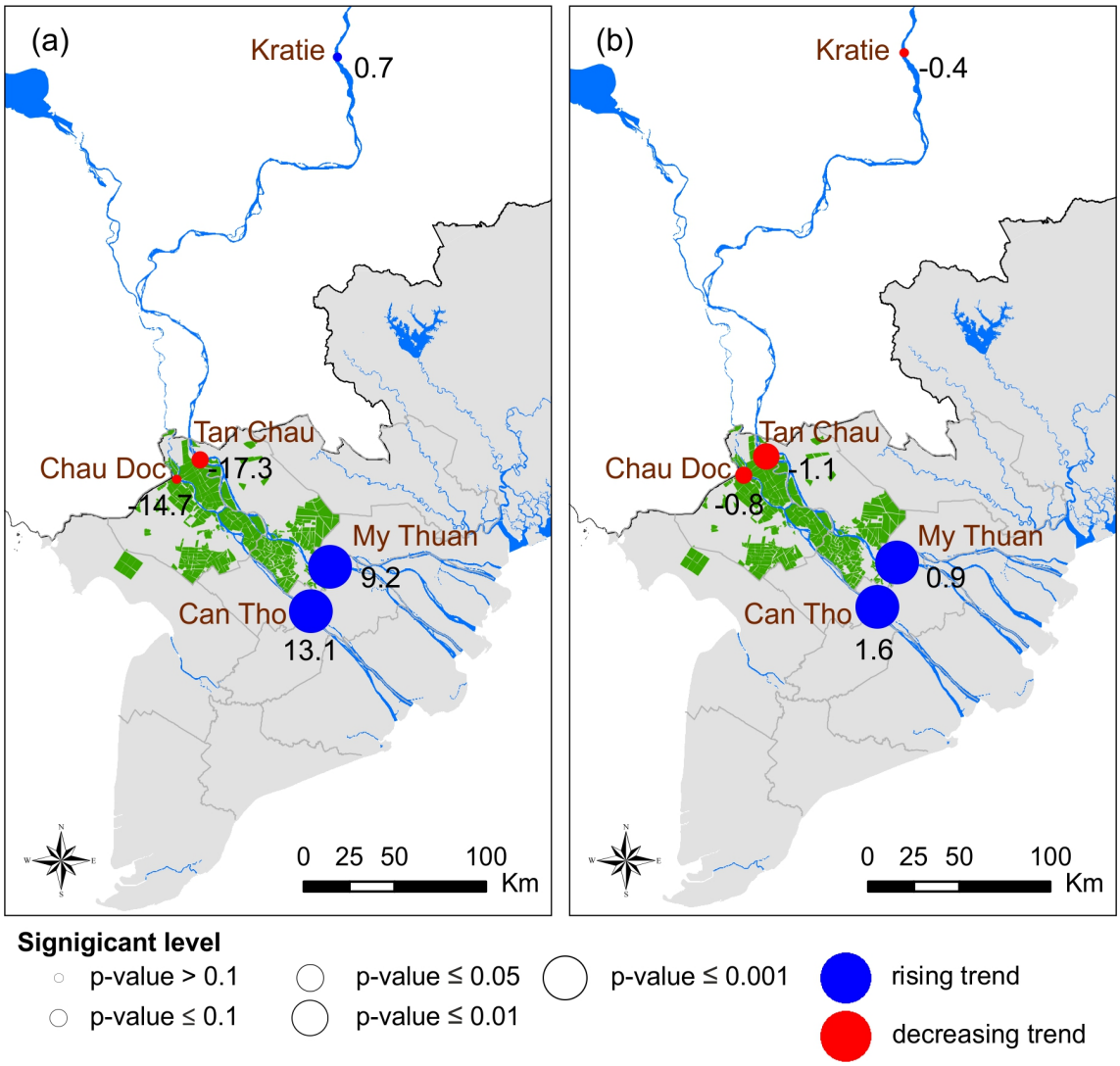

Figure 2.5: Flood trends at key locations during the study period 1978-2015. (a) Trend of annual maximum water level, slope presented in mm year^{-1}. (b) Trend of duration of peak over threshold and annual flood volume, slope presented in day year^{-1} (DOT) and in km^3 year^{-1} (flood volume). Blue circles indicate rising trends and red circles imply decreasing trends. Circle size is proportional to significance level. The numbers present estimated slope. High-dyke areas are marked in green.

Doc decreases by 17 *mm year*$^{-1}$ ($p \leq 0.1$) and 15 *mm year*$^{-1}$ ($p > 0.1$), respectively. Interestingly, Fujihara et al. [2016] found increasing, non-significant trends of 40.5–45.6 *mm year*$^{-1}$ ($p > 0.1$) for the period 1987-2006 for these stations. This mismatch between our study and Fujihara et al. [2016] can be explained by the different time periods, as trend tests can be very sensitive to the selection of the time period [e.g. Hall et al., 2014], particularly at these low significance levels. This is also expressed by our test for robustness, where the assumed data errors can change the significance of the trends even for an assumed error of ±5 *cm* only (Table 2.4). A pronounced downward trend in *DOT* is obtained at Tan Chau, with an estimated slope of –1.0 *day year*$^{-1}$ ($p \leq 0.05$). This trend is rather robust, even when data errors of ±20 *cm* are added. Over 96% of the 1000 disturbed time series indicate a negative slope at $p \leq 0.05$, and the coefficient of variation

is less than 5%. A similar trend is obtained at Chau Doc, although smaller and less robust against errors (slope: –1.0 $day\ year^{-1}$, $p > 0.1$). In summary, there are weak negative trends in terms of flood peak and duration at the entrance of the VMD during the study period 1978-2015, of which the trends in DOT are more pronounced and robust. This result is comparable with the findings in Dang et al. [2016], who showed decreasing but non-significant trends of annual mean water levels for Tan Chau and Chau Doc.

Trends downstream of high-dyke development areas

Contrary to the three upstream locations, the two stations downstream of high-dyke areas, i.e. Can Tho and My Thuan, show significant upward trends in both $AMWL$ and DOT. $AMWL$ increases by 13.1 and 9.2 $mm\ year^{-1}$ ($p \leq 0.001$) at Can Tho and My Thuan, respectively. This is similar to the findings of Fujihara et al. [2016]. Dang et al. [2016] analysed annual mean water levels and detected a significant upward trend at Can Tho, but no trend in My Thuan (Fig. 2.6). This, at first sight, contradictory result can be explained by the different relation between annual maximum and mean water levels at the two stations. There is a strong correlation between maximum and mean water levels for Can Tho ($r = 0.84$), but only a weak correlation is seen for My Thuan (Fig. 2.6). The MK test for DOT indicates upward trends at $p \leq 0.001$, whereas the slope varies from 0.9 $day\ year^{-1}$ at My Thuan (Mekong River) to 1.6 $day\ year^{-1}$ at Can Tho (Bassac River). Both trends in $AMWL$ and DOT are exceptionally robust. Only for an error level of 20 cm does the significance at My Thuan drop (i.e. 27% of the disturbed time series at $p \leq 0.01$ and 67% at $p \leq 0.001$), while the trend at Can Tho remains highly significant (99% at $p \leq 0.001$) as given in Table 2.4. These results support public claims of higher and longer floods at Can Tho in the past decade. The opposite direction of the trends at Can Tho and My Thuan compared to those at Tan Chau and Chau Doc supports the hypothesis that high-dyke construction in the upper part of the VMD has altered the flood hazard downstream.

2.3.2 Step-change analysis and uncertainty analysis

Figure 2.7 presents the results of the step-change analysis for the four main gauges in the VMD. We did not apply the Pettitt test for station Kratie, since flood changes in Kratie were negligible during the study period. The detected change points for both $AMWL$ and DOT differ between upstream and downstream stations. The test identified step changes in 2005/2006 at the upstream stations Tan Chau and Chau Doc and in 2000/2001 at the stations Can Tho and My Thuan downstream of the high-dyke areas.

$AMWL$s at the upstream stations Tan Chau and Chau Doc decrease by roughly 10%

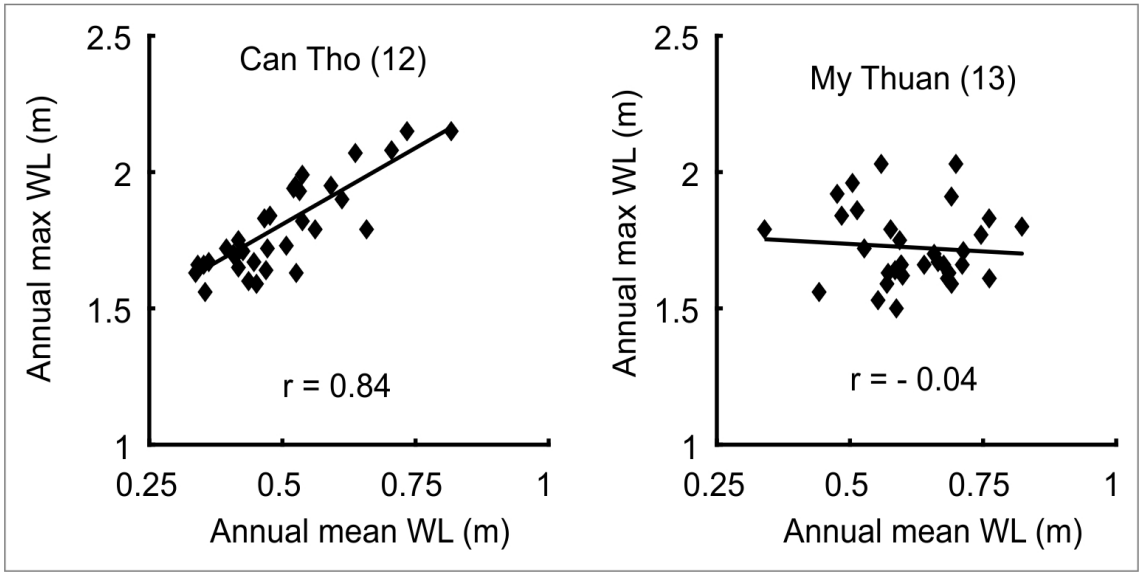

Figure 2.6: Strong correlation between annual maximum and mean water level at Can Tho, but no correlation at My Thuan; data from 1978 to 2015. The numbers next to the station names refer to the numbers in Fig. 2.1.

but are not significant (both $p > 0.1$). The test on DOT also identifies a change point in 2005 for both stations, where the mean DOT decreases over 50%, but again with low significance (Tan Chau: $p = 0.14$; Chau Doc: $p = 0.12$). Arguably, this low significance can be attributed to the limited number of data points after the change point (10 data points). The test for robustness indicates that the detected step changes are not robust against data errors, particularly for $AMWL$, as indicated by the markers in Figure 2.7. Even assuming a small error of at most 5 cm, the timing of the step change can vary by about 20 years.

In contrast, the detected step changes in both $AMWL$ and DOT for the downstream stations Can Tho and My Thuan are highly significant and robust. They amount to an increase in $AMWL$ of 17% at Can Tho and 12.5% at My Thuan (both $p \leq 0.001$). DOT is even 3 times longer in the post-2000 period compared to the pre-2000 period ($p \leq 0.001$). The test for robustness indicates that the step change of DOT is almost always detected in the year 2000, even for an assumed error of up to 20 cm. For $AMWL$ the assumed errors can cause slight shifts of the detected step change in 2000, but the distribution of the MC-detected step changes is almost normally distributed around the median of 2000 (Fig. 2.7).

Dang et al. [2016] also reported a reduction of 21 and 14% ($p > 0.05$) in the annual mean water level at Tan Chau and Chau Doc, while for Can Tho they found that the water level increased by 27% ($p \leq 0.05$) between the pre- and post-2007 periods. However, we have to note the differences in the study designs. Dang et al. [2016] used the annual mean water level and set the year 2007 as a separation year based on the analysis of satellite images of inundation extents. Our study, in contrast, analyses flood indicators and derives the

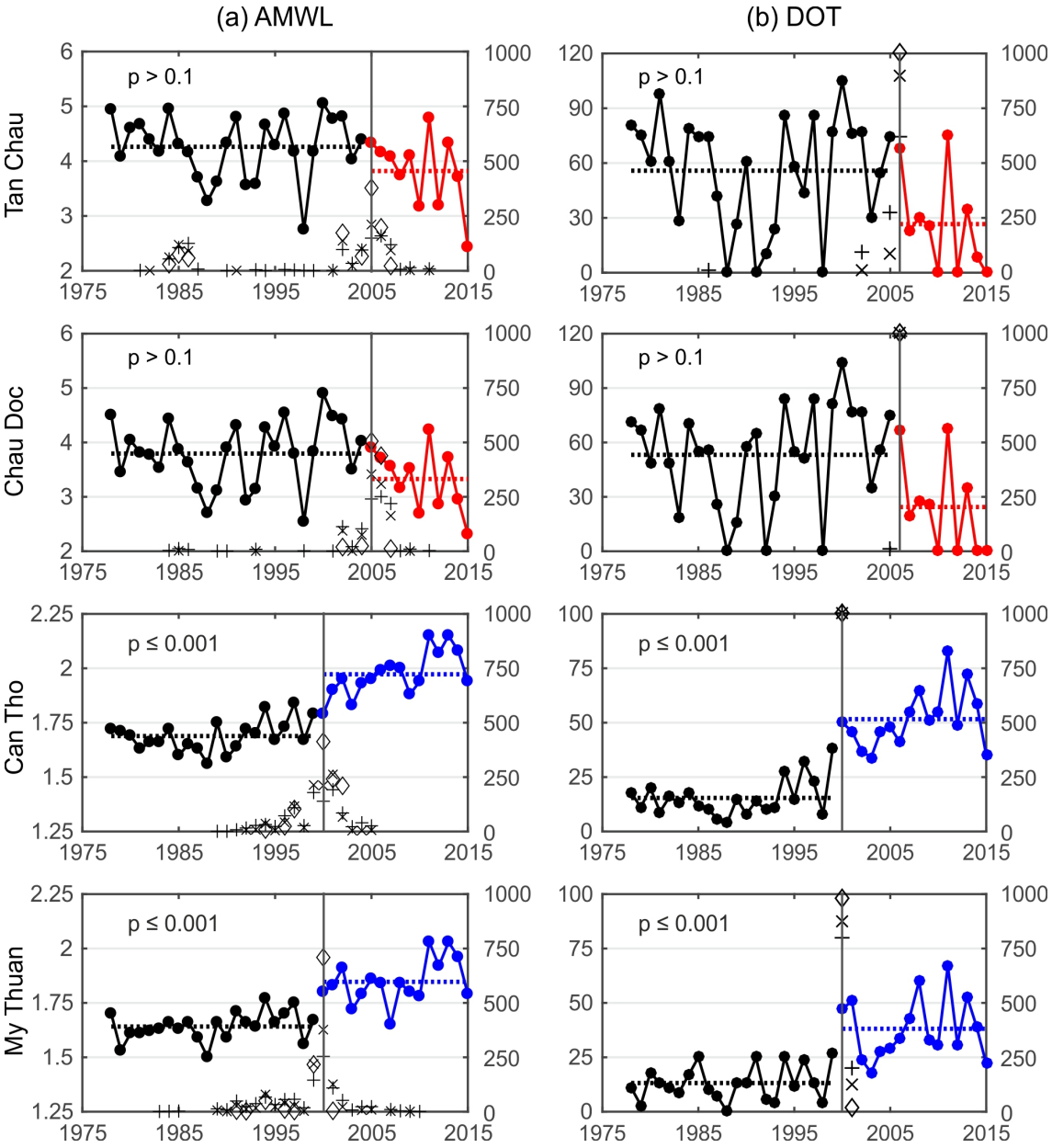

Figure 2.7: Step-change analysis including the uncertainty analysis at four stations in the VMD. Panel (a) presents results for annual maximum water level (in metres) and (b) for flood duration over thresholds (in days). Data before the change point are presented in black. The second period is presented in red for negative step change and in blue for a positive change. Dashed lines are mean values of partial datasets. Results of the uncertainty analysis are presented using the second vertical axis on the right, as the number of times that a step change occurred in a certain year at three error levels (± 5 cm: diamond; ± 10 cm: cross; ± 15 cm: plus).

timing of step changes directly from the water level data. Hence, Dang et al. [2016] used the completion year of the majority of dyke systems, which were built during a number of years following the 2000 flood, whereas our approach rather detects the year where the construction starts to have its largest impact on the flood indicators. Thus, it is likely that the different timing of the step changes refers to the same cause.

The facts that, at both downstream stations, step changes with identical timing are detected, that this timing corresponds to the start of the high-dyke construction in the upstream provinces An Giang and Dong Thap, and that these step changes are not detectable upstream of the high-dyke areas suggest adverse impacts of upstream dyke development on downstream inundation dynamics. This suggestion is further analysed in the following sections presenting the hydraulic modelling results.

2.3.3 Impact of high-dyke development derived from hydraulic modelling

In the following the results of the hydrodynamic model for the two model setups, i.e. with and without high-dyke systems in An Giang and Dong Thap, are presented. Differences in inundation areas, depths and duration between the two model setups are given in Figure. 2.8, 2.9 and Table 2.5 for the two floods 2000 and 2011. Table A2 summarizes the impact on inundation area for the nine flood-prone provinces in the VMD.

A first observation is that the high-dyke development leads to almost identical impacts for the two floods (e.g. compare the upper and lower panel of Fig. 2.8). The maximum difference in terms of impact on inundation depth is 3.4 *cm* (station Tan Hiep, Table 2.5), whereas the differences in terms of impact on inundation duration are at most 1 day between the two floods. Although this similarity does not prove that the dyke system development has the same effect for other large flood events, it strongly suggests that the effect of dyke development is similar for large floods.

The results reveal that the high-dyke development increases inundation depth and duration at many locations in the VMD. The impacts are not only found downstream of the high-dyke areas, e.g. at Can Tho or My Thuan, but can also be seen upstream of high-dyke areas, e.g. at Chau Doc or Tan Chau. This is a consequence of losing flood retention capacity in those areas protected by high dykes and consequently backwater effects due to changes in in-channel flow. The impact varies from location to location (Table 2.5). It is rather minor for the two important floodplains in the VMD, i.e. POR and LXQ. An increase in maximum depth of $\sim$5 *cm* and a change in inundated area of less than 2% is found for the provinces Long An (POR) and Kien Giang (LXQ), which are located farthest from the main rivers Table A2. A significant reduction in inundation area of 32 and 19 % is quantified for the provinces at An Giang and Dong Thap, respectively. The increase in $AMWL$ of 5–6 *cm* at the two stations in these provinces (Chau Doc, Tan Chau) is far less than the negative slope detected (15–17 $mm\ year^{-1}$ at these locations (Sect. 2.3.1). This indicates that only a part of the detected weak downward trends at these locations could be explained by the construction of the high-dyke system.

Table 2.5: Contribution of each of the three factors, i.e. upstream boundary, high-dyke construction and lower boundary, to the alteration of maximum water level (in cm) and duration over threshold (in days) at key gauge stations in the VMD.

Station code	Gauge station[1]	Change in maximum water level									Change in duration over threshold [2]								
		upstream boundary			high-dyke development			downstream boundary			upstream boundary			high-dyke development			downstream boundary		
		S5-S1[3]	S3-S6	mean	S2-S1	S3-S4	mean	S7-S1	S3-S8	mean	S5-S1	S3-S6	mean	S2-S1	S3-S4	mean	S7-S1	S3-S8	mean
8	Chau Doc	-27.6	-24.8	-26.0	5.0	4.2	4.6	-0.3	2.9	1.3	-18.0	-16.0	-17.0	0.0	0.0	0.0	0.0	2.0	1.0
7	Tan Chau	-28.9	-26.0	-28.0	6.0	4.9	5.5	-1.0	1.9	0.5	-19.0	-18.0	-19.0	1.0	0.0	1.0	0.0	1.0	1.0
9	Vam Nao	-18.4	-23.4	-21.0	6.9	6.9	6.9	5.0	1.0	3.0									
10	Long Xuyen	-8.2	-8.7	-8.5	10.1	12.1	11.1	13.0	12.8	12.9									
11	Cao Lanh	-0.5	-5.4	-2.9	12.1	11.1	11.6	13.9	9.1	11.5									
12	Can Tho	10.2	4.0	7.1	13.5	11.9	12.7	35.7	29.8	32.8	12.0	-5.0	4.0	18.0	18.0	18.0	38.0	21.0	30.0
13	My Thuan	12.8	3.5	8.1	8.1	9.0	8.5	23.7	14.1	18.9	13.0	-4.0	5.0	13.0	12.0	13.0	24.0	6.0	15.0
16	Moc Hoa	-31.8	-31.1	-32.0	5.3	5.0	5.1	0.7	2.2	1.5									
14	Hung Thanh	-24.5	-25.2	-25.0	4.0	3.5	3.7	1.6	0.8	1.2									
15	Kien Binh	-17.2	-12.4	-15.0	5.0	4.8	4.9	1.1	6.0	3.6									
17	Xuan To	-27.6	-24.8	-26.0	4.3	3.3	3.8	-0.6	3.3	1.3									
18	Tri Ton	-15.5	-18.4	-17.0	7.3	6.0	6.7	2.7	0.7	1.7									
19	Tan Hiep	-5.7	-1.1	-3.4	5.9	2.5	4.2	2.7	9.0	5.9									
20	Vi Thanh	-15.8	-11.1	-14.0	3.1	3.6	3.4	20.0	24.4	22.2									

[1] Gauge stations are listed from upstream to downstream and from small to large distance from main rivers, station locations are given in Fig. 2.1 and Table 2.1.

[2] Calculated for 4 stations where trend tests were performed.

[3] S5 – S1: (u11nHDd00) - (u00nHDd00); S3 – S6: (u11yHDd11) - (u00yHDd11);
S2 – S1: (u00yHDd00) - (u00nHDd00); S3 – S4: (u11yHDd11) - (u11nHDd11);
S7 – S1: (u00nHDd11) - (u00nHDd00); S3 – S8: (u11yHDd11) - (u11yHDd00).

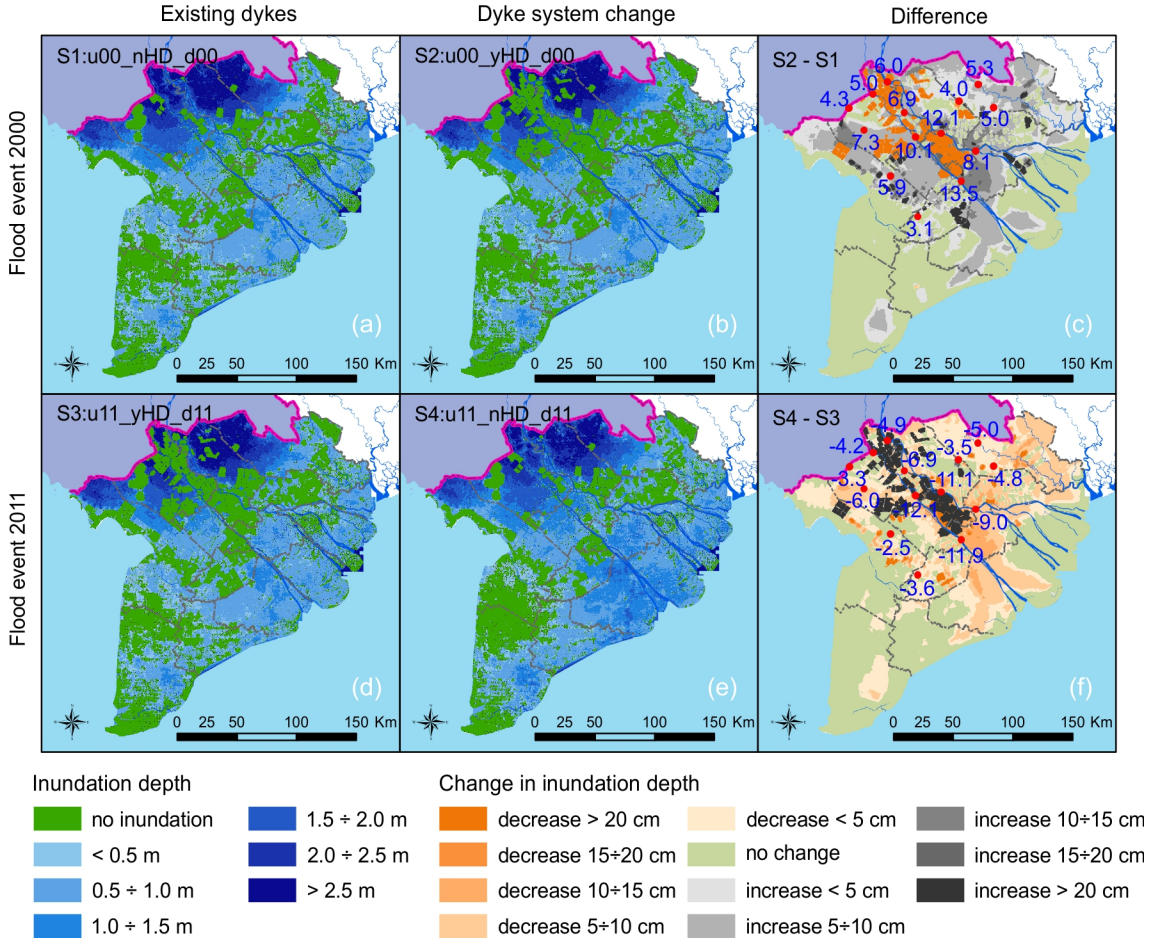

Figure 2.8: Impacts of upstream high-dyke development on downstream inundation area and depth for the flood event 2000 (a, b, c) and the flood 2011 (d, e, f). (a, d) Dykes as existing in the respective year. (b, e) Dyke system interchanged between the two years. (c, f) Difference between the two dyke scenarios.

High-dyke construction is found to have a notable impact on water levels along the Mekong and Bassac rivers downstream of the Vam Nao River connecting both rivers. Along the Mekong River, the impact ranges from 12 *cm* at station Cao Lanh to 8 *cm* at station My Thuan (Table 2.5). Along the Bassac River, the impact increases from station Vam Nao (7 *cm*) to Long Xuyen to Can Tho (12 *cm*). Downstream of stations Can Tho and My Thuan, the impacts are smaller, in the range of 3–7 *cm*.

Our results indicate that high-dyke development increases the duration of water levels exceeding alarm level 1 by 17 *days* at Can Tho and 13 *days* at My Thuan (Table 2.5). This is expected to exacerbate urban flooding in Can Tho with its very low topography and poor drainage system as reported in Apel et al. [2016] and Huong and Pathirana [2013]. In Can Tho the total inundation area is not affected by the high-dyke construction; however, 6% of the city area is converted from shallow inundation with depths below 1.5 *m* to deep inundation above 1.5 *m* (Table A2). The Vinh Long province, which is located between the Mekong and Bassac rivers directly downstream of Can Tho and My Thuan, experiences large changes in inundation extent. Over 12% of the total area of the province is altered

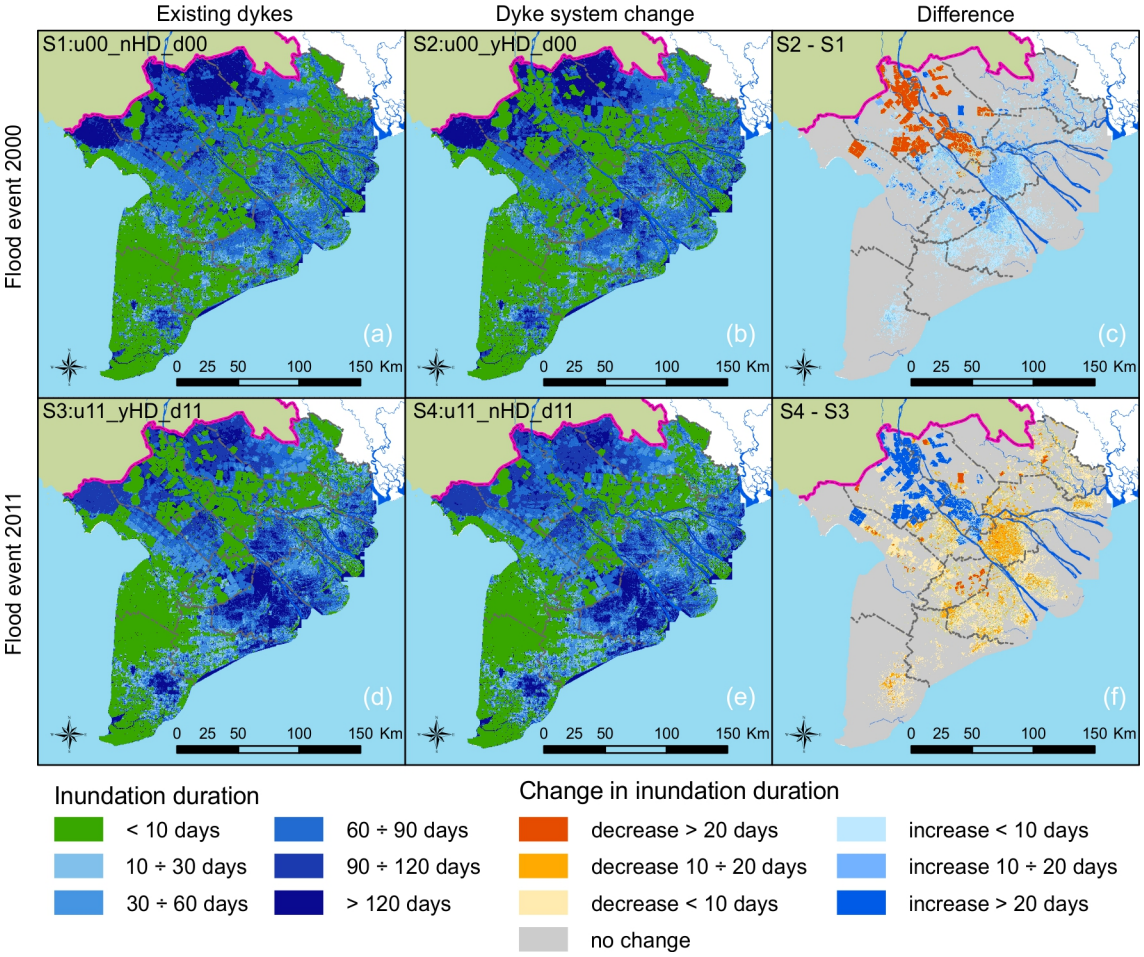

Figure 2.9: Impacts of upstream high-dyke development on downstream inundation duration for the flood event 2000 (a, b, c) and the flood 2011 (d, e, f). (a, d) Dykes as existing in the respective year. (b, e) Dyke system interchanged between the two years. (c, f) Difference between the two dyke scenarios.

from no/shallow inundation to deep inundation due to high-dyke development.

Notably, the impact on $AMWL$ and DOT at the stations Can Tho and My Thuan is almost identical to the range estimated from the trend analysis. Applying the obtained trend slopes to the interval 2000–2011 yields an increase of 11–15 cm for $AMWL$ and 12–18 *days* for DOT. This agreement between the two independent methods enhances the credibility of the results.

2.3.4 Comparison of impacts driven by changes in the upper and lower boundaries and in the dyke system

In this section the relative impact of the three factors (i) changes in the upper boundary, (ii) high-dyke construction, and (iii) changes of the lower boundary is evaluated by interchanging the upper boundary, the dyke system and the lower boundary of the model simulation for the reference years 2000 and 2011. The scenario set is given in Table 2.3

and the results are summarized in Table 2.5. The contributions of the three factors are compared to the baseline difference, which is defined as the difference in maximum water level of 2011 (scenario S3) and 2000 (scenario S1). The contributions were calculated as the mean of the two scenarios for each factor. The relative contributions are presented in Table 2.6 and Figure 2.10. Table 2.6 reveals that for most stations the maximum water levels and the duration over threshold levels decrease when as upper boundary the flood hydrograph of 2000 is replaced with the lower volume flood of 2011.

Interestingly, this is not the case for Can Tho and My Thuan. These stations are located in areas where the magnitude of both river discharge and tidal water levels is important for $AMWL$ and DOT during the annual flood events. Moreover, not only the magnitude but also the temporal coincidence of maximum floodwater levels and the spring tides is highly relevant. During the flood in 2000, the flood peak in Tan Chau and Chau Doc occurred on 23 September, coinciding with a neap tide period. However, the peak in 2011 occurred during the first week of October, coinciding with a spring tide period. When the upper boundaries are interchanged, this timing is reversed: the peak flood levels of 2000 coincide with the neap tide in 2011, while the peaks of 2011 are combined with high tidal levels in 2000. This means that for the flood event of 2011 with the upper boundary of 2000, lower $AMWL$s for Can Tho and My Thuan are simulated, although the peak discharge of the flood hydrograph of 2000 was lower than 2011. Analogously for the flood in 2000, with the upper boundary of 2011, higher $AMWL$s are simulated due to the temporal coincidence of high floodwater and spring tide condition. This effect causes positive differences in

Table 2.6: Contribution of each factor to the alteration of water level between the floods 2000 and 2011 for key gauge stations in the VMD. The stations are listed from upstream to downstream and from small to large distance to the main rivers to remote. Station numbers refer to Fig. 2.1.

Gauge station	Baseline (S3-S1) *(cm)*	Upper bound. *(cm)*	High-dyke *(cm)*	Lower bound. *(cm)*	Summed changes *(cm)*	Upper bound.	High-dyke	Lower bound.	Summed changes
						(in % of baseline)			
Chau Doc[8]	-19.6	-26.2	4.6	1.3	-20.3	-133.7	23.5	6.6	103.6
Tan Chau[7]	-20.6	-27.5	5.5	0.5	-21.5	-133.5	26.7	2.4	104.4
Vam Nao[9]	-10.4	-20.9	6.9	3.0	-11.0	-201.0	66.3	28.8	105.8
Long Xuyen[10]	17.1	-8.5	11.1	12.9	15.5	-49.7	64.9	75.4	90.6
Cao Lanh[11]	14.1	-2.9	11.6	11.5	20.2	-20.6	82.3	81.6	143.3
Can Tho[12]	40.1	7.1	12.7	32.8	52.6	17.7	31.7	81.8	131.2
My Thuan[13]	28.0	8.1	8.5	18.9	35.5	28.9	30.4	67.5	126.8
Moc Hoa[16]	-25.1	-31.5	5.1	1.5	-24.9	-125.5	20.3	6.0	99.2
Hung Thanh[14]	-19.7	-24.9	3.7	1.2	-20.0	-126.4	18.8	6.1	101.5
Kien Binh[15]	-7.8	-14.8	4.9	3.6	-6.3	-189.7	62.8	46.2	80.8
Xuan To[17]	-20.5	-26.2	3.8	1.3	-21.1	-127.8	18.5	6.3	102.9
Tri Ton[18]	-7.1	-17.0	6.7	1.7	-8.6	-239.4	94.4	23.9	121.1
Tan Hiep[19]	11.6	-3.4	4.2	5.9	6.7	-29.3	36.2	50.9	57.8
Vi Thanh[20]	16.2	-13.5	3.4	22.2	12.1	-83.3	21.0	137.0	74.7

AMWL for these two locations, when the upper boundaries are interchanged. This effect also explains the comparatively large positive differences listed in Table 2.5 at these two stations when the lower boundaries are interchanged. For the *DOT* this effect is also observable for the scenario S5–S1, but for the analogous scenario the long period of high water levels in 2000 causes higher *DOT*, even if the period of high water levels does not coincide with the spring tide period.

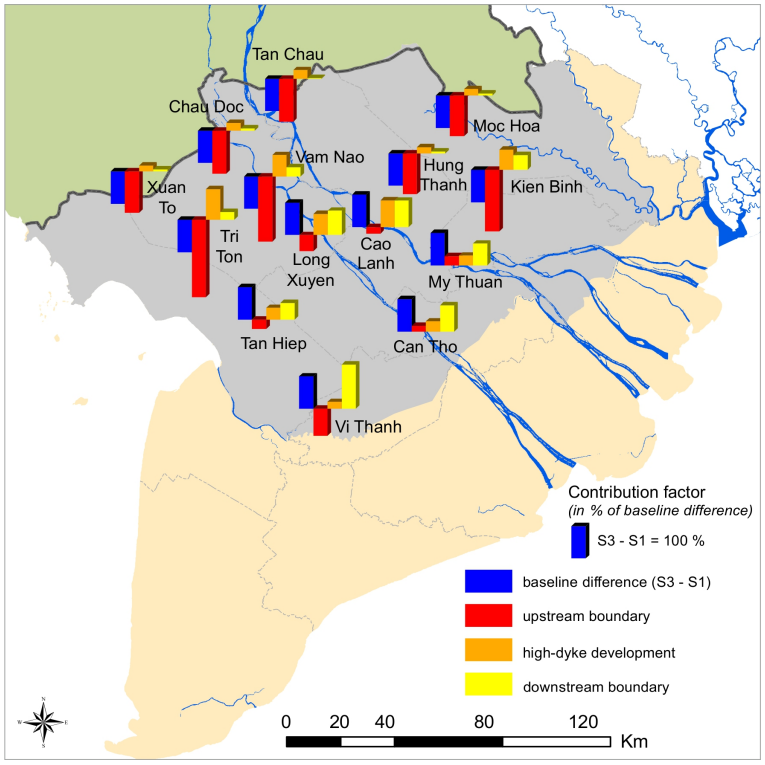

Figure 2.10: Contribution of each factor to the alteration of water levels between the floods 2000 and 2011 for key gauge stations in the VMD. The difference between the two scenarios S3 and S1 is considered to be 100%.

A comparison of the changes in *AMWL* and *DOT* in Table 2.5 reveals a spatial pattern: the upstream boundary has the largest impact on the stations located north of Long Xuyen and Cao Lanh, and at stations with larger distances from the main rivers. In these areas the tidal amplitude is attenuated due to the large distance from the sea and/or the length of the channel network. The situation at the stations downstream of the high-dyke areas and along the main rivers (stations Long Xuyen, Cao Lanh, Can Tho, My Thuan) is more complex. Here the changes caused by the different factors have similar magnitudes, whereas the tidal influence increases in downstream direction. Hence, the factors can partly compensate for each other, and an attribution of observed changes to individual factors requires a careful inspection.

Table 2.6 and Fig. 2.10 present the contributions of the three factors in relation to the observed differences between the floods in 2000 and 2011. Apparently, the sum of the single

contributions does not equal the observed differences. This is a consequence of non-linear interactions, including, for example, the problem of timing between flood peaks and tidal characteristics. The magnitude of the discrepancy varies widely between the stations from a close match to almost 50%. Most of the stations with small discrepancies are located farthest north and farthest away from the main rivers. For those stations the upstream boundary causes changes of 120–130% of the baseline difference. Dyke construction and, to a lesser extent, the change in the lower boundary counteract these changes.

Downstream of Vam Nao the contribution of the upper boundary diminishes to only 20–50% of the baseline difference. In this region the other two factors have higher importance, but the relative contribution changes from station to station. With respect to the motivation of the study, i.e. the quantification of the impact of high-dyke construction on floodwater levels, this region is the most affected by the high-dyke development. This factor amounts to 65–80% of the baseline difference. Further downstream, i.e. at Can Tho and My Thuan, the lower boundary becomes the prevailing factor, amounting to more than 80% of the baseline difference. The water level changes caused by the high-dyke system is reduced to about 30%.

These findings disagree with public and several officials' claims that the high-dyke development in the upper part of the MD is the main factor for the higher and longer floods in Can Tho and the central part of the Mekong Delta. For this region it is rather the combination of all three factors, with the lower boundary, or the timing of high flood levels and tidal levels that is dominating. The further downstream the station location, the higher the impact of the tidal water level. Hence, sea level rise and land subsidence are important factors for future inundation dynamics in the central and coastal areas of the VMD. These findings are in line with Fujihara et al. [2016], who identified sea level rise and land subsidence as the main factors controlling alteration of minimum and maximum water levels in the middle part and coastal zones of the VMD.

2.4 Conclusions

The present study sheds light on the link between changes in flood dynamics in the VMD and high-dyke construction in the northern provinces An Giang and Dong Thap. The research was motivated by the recent discussions of the Vietnamese public, as well as by the media and officials regarding the role of the high-dyke development. These discussions were triggered by a flood in 2011, where higher flood levels occurred in the middle part of the VMD compared to the flood in 2000, which had a much larger flood volume and a longer duration of high water levels, but lower peak discharges. However, the widespread claim that high-dyke development is the sole cause of increased floodwater levels has not been investigated in detail. Particularly, the effects of the possible causes –different flood

hydrograph characteristics, high-dyke construction, and different tidal dynamics –have not been quantified to date.

In a first step we performed a trend analysis of indicators of flood severity, i.e. annual maximum water levels ($AMWLs$) and the duration of water levels above a warning threshold (DOT) for the period 1978-2015. Negative trends of low significance were found for the upper part of the delta (stations Chau Doc, Tan Chau). However, strongly increasing and highly significant trends were detected downstream of the areas with the large-scale high-dyke development. These trends were also highly robust against measurement errors. The Pettitt test revealed a step change at the stations downstream of the high-dyke areas around the year 2000, with high significance and robustness. The timing of the step change coincides with the initiation of the high-dyke development. This result differs from the step change identified by Dang et al. [2016] at the year 2006. However, this difference is a consequence of different methodologies; our statistical approach identified the start of the high-dyke construction period, while Dang et al. [2016] defined the end of the main construction period as step-change date. Thus, our analyses are in line with the widespread public claim about the adverse impacts of the high-dyke construction on downstream water levels. Our trend analyses also strengthen the conclusions of the earlier, less refined, studies of Fujihara et al. [2016] and Dang et al. [2016].

However, trend analyses do not allow for separating the contribution of high-dyke development from the other important factors, i.e. the severity of the flood entering the MD, and the tidal influence. This separation was achieved by running an up-to-date hydrodynamic flood model of the whole MD for a set of scenarios with interchanged boundaries and dyke system state. The model simulations indicated that, at Can Tho and My Thuan in the central VMD, an increase of 9–13 cm in maximum water level and of 15 $days$ in duration above the first official warning level can be attributed to the high-dyke development. However, this explains only about 30% of the observed differences between the floods in 2011 and 2000.

The hydraulic model scenarios also demonstrated the importance of the different boundary conditions and how this importance varies in space. In the northern part of the VMD the flood hydrograph entering the MD has the highest importance, while further downstream the tidal influence dominates. The simulations further revealed that not only the tidal level but also the timing of spring tides in relation to maximum floodwater level plays an important role for the flood hazard in the central and coastal VMD. For the central VMD (Can Tho and My Thuan) it was found that the most dominant factor was the tidal impact. The isolated tidal impact amounts to about 80 % of the observed differences between the floods in 2011 and 2000. The higher tidal level of 2011 and the coincidence of spring tide and high flood levels caused differences of about +19 and +32 cm at My Thuan and Can Tho, respectively, whereas the upper boundary caused an increase of 7–8

cm. Thus, the claims that the dyke development has altered the flood hazard in the areas downstream can be partially confirmed, but not the claim that it is the only cause. In fact, for the central VMD the lower boundary has a 2–3 times higher influence.

For the flood in 2011 the coincidence of a late flood peak in October with a spring tide period was the main cause for the exceptional flooding in My Thuan and particularly Can Tho. Hence, flood risk management plans should consider changes in the lower boundary and the timing of high flood flows and spring tides. A clear implication of our research is that higher flood levels than usual have to be expected in the central and coastal VMD if floodwater levels peak in October, which is the period of spring tides in the East Sea. This insight should be considered when flood warnings are issued.

Another important implication resulting from the link between inundation dynamics and lower boundary is that flood levels in the central and coastal VMD have to be expected to increase in the coming decades. Sea levels in the East Sea surrounding the MD rose by 3.1 $mm\ year^{-1}$ at My Thanh and 3.5 $mm\ year^{-1}$ at Vung Tau during 1985–2010 [Hak et al., 2016], and sea level rise is expected to continue [IPCC, 2014a]. To make the situation even more alarming, several cities in the VMD suffer from local subsidence due to overexploitation of groundwater, for instance, 20 $mm\ year^{-1}$ for Can Tho during 2006-2010 [Erban et al., 2014]. This development adds to the climate driven sea level rise and will cause even higher effective tidal water levels.

Against this background, it is worth noting that the high-dyke system has the potential to be harnessed for flood mitigation in the central VMD. Including the operation and flooding of the floodplains in Dong Thap and An Giang in flood management plans on a delta-wide organizational level would reduce the flood hazard in the central VMD by reusing the natural floodplain storage. This could be organized for individual flood events, if large floods, and particularly flood peaks in October, are forecasted. Another option would be a long-term plan for counteracting the effective sea level rise by partial flooding of the floodplains protected by high dykes on an (multi-)annual rotation basis. Such management options would require close cooperation and coordination between the provinces and districts, possibly overseen by national agencies. Additionally, compensation schemes would be required for farmers affected by emergency flooding of their fields where a summer crop has already been planted.

Finally, the updated quasi-2-D flood model performs better than the previous versions and proved to be a valuable tool for understanding and quantifying temporal changes in flood characteristics in this highly complex delta. The model can be used to investigate the impacts of hydropower dam development, climate change and water management, such as the very likely expansion of high-dyke areas in the VMD, on delta inundation.

Chapter 3 Flood damages and risks to paddy rice cropping in the Mekong Delta

Abstract

Flooding is an imminent natural hazard threatening most river deltas, e.g. the Mekong Delta. An appropriate flood management is thus required for a sustainable development of the often densely populated regions. Recently, the traditional event-based hazard control shifted towards a risk management approach in many regions, driven by intensive research leading to new legal regulation on flood management. However, a large-scale flood risk assessment does not exist for the Mekong Delta. Particularly, flood risk to paddy rice cultivation, the most important economic activity in the delta, has not been performed yet. Therefore, the present study was developed to provide the very first insight into delta-scale flood damages and risks to rice cultivation. The flood hazard was quantified by probabilistic flood hazard maps of the whole delta using a bivariate extreme value statistics, synthetic flood hydrographs, and a large-scale hydraulic model. The flood risk to paddy rice was then quantified considering cropping calendars, rice phenology, and harvest times based on a time series of enhanced vegetation index (EVI) derived from MODIS satellite data, and a published rice flood damage function. The proposed concept provided flood risk maps to paddy rice for the Mekong Delta in terms of expected annual damage. The presented concept can be used as a blueprint for regions facing similar problems due to its generic approach. Furthermore, the changes in flood risk to paddy rice caused by changes in land use currently under discussion in the Mekong Delta were estimated. Two land-use scenarios either intensifying or reducing rice cropping were considered, and the changes in risk were presented in spatially explicit flood risk maps. The basic risk maps could serve as guidance for the authorities to develop spatially explicit flood management and mitigation plans for the delta. The land-use change risk maps could further be used for adaptive risk management plans and as a basis for a cost–benefit of the discussed land-use change scenarios. Additionally, the damage and risks maps may support the recently initiated agricultural insurance programme in Vietnam.

Published as: Triet, N. V. K., Dung, N. V., Merz, B., and Apel, H.: Towards risk-based flood management in highly productive paddy rice cultivation - concept development and application to the Mekong Delta, Natural Hazards and Earth System Sciences, 18, 2859-2876, 10.5194/nhess-18-2859-2018, 2018.

3.1 Introduction

Characterized by low topography, the Mekong Delta (MD) is subjected to flooding caused by high river discharge, tidal backwater effects, and storm surges. Floods in the Mekong Delta are annual events, mainly triggered by the Asian monsoons, but also by tropical cyclones (typhoons). On the positive side, floods bring various benefits to the MD with an estimated annual value of USD 8–10 *billion* [MRC, 2012]. These benefits include provision of sediment to counter delta subsidence, increase in wild fish catch and enhancement of soil fertility through deposited sediment [Manh et al., 2014]. On the other hand, extreme floods can result in extensive damages as recorded during the floods in 2011 and 2000. For example, the 2000 flood, considered as a 50-year flood [Dung et al., 2015], resulted in over 450 fatalities and economic losses of USD 250 *million* [MRC, 2012]. Recent studies suggest that the frequency of such extreme events is likely to increase [Delgado et al., 2010, Hirabayashi et al., 2013]. For instance, the 100-year flood in the Mekong basin in the 20th century is projected to occur every 10–20 years in the 21st century due to impacts of climate change [Hirabayashi et al., 2013]. Therefore, assessing hazards and risks induced by extreme floods is a crucial task for developing flood management strategies and climate change adaptation measures.

Traditionally, flood management in the Vietnamese Mekong Delta (VMD) has focussed on engineering solutions aiming at flood control. Structural flood defence measures, such as sluice gates and dyke lines, were implemented across the whole delta. The water level of the flood in 2000 was commonly chosen as the design flood event. Flood risk assessments, taking into account not only flood probabilities and water levels, but also flood losses, were not undertaken to support flood management. Recently, non-structural measures (e.g. shifting of cropping calendar) have gained more interest. This alteration is in agreement with the global trend of moving from flood hazard control toward flood risk management [Merz et al., 2010]. By definition, risk assessment is the evaluation of the frequency and magnitude of floods, or flood hazard, and their consequences. Hence, damage assessment is an essential task for the transition from traditional hazard control to flood risk management.

The majority of the literature on flood hazard assessments for the VMD focusses on changes in delta inundation hazards driven by upstream infrastructure development (e.g. hydropower dams), local flood control (e.g. dyke systems), climate change impacts, and sea level rise by hydrodynamic modelling [Le et al., 2007, Van, 2009, Dinh et al., 2012, Van et al., 2012, Toan, 2014, Triet et al., 2017, Dang et al., 2018]. A comprehensive flood hazard analysis for the whole MD can only be found in the study of Dung et al. [2015]. They developed different copula-based bivariate statistical models to quantify the probability of joint occurrence of peak discharge and flood volume of the Mekong River at

Kratie, commonly defined as the upstream entrance of the MD. Apel et al. [2016] presented a detailed probabilistic fluvial–pluvial flood hazard assessment for the city of Can Tho in the centre of VMD using the results of Dung et al. [2015] as a boundary condition for a fluvial 2-D urban flood model.

Studies on flood damage are rare for the VMD. Damage assessments require rather extensive data sets, such as land-use, cropping systems and crop timing, asset values, damage functions for the different land-use types, and damage data to calibrate and validate the damage models. Consequently, flood damage and risk assessments have been conducted on the scale of districts or provinces only. For example, Chinh et al. [2017] developed a model to estimate flood losses using surveyed damage data of the flood in 2011 and assessed flood risk for an urban district of Can Tho city. Similarly, publications on agro-economic flood damage are practically non-existent for the VMD. The literature search on damage to agriculture in the VMD resulted in a single publication, a report by the Mekong River Commission [MRC, 2009]. The MRC developed a loss model for paddy rice in two provinces in the VMD: An Giang and Dong Thap. Two damage functions were developed using observed maximum water levels at two gauging stations, and statistical damage data for the period of 2000-2007. These depth-damage functions were then applied to estimate flood losses for the period 1910-2006. Since this model requires only the water level as input, it can provide a quick assessment of flood damage to rice crops. Applying these damage functions to the current situation is, however, not recommended due to the massive changes in land use and cropping system over the last two decades. For example, [Le et al., 2018] calculated an annual rate of change in land use in the VMD of 14.9% during 2001-2012. Hence, to our best knowledge, large-scale economic assessments of flood damage to agriculture crops for the whole delta and appropriate damage models are missing.

Against this background, we provide the first large-scale flood risk assessment for the agricultural sector covering the whole VMD. Our assessment is focussed on paddy rice, the predominant land-use type in the delta. We limit our calculation to direct losses, i.e. yield reduction as consequence of physical contact with floodwater. The methodological novelty is the detailed consideration of cropping calendar and plant phenology in combination with synthetic probabilistic flood hydrographs mapping different flood regimes of the Mekong. By this, the important aspect of plant phenology and temporal occurrence of flood peaks is introduced into the probabilistic flood risk assessment approach.

The flood hazard is quantified following the methodology of [Dung et al., 2015]. To obtain spatially explicit flood hazard maps, a large-scale hydraulic inundation model is driven by synthetic flood discharge time series, which are associated with probabilities of occurrences. Based on these hazard maps, crop damages are estimated using published damage functions, and explicitly considering the temporal occurrence of high water levels,

the cropping calendar, and plant phenology. Finally, the consequences of two land-use development scenarios proposed in the Mekong Delta Plan were estimated in terms of crop damages by floods.

3.2 Study area and data

3.2.1 Study area

The VMD covers an area of approximately 40,500 km^2 in the south of Vietnam, where the Mekong River discharges into the South China Sea through a number of estuary branches. The landscape is dominated by flat floodplains formed by deposited river sediments. Floodplain sedimentation is estimated to approximately 9.5 $mmyear^{-1}$ on average [Manh et al., 2013]. The properties of the deposits and the associated nutrients in combination with the tropical climate form ideal conditions for high agricultural productivity. Official statistics indicate that over 64% of the delta (2.6 *million ha*) is used for agriculture, with rice as the dominant crop (three quarters of the total cultivation land), followed by orchard farms and sugar cane [GSO, 2015]. Covering only 12% of the total land area of Vietnam, the delta contributes 52% to the national food production and over 80% to the Vietnamese rice export [GSO, 2015].

From July to December, high discharge of the Mekong River triggered by the Asian monsoons cause a large-scale inundation in the delta. Our study area, referred to as the delta flood-prone region in Vietnam, comprises 2 million hectares of nine provinces. The area is commonly divided into two ecological regions on the basis of inundation depth, named "deep inundation" (above 1.5 m) and "shallow inundation" (below 1.5 m). The deep-inundation areas (marked in yellow in Fig.3.1) encompass the two most important floodplains in the delta, i.e. the Plain of Reeds (PoR), and the Long Xuyen Quadrangle (LXQ).

Flooding in the VMD is characterized by slowly rising and receding rates, with a mean value of 5–10 $cmday^{-1}$. The flood hydrograph at Tan Chau and Chau Doc (blue points 1 and 2 in Fig.3.1) usually has two peaks. The first peak normally falls from mid-July to mid-August. The second, often higher peak, arrives from September to October. Floodwater from Cambodia enters the VMD via three main routes. The mainstream branches of the Mekong, i.e. Mekong and Bassac rivers, convey 90% of the total flood volume. The remaining 10% are the transboundary overland flow from Cambodian lowlands to the PoR east of the Mekong River, and the LXQ west of the Bassac River [Hung et al., 2012, Tri, 2012]. Besides inundation caused by high river discharge, tidal floods occur in the vicinity of rivers/canals in the coastal areas, characterized by short but repeated durations following the high tides of the South China Sea and the Gulf of Thailand [Apel et al., 2016].

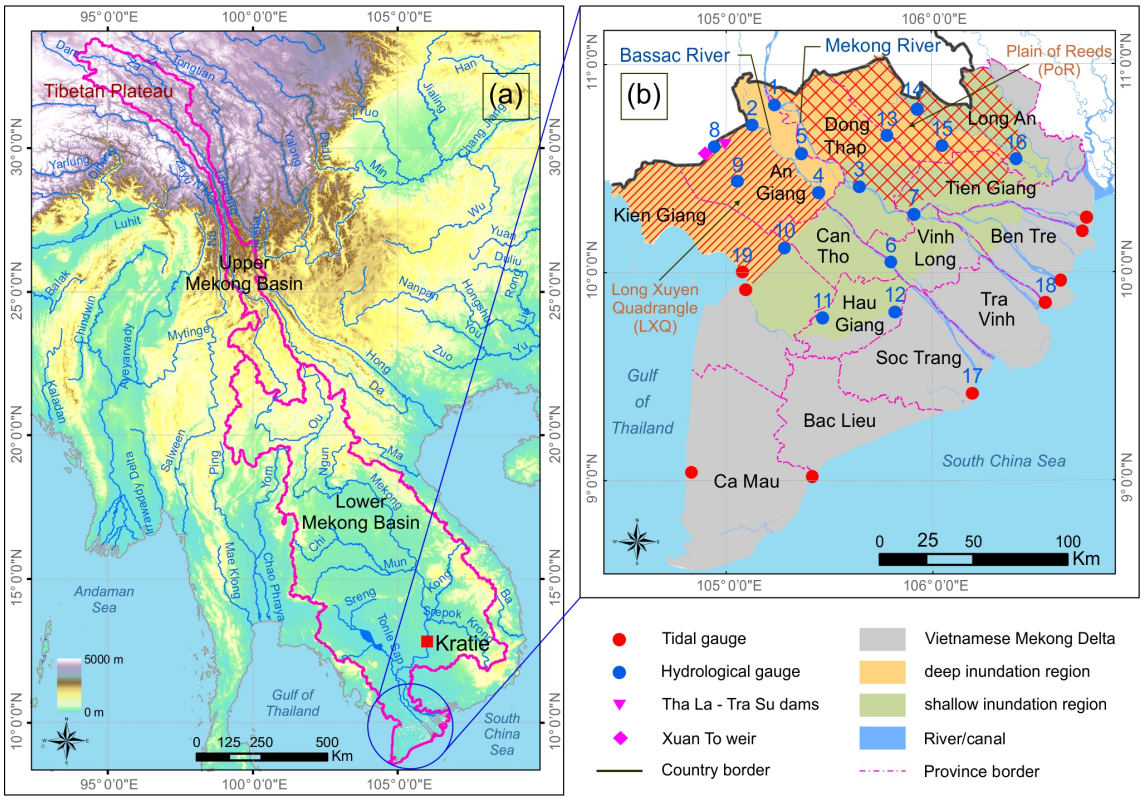

Figure 3.1: Geographical location of the Mekong Basin (a). The Vietnamese Mekong Delta and its flood-prone area (b). Deep-inundation region (above 1.5 m) marked in yellow, shallow-inundation region (below 1.5 m) presented in green. Red dots are locations of tidal gauges. Blue dots are locations of water level gauges. The numbers above blue and red dots present station codes.

3.2.2 Data

Topography data, tidal levels and operation schemes of flood control structures

Tidal level data are used as downstream boundary condition of the flood propagation model. Hourly tidal level records at 10 gauge stations were collected, covering the entire flood season of the year 2011 from 1 June to 30 November. The locations of these tidal gauges are given in Fig.3.1. These data were provided by the Southern Regional Hydro-Meteorology Centre of Vietnam (SHRMC). To generate inundation maps, a high-resolution (5x5 m) lidar-based digital elevation model (DEM) for the whole VMD was acquired from the Ministry of Environment and Natural Resources of Vietnam (MONRE). The lidar data were collected and processed during 2009-2010. Operation schemes of the flood control structures in 2011 were collected from the Departments of Agriculture and Rural Development (DARD) of the delta provinces.

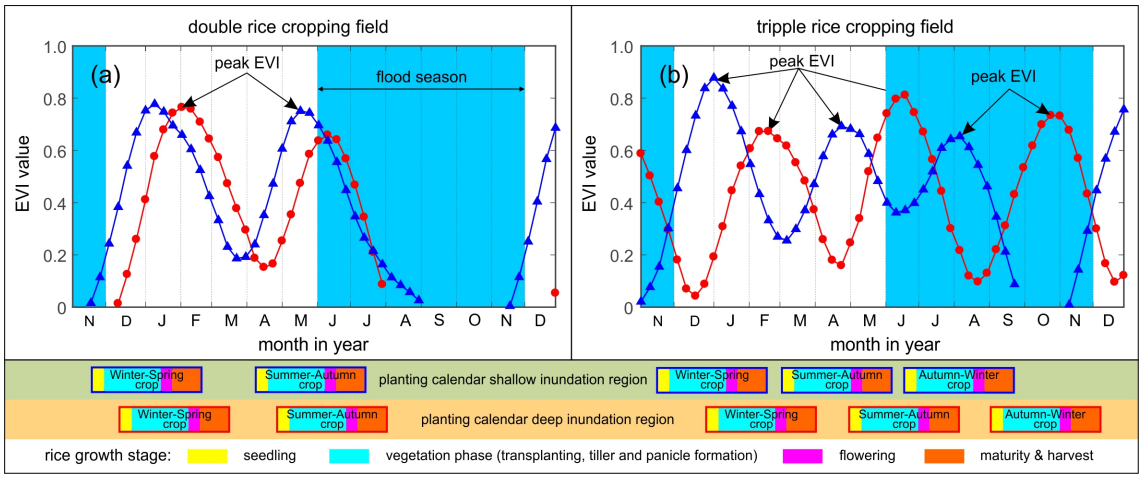

Figure 3.2: Time series of the smoothed enhanced vegetation index (EVI) for double (a) and triple (b) rice cropping fields in the Vietnamese Mekong Delta. The blue lines denote paddy fields in the shallow-inundation zone. Red lines represent paddy fields in the deep-inundation zone. The cropping season ends 40 days after the EVI peak [Kotera et al., 2016]

Rice cropping system and planting calendar

The rice cropping system in the VMD is strongly related to water availability, soil fertility and irrigation/drainage facilities (e.g. flood control structures). Rice fields are generally encircled by dyke systems to protect them against the regular flood pulse of the Mekong. These dyke systems can be classified as low dykes and high dykes. Low dykes protect the summer–autumn crop against the early flood peak from mid-July to mid-August. They are regularly overtopped during the later stages of the flood period. Farmlands protected by high dykes can be, however, completely cut off from floodwater. The design level of the dykes was chosen to withstand water levels observed during the historical flood in 2000 [Triet et al., 2017]. The inundation of those areas is thus controlled by the operation of sluice gates included in the dyke lines.

Traditionally, farmers were only able to grow a single rice crop per year during the wet season. This crop was known as rainfed crop. Today, the majority of rainfed crops have been replaced by irrigated rice, except for small areas affected by saline water intrusion or poor soil quality (acid sulphate soil). Farmers are able to grow two or even three crops per year. One crop is planted in the dry season in November–December and harvested in February–March (called winter–spring crop or Dong Xuan). During the wet season, farmers plant one or two crops. The first crop (summer–autumn crop or He Thu) is planted in April–early June and harvested by July–early August. The second crop (autumn–winter crop or Thu Dong) depends on how farmlands are protected against floodwater. Farmlands with full protection (located in the deep-inundation region) plant in August and harvest in November–December. In the shallow-inundation region, farmers harvest in late August–early September, before the arrival of the main flood peak.

The rice cropping system and planting calendar in the VMD have been well studied using optical and radar satellite data [e.g. Bouvet and Le Toan, 2009, 2011, Nguyen et al., 2015]. Figure 3.2 illustrates the planting calendar in 2011 for four paddy fields positioned in the deep versus shallow-inundation region for double- and triple-season rice fields. There is a shift of 1–1.5 months in the planting calendar between the shallow- and deep-inundation regions. The enhanced vegetation index (EVI) time series used to construct this plot were provided by Akihiko Kotera (personal communication, 1 March 2017). An EVI value of 0 indicates no vegetation cover, whereas a value of 1 means complete vegetation cover. The methodology used to derive the data set has been presented in Kotera et al. [2016] and applied to assess economic flood damage to rice crop in the Chao Phraya delta in Thailand from 2000 to 2011.

Land-use data

The land-use map of 2014, with a resolution of 250 x 250 m, covering all 13 provinces in the VMD was provided by the German Aerospace Centre (DLR). The VMD land use is part of the product MEKONG LC2010, covering the entire Mekong Basin at a spatial resolution of 500 m. MEKONG LC2010 was developed within the German–Vietnamese project "Water-related Information System for a Sustainable Development of the Mekong Delta" (WISDOM, http://www.wisdom.eoc.dlr.de/, last access: 20 July 2018). Land cover data were derived using the Moderate Resolution Imaging Spectroradiometer (MODIS) instrument aboard the Terra and Aqua satellites. Different MODIS products were combined to provide cloud free composites. The enhanced vegetation index (EVI) was calculated following Eq. 3.1.

$$EVI = G \times \frac{NIR - RED}{NIR + C_1 \times RED - C_2 \times BLUE + L} \tag{3.1}$$

where G is the gain factor ($G = 2.5$). C_1 and C_2 are the coefficients of the aerosol resistance term, which uses the 500 m blue band of MODIS to correct aerosol influences on the red band ($C_1 = 6.0$ and $C_2 = 7.5$).L is the canopy background adjustment ($L = 1$) [Huete et al., 2002].

Land-use classification was performed on the basis of the EVI time series from 2001 to 2011 (for a detailed description see Leinenkugel et al. [2013]. Within the 12 classes of the VMD land-use raster, three classes indicate rice cultivation areas: single-season rice, double-season rice, and triple-season rice (values 5–7 in Fig. 3.3a).We reclassified the original product to two raster images presenting the summer–autumn crop, hereafter referred as SAC, and the autumn–winter crop, hereafter referred to as AWC, since their growth stages

partially or fully fall in the flood season. The SAC image was created by merging all pixels with double-season and triple-season rice. The other landuse classes (e.g. orchards, sugar cane) were considered non-rice pixels (presented in Fig. 3.3b). To produce the AWC image, which is only grown in triple-season cropping schemes, only pixels with original values of 7 were considered (see Fig. 3.3c).

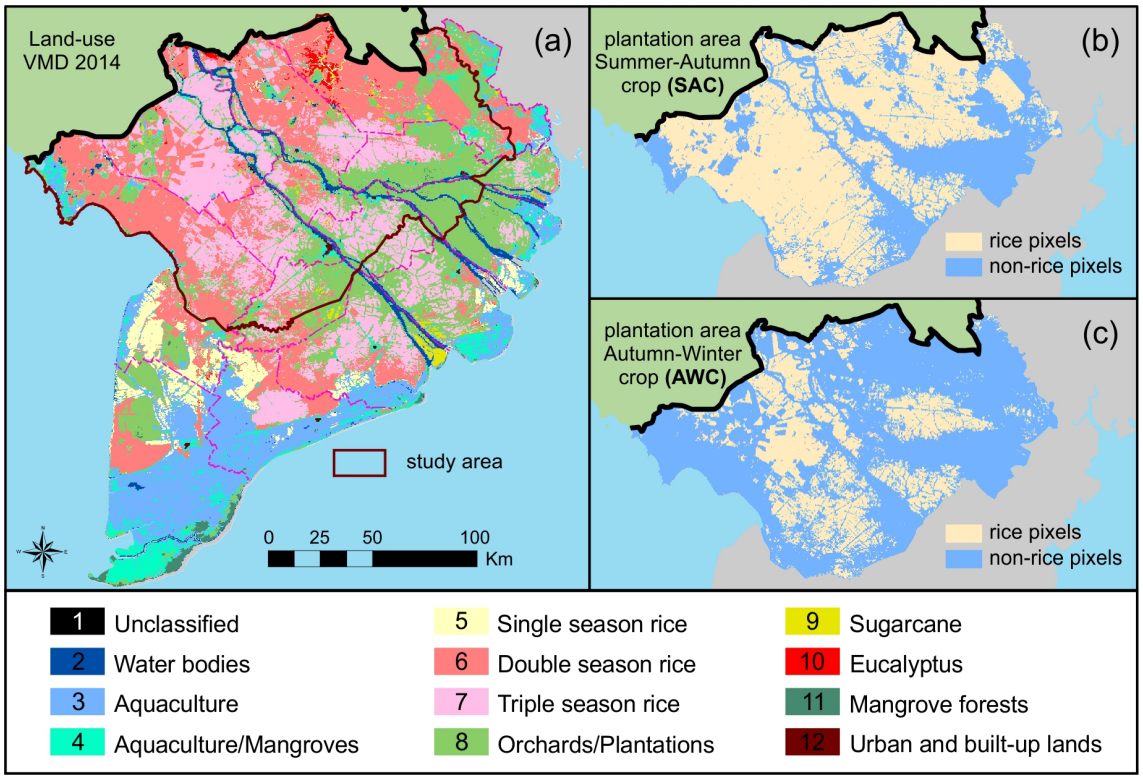

Figure 3.3: Panel (a) presents the land-use map of the Vietnamese Mekong Delta in 2014. Panels (b) and (c) show plantation areas of the summer–autumn crop (SAC) and the autumn–winter crop (AWC).

3.3 Methodology

For the large-scale flood risk assessment, the temporal relationship between the inundation hazard and the rice planting calendar was taken into consideration. The next sections describe the procedure that derives the area of rice crops exposed to floods, flood damage (D) from a given extreme event, and the expected annual damage (EAD). These risk indicators were estimated for the current situation and for two land-use development scenarios, namely the reduction or expansion of the triple-season rice area as given in the Mekong Delta Plan of the Vietnamese government. The methodology is outlined in Fig. 3.4a.

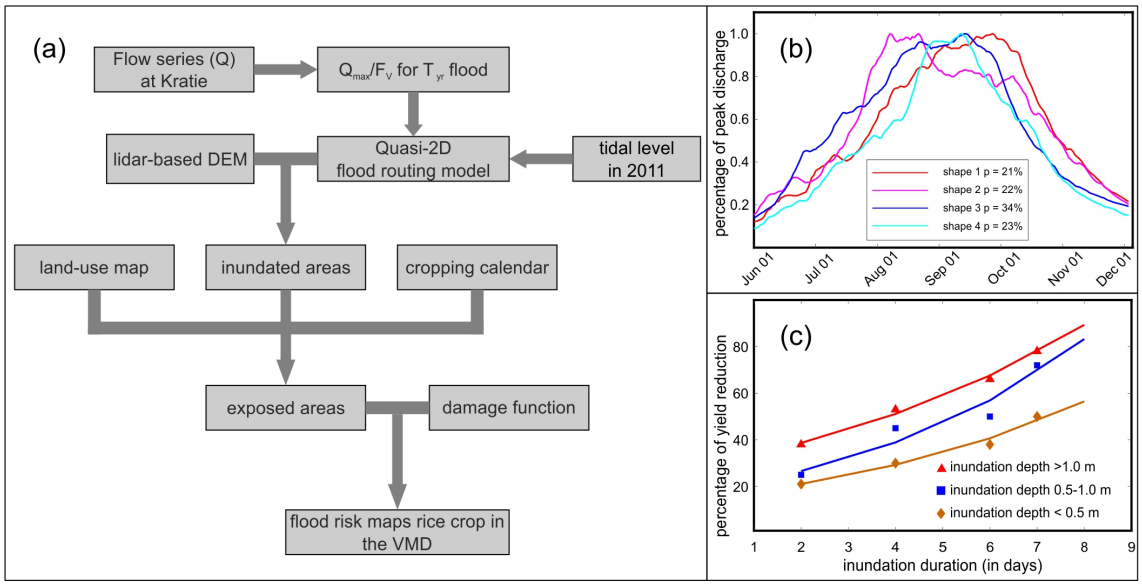

Figure 3.4: (a) Procedure for estimating flood risk to rice production in the Vietnamese Mekong Delta. (b) The four normalized discharge hydrographs at Kratie, together with their probability of occurrence Dung et al. [2015] used for the derivation of synthetic flood events as the upper boundary of the hydraulic model. (c) Stage-damage curve for paddy rice Dutta et al. [2003].

3.3.1 Determining event hydrographs corresponding to the T -year flood

Synthetic flood events were estimated for station Kratie (Fig.3.1, left panel) with 10-, 20-, 50-, and 100-year return periods, referred to as T_{10}, T_{20}, T_{50}, and T_{100}. This station is commonly defined as the upstream entrance of the MD and is used as upper boundary of the hydraulic inundation model of the MD. The estimation of flood events is based on Dung et al. [2015]. The authors developed and tested different bivariate copula-based statistical models on extreme values, using annual maximum discharge Q_{max} and flood volume FV. Both variables are important for the characterization of the long-lasting annual floods in the MD. From different models that were tested, the Gumbel–Hougaard copula was selected as most suitable, with log-normal distributions describing the marginals of Q_{max} and FV . The outcomes of the mentioned study is the very first publication on flood frequency analysis for the MD, considering both peak discharge and flood volume. We refer readers to the original paper for a detailed description.

Four pairs of peak discharge (Q_{max}) and volume at Kratie (FV), corresponding to T_{10}, T_{20}, T_{50}, and T_{100} floods were selected from the bivariate copula model. The most probable pairs were selected from the Q_{max}/FV pairs with equal joint probabilities corresponding to the return periods specified above. A full probabilistic analysis using a large number of Q_{max}/FV pairs with equal joint probabilities was not performed due to the high computational demand of the large scale hydraulic model (on average, 2–3 *hours* are required for one simulation of the whole flood season June–November on a PC installed with Intel i7-CPU 3.0 GHz, 16 GB RAM). The selected Q_{max} and FV values range from 56,500 to

66,000 m^3s^{-1} and from 459 to 525 km^3, from the different return periods.

Damages to agriculture crops are highly dependent on the time of occurrence of flooding [Penning-Rowsell et al., 2003, Förster et al., 2008, Klaus et al., 2016]. To account for the timing, each of the four Q_{max}/FV pairs were scaled to synthetic flood hydrographs covering the whole flood season from 1 June to 30 November using four typical hydrograph shapes (shp_i, i = 1–4), representing different flood patterns and, consequently, different possible damages. These shapes were adapted from Dung et al. [2015] (see Fig. 3.4b). The shape shp_3 has the highest possibility of occurrence (p = 0.34). The flood in 2000 closely followed this shape, with a minor alteration as the first peak arrived some days earlier. The other three hydrograph shapes have equal probabilities of occurrence (p = 0.21–0.23). The shape shp_2 has an early flood peak, while shp_1 shows a late peak. The disastrous flood in 2011 resembled shp_1.

This procedure results in 16 synthetic discharge time series at Kratie. They serve as the upper boundary condition for the flood propagation model. In each simulation, the lower boundaries (i.e. tidal levels), dyke scenarios and operation schemes of flood control structures were fixed as recorded in 2011, i.e. the most recent damaging flood. The scenarios are denoted using the return period and the hydrograph shape. For example, scenario $T_{100}shp_3$ corresponds to the 100-year return period of Q_{max}/FV and the hydrograph shp_3.

3.3.2 Transformation of discharge to water levels

To transform the discharge series into spatially distributed inundation water levels and associated timing in the VMD, a quasi-2-D, large-scale hydraulic model was used. The model domain covers the entire MD, including the VMD and Cambodia lowlands and the Tonle Sap Lake. It uses Kratie as the upper boundary condition and the tidal level monitoring gauges along the South China Sea and the Gulf of Thailand as downstream boundaries.

The model was initially developed by Dung et al. [2011], using the 1-D river model modelling package MIKE11-HD developed by Danish Hydraulic Institute (DHI). The hydrodynamic module (HD) provides the full dynamic solution of the 1-D Saint-Venant equations. The solution is based on an implicit finite difference scheme developed by Abbott and Ionescu [1967]. Floodplain inundation (2-D flow) was presented by the 1-D model through wide cross sections for the Cambodian part of the model domain, which is appropriate for the comparatively low anthropogenic impacts on the channel network, and natural inundation dynamics of in this part of the MD. In the Vietnamese part of the delta, flood compartments were represented by virtual canals and control structures presenting the

dykes. The original model was later refined and updated by Manh et al. [2014] and Triet et al. [2017] (see Fig.3.5). The model was calibrated and validated with gauged data and maximum inundation extents derived from satellite data for a number of flood events, including the moderate flood of 2009, the low flood of 2010, and the extreme floods in 2011 and 2000. For a detailed description of the 2-D model see the original paper by Dung et al. [2011].

3.3.3 Transformation of water levels to flood hazard indicators

The hydraulic simulations provided discharge and water level time series at the model calculation nodes. Inverse distance weighting (IDW) was applied to interpolate between nodes for complete spatial coverage. Inundation extent and depth were then obtained by intersecting the water levels with the lidar-based DEM.

Based on the rice cropping system and cropping calendar, three gridded inundation maps were produced for each simulation scenario. The first map, labelled "*July*", was generated using the maximum water level of 61 days from the beginning of simulation from 1 June to 31 July. It was applied to calculate damage to the summer–autumn crop (SAC) in both shallow- and deep-submergence regions. The second map (*August*) was based on the maximum water level from 1 June to 15 September in order to calculate damage to the autumn–winter crop (AWC) in the shallow-submergence region. For the AWC in the deep-submergence region, we used the map defined by the maximum annual submergence (*annual*) within 1 September to 30 November. The inundation grid cells of these maps were classified into three inundation depth classes to assign a stage-damage curve (Fig. 3.4c) to each grid cell. Exposed areas of rice crops were calculated by intersecting the inundation maps with the two land-use maps presenting the SAC and the AWC, as summarized in Table 3.1.

All these procedures were performed using Python scripts (Python version 2.7) and the Python-supported module of ArcGIS (ArcGIS 10.4).

Table 3.1: Inundation maps for estimating damage to rice crops in the Vietnamese Mekong Delta.

Inundation region	Cropping system system	Rice crop	Planting calendar	Input inundated raster name	period
Shallow (<1.5 m)	double-season rice	Summer–Autumn (SAC)	mid-April–mid-July	*July*	1 Jun–31 Jul
	tripple-season rice	Summer–Autumn (SAC)	March–May/early June	*July*	1 Jun–31 Jul
		Autumn–Winter (AWC)	mid-June–mid-September	*August*	1 Jun–15 Sep
Deep (≥1.5 m)	double-season rice	Summer–Autumn (SAC)	May–July	*July*	1 Jun–31 Jul
	tripple-season rice	Summer–Autumn (SAC)	May–July	*July*	1 Jun–31 Jul
		Autumn–Winter (AWC)	September–November	*Annual*	1 Sep–30 Nov

3.3.4 Calculation of flood damage (D) and expected annual damage (EAD)

Flood damage (D) was calculated on a pixel basis following equation (Eq.3.2) and aggregated to damage per province and to the whole study area.

$$D = Y \times MP \times (A_1 \times RD_1 + A_2 \times RD_2) \tag{3.2}$$

where D is the total monetary damage (in USD). Y and MP are the average rice yield and market prices taken from official statistical data for 2011: $Y = 5.0$ ton per hectare, and $MP =$ USD 280 per ton. A_1 and A_2 are the total exposed areas classified as partial and full losses. RD_1 and RD_2 are the relative damage factors specified on the basis of the damage curves adopted from Dutta et al. [2003] (see Fig.3.4c). The percentage of damage (i.e. in terms of yield reduction) depends on the duration of contact with floodwater (in days) and inundation depth, which was classified into two groups, i.e. below 0.5 m and above 0.5 m. Because flooding in the VMD is characterized with a long duration of submergence of 2–5 months Toan [2014], loss factor RD_2 was set to 1 for the areas where inundation depth is above 0.5 m (A_2), while the partial loss factor RD_1 was set to 0.5, which is the maximum damage of this class in the damage functions, for areas with inundation depth below 0.5 m (A_1).

We calculated the EADs for each of the four hydrograph shapes following Apel et al. [2016]. EAD is defined as the product of probability of exceedance of a given flood event and its damage:

$$EAD = \sum_{i=1}^{n} \Delta P_i \times \overline{D}_i \tag{3.3}$$

ΔP_i and $\overline{D}_i$ are calculated as follow:

$$\overline{D}_i = \frac{1}{2}(D_i + D_{i+1}) \tag{3.4}$$

$$\Delta P_i = p_{i+1} - p_i \tag{3.5}$$

where Δ_P is the increment of annual probability of exceedance $= \Delta(1-p)$, with p as the annual probability of non-exceedance. In this work $p = 0.90$, 0.95, 0.98 and 0.99 according to the selected return periods; D is the calculated damage induced by the given event; i is the numerator of the probability levels considered, and n is the number of probability levels.

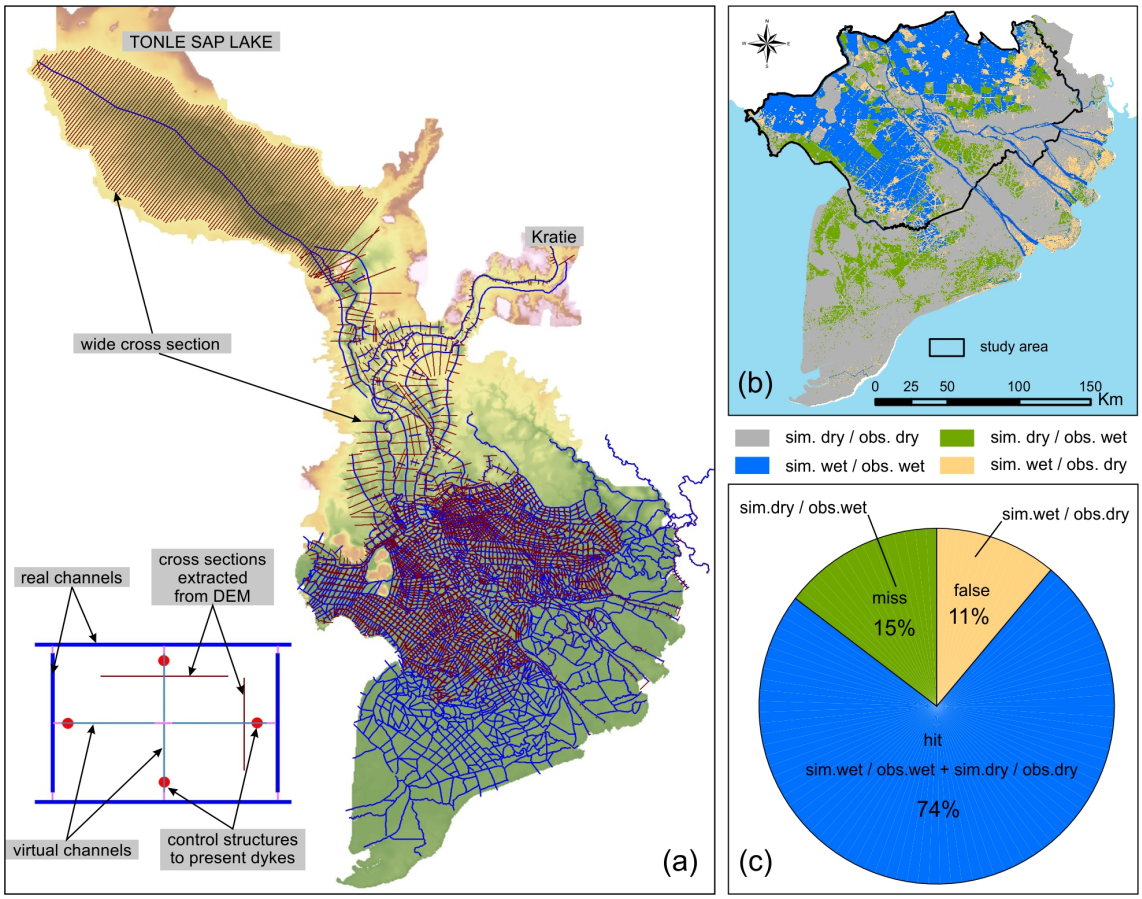

Figure 3.5: (a) Schematization of the quasi-2-D flood propagation model for the Mekong Delta and the concept of simulation of compartmented floodplains in the VMD. Comparison of observed inundation extent derived from satellite data and simulated maximum inundation extent for the flood event in 2011 for the whole delta (b), and evaluation of inundation simulation (c) adapted from Triet et al. (2017).

The average estimated annual damage (EAD) of the four hydrograph shapes was computed as the weighed sum of the EAD values, with the probability of occurrence of the hydrograph (Pr) as weights (Eq.3.6). The average crop risk indicator was computed by dividing the average EAD by the total annual rice plantation area.

$$\overline{EAD} = \sum_{i=1}^{4} Pr(shp = shp_i) \times EAD_i \tag{3.6}$$

3.3.5 Estimation of risk variation as a result of two land-use scenarios

In the final step, we investigated how flood risk will change in two land-use scenarios. Triet et al. [2017] proved that the construction of high-dyke areas in the northern delta provinces An Giang and Dong Thap increased the flood hazard in the centre of the delta. Thus, the first scenario considers the opening of the sluice gates in the high-dyke areas in these two provinces to introduce floodwater to the paddy fields during the main flood period, September-October. In response to this change in the flood management the farming

system also changes: farmlands with triple-season cropping are converted to double-season cropping, i.e. no cultivation of the AWC. The second scenario considers an expansion of high dykes, i.e. an increase in the height of the existing low dykes, in these two provinces to enlarge the area with triple rice crop production. This scenario follows the development scenario, the so-called "food production scenario", proposed in the Mekong Delta Plan [Deltares, 2013]. Dyke height was increased using information of dyke elevation from neighbouring compartments and maximum water level of the historical flood in 2000, which was chosen as the design event for flood control infrastructures in the delta.

The flood propagation model simulated the 16 synthetic floods for these two dyke scenarios, while the lower boundary conditions were preserved as in 2011. Figure 3.6 exemplarily illustrates the simulated inundation extent for the 10-year flood for three scenarios (current situation, expansion and removal of high dykes).

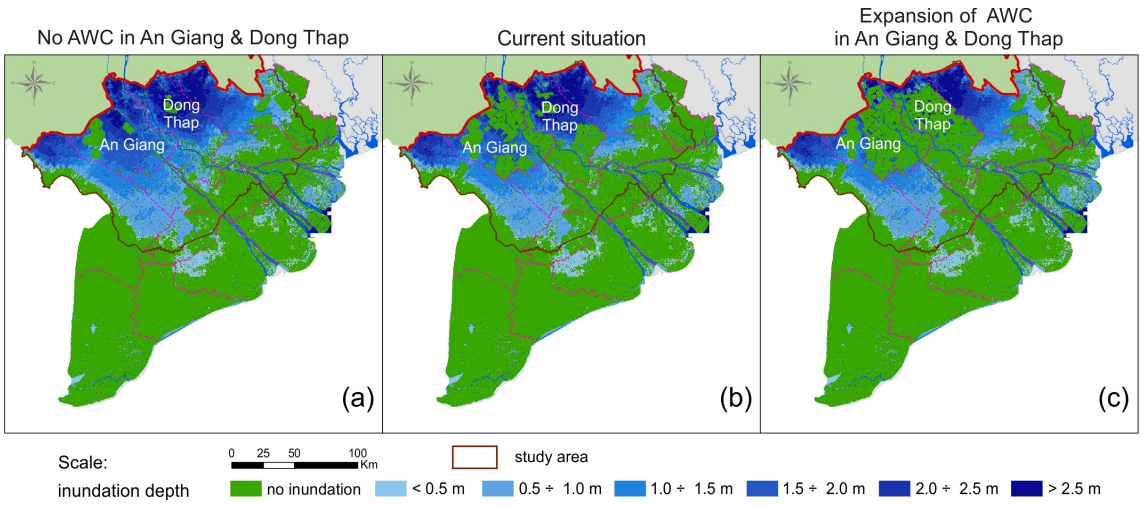

Figure 3.6: Simulated maximum inundation extent for a 10-year return period flood ($T_{10}shp_1$) for three land-use scenarios. (a) No plantation of autumn–winter crop in An Giang and Dong Thap, (b) present condition as of 2011, and (c) expansion of high-dyke areas in An Giang and Dong Thap to enlarge triple-season rice crops.

3.4 Results and discussion

3.4.1 Validation of estimated damage

The damage estimation was validated by comparing the estimated damage for the flood in 2011 with official damage data. The exposed cropping area was overestimated by 18%, i.e. 32,500 *ha* in comparison with a reported area of 27,000 *ha* [Tinh, 2012]. We estimated rice crop losses of USD 42.7 *million*. This number is equivalent to 81% of the reported agricultural damages from the National Steering Committee for Flood and Storm Prevention and Control (USD 52.8 *million*) [MRC, 2011]. Flood damages to other agriculture crops and

facilities, e.g. farmhouses, which were included in the reported damages (lumped into a single value categorized as agriculture losses), were not yet incorporated in the presented damage estimation. Considering that paddy rice is the predominant crop in the delta, it is very likely to share a large part of the reported losses. Paddy fields derived from the land-use LC2014 raster account for 72% of whole agriculture land within the focus area of this study (deep- and shallow-inundation areas). Assuming a linear distribution of damages in the lumped official reported damages with landuse proportion, it can be reasoned that the simulated damages are in the range of the reported. However, it has to be acknowledged that spatial distribution and market prices of different crops are likely to be important for the damage estimation. In any case, although not the ideal piece of information, the reported agriculture losses were the only available data with which to evaluate our rice crop damage calculation.

A large share of the overestimated exposed area of rice crops can be attributed to the simulated inundation extents, although efforts have been made to update, refine, and calibrate the model [Dung et al., 2011, Manh et al., 2014, Triet et al., 2017]. The main source of uncertainty stems from the interpolation of 1-D model results to a 2-D raster, which could not be reduced even by the high-resolution lidar DEM. Triet et al. [2017] reported a flood area index (FAI) of 0.64 for the comparison of modelled and observed inundated areas for the whole VMD. The FAI was computed by dividing the sets of pixels presenting the intersection of observed and simulated inundation with the set of pixels presenting the union of observed and simulated (Eq.3 in Aronica et al. [2002]). This value increased to 0.74 only if the flood-prone area of the VMD was considered. According to Aronica et al. [2002], who suggested that a FAI higher than 0.7 is considered acceptable for an inundation simulation model, it can be concluded that the performance of the inundation model for the VMD is acceptable for the flood-prone area of the VMD, where the bulk of flood damages occur.

A small share of the overestimation of the 2011 flood might stem from the land-use data. Considering the rapid expansion of the triple-season rice areas in the delta [Le et al., 2018], it can be expected that the used land-use product of 2014 overestimates the spatial coverage of triple season rice paddies, possibly resulting in an overestimation of the flood damage. Also, land-use data have a resolution of 250×250 m; therefore the majority of inland canals (width 10–30 m) were likely classified as rice pixels (see Fig.3.3). Considered the channel density in the delta of 14 mha^{-1} [Hung et al., 2012], not separating these inland water pixels might contribute with a small share to the overestimation. Additionally, other important factors were not considered, such as dyke failures and local flood management measures, i.e. early harvesting of rice crops despite not being 100% ripe or local raising of dyke segments with sandbags.

Some of these error sources might be resolved by further refining the model. For instance,

the land-use data set can be improved by considering the inland canals when the crop areas are extracted. Enhancing model performance is, however, not that straightforward considering the huge amount of data required for the large-scale model domain. Despite these deficiencies, the flood damage assessment proposed in this study can produce reliable results, particularly when the typically large errors in flood damage estimation are taken as a reference [e.g. Shroder et al., 2014]. Thus, the proposed method is judged to be appropriate to estimate flood hazard and risk to rice cropping in the VMD.

3.4.2 Flood hazard assessment

The flood event time series at Kratie were transformed into four hazard indicators: maximum water level, date of occurrence, inundation extent, and depth. The simulated annual maximum water levels ($AMWLs$) at locations with water level gauges in the VMD are summarized in Table 3.2. Figure 3.7 presents the date of occurrence (DO) of the $AMWLs$ at these points. The chosen locations encompass nine gauges in the mainstream Mekong (i.e. Mekong River and Bassac River), and seven inland gauges in the two most important floodplains, i.e. LXQ (Long Xuyen Quadrangle) and PoR (Plain of Reeds). Inundated areas were calculated for the three periods specified in Table 3.1 and aggregated to the flood-prone area of the VMD on the basis of the four hydrograph shapes (Fig. 3.8).

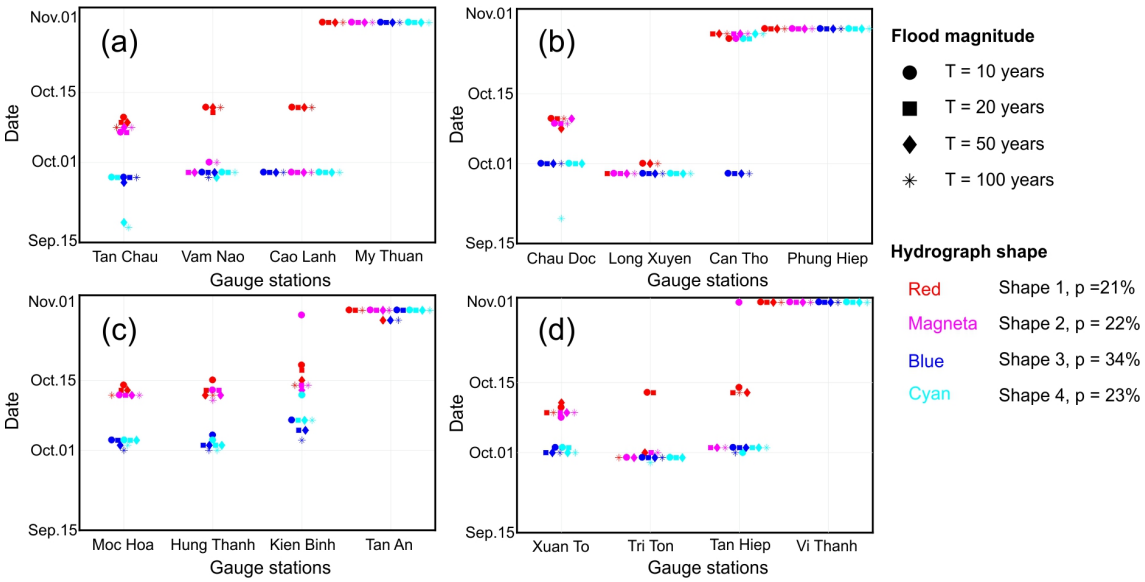

Figure 3.7: Date of occurrence (DO) of the annual maximum water level at key monitoring gauges in the Vietnamese Mekong Delta (a) stations in the Mekong branch, (b) stations in the Bassac branch, (c) stations in the Plain of Reeds, and (d) stations in the Long Xuyen Quadrangle. The four hydrograph shapes (indicated by colours) are shown in combination with different flood magnitudes (indicated by markers).

The simulation results show that the $AMWLs$ in the VMD vary substantially depending on flood magnitude (T_F) and hydrograph shapes. We estimated a relative change of

Table 3.2: Simulated annual maximum water level at key gauge stations in the Vietnamese Mekong Delta in correspondence with T-year flood event.

Simulation	Mekong River				Bassac River			Plain of Reeds			Long Xuyen Quadrangle			Inland stations		
	Tan Chau [1]*	Vam Nao [5]	Cao Lanh [3]	My Thuan [7]	Chau Doc [2]	Long Xuyen [4]	Can Tho [6]	Moc Hoa [14]	Hung Thanh [13]	Kien Binh [15]	Tan An [16]	Xuan To [8]	Tri Ton [9]	Tan Hiep [10]	Vi Thanh [11]	Phung Hiep [12]
$T_{10}Shp_1$	4.94	3.71	**2.69**	**2.04**	4.71	2.78	**2.27**	3.20	3.29	2.09	**1.58**	4.69	2.90	**1.80**	**1.01**	**2.01**
$T_{20}Shp_1$	5.15	3.88	**2.83**	**2.07**	4.92	2.89	**2.30**	3.45	3.51	2.30	**1.61**	4.90	3.05	**1.91**	**1.04**	**2.03**
$T_{50}Shp_1$	5.37	4.06	**2.98**	**2.09**	5.12	3.02	**2.33**	3.71	3.74	2.49	**1.64**	5.12	3.20	**2.02**	**1.08**	**2.05**
$T_{100}Shp_1$	5.50	4.17	**3.07**	**2.11**	5.26	3.10	**2.35**	3.87	3.89	2.61	**1.67**	5.25	3.29	**2.09**	**1.11**	**2.07**
$T_{10}Shp_2$	4.54	3.41	**2.53**	**1.99**	4.33	2.66	**2.22**	2.75	2.91	1.76	**1.50**	4.31	2.75	**1.66**	**0.96**	**1.98**
$T_{20}Shp_2$	4.72	3.55	**2.64**	**2.02**	4.51	2.74	**2.25**	2.99	3.11	1.94	**1.54**	4.49	2.89	**1.74**	**0.99**	**2.00**
$T_{50}Shp_2$	4.92	3.70	**2.76**	**2.05**	4.70	2.84	**2.28**	3.24	3.32	2.15	**1.58**	4.68	3.02	**1.83**	**1.02**	**2.02**
$T_{100}Shp_2$	5.05	3.81	**2.84**	**2.06**	4.82	2.91	**2.30**	3.39	3.45	2.27	**1.60**	4.81	3.11	**1.91**	**1.03**	**2.03**
$T_{10}Shp_3$	4.93	3.75	**2.79**	**1.95**	4.68	2.87	**2.21**	3.22	3.29	2.09	**1.50**	4.66	3.05	**1.83**	**0.94**	**1.95**
$T_{20}Shp_3$	5.13	3.91	**2.92**	**1.98**	4.87	2.98	**2.25**	3.46	3.51	2.29	**1.53**	4.85	3.19	**1.95**	**0.96**	**1.97**
$T_{50}Shp_3$	5.35	4.09	**3.06**	**2.01**	5.08	3.10	**2.28**	3.72	3.75	2.50	**1.56**	5.06	3.34	**2.07**	**0.99**	**1.99**
$T_{100}Shp_3$	5.49	4.20	**3.17**	**2.04**	5.21	3.19	**2.33**	3.88	3.89	2.62	**1.60**	5.19	3.43	**2.14**	**1.02**	**2.03**
$T_{10}Shp_4$	4.54	3.44	**2.55**	**1.96**	4.31	2.67	**2.19**	2.73	2.87	1.72	**1.47**	4.28	2.77	**1.65**	**0.94**	**1.96**
$T_{20}Shp_4$	4.73	3.59	**2.67**	**1.99**	4.49	2.77	**2.22**	2.99	3.08	1.90	**1.51**	4.46	2.92	**1.74**	**0.96**	**1.98**
$T_{50}Shp_4$	4.94	3.76	**2.80**	**2.02**	4.69	2.88	**2.25**	3.26	3.32	2.13	**1.55**	4.66	3.07	**1.85**	**0.99**	**2.00**
$T_{100}Shp_4$	5.09	3.87	**2.89**	**2.04**	4.82	2.95	**2.27**	3.42	3.47	2.27	**1.57**	4.79	3.16	**1.93**	**1.01**	**2.01**

* The numbers below the station names refer to the codes in Fig. 3.1b. Deep-inundation regions are indicated by plain text, shallow-inundation regions are indicated in bold.
Stations are listed from upstream to downstream and grouped according to their location as Mekong River, Bassac River, Plain of Reeds, Long Xuyen Quadrangle, and inland stations.

10–20% (40–60 *cm*) in simulated $AMWL$ for an event with T_{100} compared to T_{10} in the deep-submergence region (DSR), and 4–8% (5–10 *cm*) in the shallow-submergence region (SSR). The minor increase in the SSR can be attributed to the strong tidal influence at these stations. Hung et al. [2012] and Triet et al. [2017] reported a tidal influence of 70–80% to the river flow and water level at Can Tho and My Thuan during the flood season. Towards the northern part of the VMD the tidal influence reduces to below 2% at Tan Chau and Chau Doc at the border with Cambodia [Hung et al., 2012].

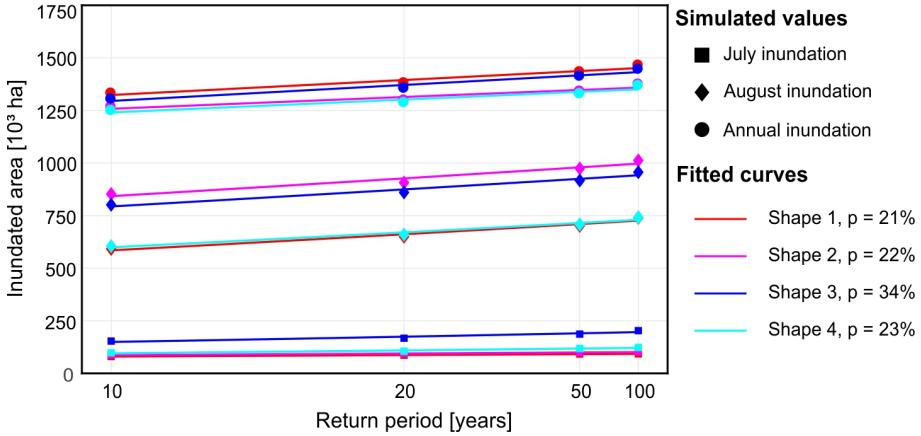

Figure 3.8: Frequency distributions of the maximum inundated area in July (squares), in August (diamonds), and over the whole year (circles) corresponding to the four flood patterns (different colours).

The hydrograph shape also influences the $AMWL$: higher $AMWL$ were obtained for events with shp_1 and shp_3. The shape shp_3 resulted in higher $AMWL$ in the DSR, while shp_1 yielded higher $AMWL$ in the SSR of the delta. In contrast to this, shp_2 and shp_4 caused lower water levels. We found a difference in $AMWL$ ranges from 9 *cm* at SSR to 45 *cm* at the DSR induced by the shapes shp_2 and shp_4 compared to the other two hydrograph shapes. These results are explained by the date of Qmax at Kratie: shp_1 and shp_3 have the second and higher peak in mid-September (shp_3) or mid-October (shp_1), about 1 month later than the other hydrographs. When this peak is routed to the VMD, it already meets partly filled floodplain compartments, and coincides with the period of highest tidal levels in the year (October-November). Therefore, the highest $AMWL$ is caused by the hydrodynamic interaction between the upstream and downstream boundaries, and preceding inundation dynamics. Our simulation thus provides numerical evidence to confirm the statement in Tri [2012] and Triet et al. [2017] that the superposition of river flood peaks with high tide periods results in substantial backwater effects and higher water levels up to the border with Cambodia.

The date of occurrence (DO) of the $AMWL$ in the VMD is less sensitive to changes in flood peak discharge and shape of hydrograph than the actual $AMWL$ (see Fig. 3.7). The DO can be divided into two groups. The first group is composed of stations with

prevailing tidal influence, e.g. Can Tho, My Thuan, and Vi Thanh. For this group $AMWL$ occurs in late October, similarly to the period of maximum tidal levels in 2011, the downstream boundary conditions of the flood propagation model. The second group contains gauges further north or gauges far from the main rivers, where the tidal influence is largely reduced. These gauges have the DO in the first half of October.

Figure 3.8 illustrates the frequency distribution of maximum inundation extent for three periods: July, August, and the whole year. This indicator varies strongly depending on the hydrograph shapes. A 10-year flood event with hydrograph shape shp_1 results in the same maximum extent as the 100-year flood with shp_4. This result proves the necessity to incorporate the temporal evolution of flood events into flood hazard and risk assessments in the MD. Our estimation of inundated areas from the T_{10} to the T_{100} event changed from 5% to 10% of the size of the flood-prone region of the VMD (2.0 *million ha*) in July, from 30% to 50% in August, and from 60% to 75% for the annual maximum extent. This means that even for the 100-year flood, 25–40% of the flood-prone region was cut off from inundation by the implementation of high dykes, initiated after the flood in 2000.

3.4.3 Exposed rice cropping area and flood damage

Exposed areas and flood damage (D) to rice crop were calculated on a pixel basis and then aggregated to the eight provinces located in the study area (Fig. 3.9 and Table 3.3). The average damage ranged from USD 39.0 *million* for a 10-year flood to USD 75.0 *million* for a 100-year flood. These numbers account for 0.23–0.45% of the total gross domestic product (GDP) of the eight provinces in 2011. Since such assessments are not available for neighbouring deltas in South Asia, e.g. Chao Phraya in Thailand or Irrawaddy in Myanmar, a comparison of these deltas is not possible. Our worst scenario, i.e. $T_{100}shp_3$, resulted in damages of USD 115.7 *million*. This value is less than half of the reported overall damage of the flood in 2000 (USD 250 *million*; reported in MRC [2012], scaled to USD 500 *million* with 2011 price levels by Chinh et al. [2016], which is considered a 50-year flood in the MD [Dung et al., 2015]. Although the damage figures from the event in 2000 were the overall damages, of which agricultural damages were an unknown part, this indicates that a large reduction in flood losses can be linked to the flood management and adaptation measures being implemented in the VMD following the Decision No. 99/1996 from the Government of Vietnam [GOV, 1996]. Note that the plan was initiated in 1996, but was implemented to a large extent after the flood in 2000 had occurred.

The hydrograph shape has a substantial effect on damage to rice crops in the VMD. The shape shp_3 resulted in a high amount of damage, roughly 1.5 times higher than the average damage. Flood hydrograph shp_2 closely matched the average damage (85–90%), while shp_1 and shp_4 resulted in approximately 60–70 % of the average damage (Fig. 3.9b).

These findings support our hazard and risk assessment approach and point to the relevance of the temporal evolution of the flood event for damage estimation. For example, the total flood damage from $T_{10}shp_3$ (USD 57.8 *million*) was about 10% higher than the $T_{100}shp_1$ event (USD 51.0 *million*).

The results provide evidence that rice cropping in the VMD is most vulnerable to flooding stemming from the early flood pulse in August-September when the total plantation area is expected to be at its maximum. During this period damage occurs to the second crop (SAC) in both DSR and SSR, and the AWC in the SSR. This finding is in line with the extremely high damages during the flood in 2000, which had a first peak at Tan Chau (point 1 in Fig. 3.1) on 2 August, i.e. 1 month earlier than usual [SIWRP, 2015]. In contrast, damage from late flood events, i.e. shp_1 or shp_4, are limited to the AWC in the DSR due to failure of dyke structure, or flood levels overtopping the current dyke height, similar to the flood damages recorded in 2011.

Aggregating the mean D values per province showed that the two northern provinces, An Giang and Dong Thap, accounted for about two-thirds of the total D of the VMD, with flood damage in An Giang being about 1.5 times higher than in Dong Thap. This difference increases up to a factor of 3 in the case of late flood peaks (Table 3.3). This can be explained by the larger areas with triple rice crops in An Giang. This third crop in the DSR is particularly vulnerable to inundation in October-November (see Fig. 3.3c). Damages for the other two provinces in the DSR also showed remarkable differences, with ∼16% of the total flood damage calculated for Long An located in the Plain of Reeds. This is 10–15 times higher than the share of Kien Giang (D in Kien Giang is less than 2% of the total D), although the rice cropping area is larger in Kien Giang [Bouvet and Le Toan, 2011, Nguyen et al., 2015].

The remaining SSR provinces accounted for about a quarter of the total D, which can be linked to their smaller rice cultivation areas in combination with their flood control

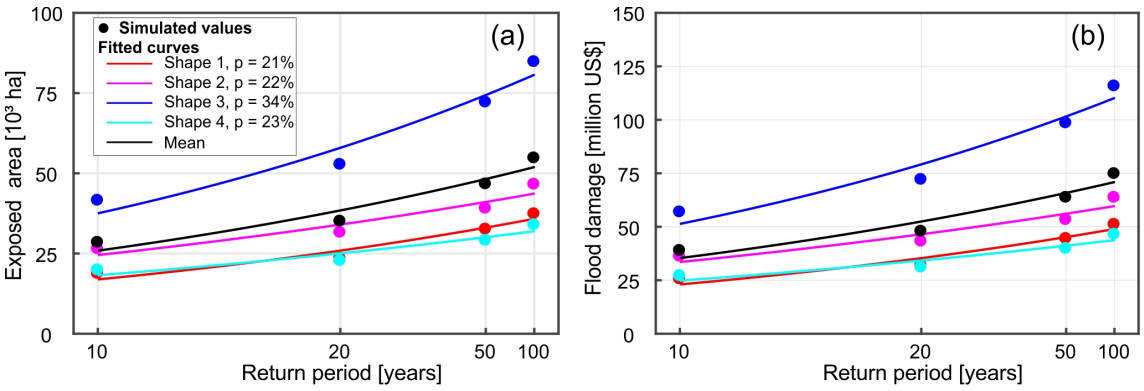

Figure 3.9: (a) Total exposed areas of rice crop in the Vietnamese Mekong Delta to floods of different return periods, calculated for the second and third rice crops and aggregated to the whole year. (b) Total damage for floods of different return periods.

Table 3.3: Flood damage to rice crop aggregated to the province level and converted to a percentage of the total damage.

Simulation	Return period	An Giang	Dong Thap	Long An	Kien Giang	Can Tho	Hau Giang	Tien Giang	Vinh Long
$T_{10}Shp_1$	10 year	50.5	18.0	13.6	0.2	6.2	1.8	0.9	8.9
$T_{10}Shp_2$		30.3	22.7	21.1	1.3	11.2	2.5	3.6	7.2
$T_{10}Shp_3$		36.3	29.8	18.9	0.5	6.5	1.6	1.7	4.7
$T_{10}Shp_4$		42.9	23.3	14.6	0.2	7.3	2.0	1.0	8.8
$T_{20}Shp_1$	20 year	54.1	16.9	12.1	0.2	6.4	1.7	1.0	7.5
$T_{20}Shp_2$		27.7	21.7	20.9	2.1	13.3	2.9	5.0	6.3
$T_{20}Shp_3$		37.5	27.7	19.9	0.8	6.7	1.5	2.0	3.9
$T_{20}Shp_4$		41.2	25.1	14.4	0.2	7.7	2.1	1.2	8.1
$T_{50}Shp_1$	50 year	61.0	14.1	10.4	0.2	5.7	1.5	1.3	5.7
$T_{50}Shp_2$		25.1	19.7	21.2	2.9	14.3	3.4	7.7	5.9
$T_{50}Shp_3$		40.6	24.6	19.5	1.0	7.0	1.6	2.3	3.2
$T_{50}Shp_4$		43.4	25.2	13.3	0.2	7.6	2.0	1.6	6.6
$T_{100}Shp_1$	100 year	62.2	13.7	10.0	0.2	5.9	1.5	1.3	5.1
$T_{100}Shp_2$		26.8	18.0	19.6	4.2	14.4	3.4	8.4	5.2
$T_{100}Shp_3$		10.1	23.8	20.2	1.3	7.2	1.7	2.9	2.9
$T_{100}Shp_4$		44.5	24.7	13.6	0.3	7.6	2.0	1.6	5.8

measures. Our calculated flood damage to rice crop for Can Tho is, on average, in the range USD 2.9–6.3 *million* from the 10-year to the 100-year flood. These figures amount to about 60% of the estimated urban damages of Can Tho (USD 5.0–9.7 *million*) for events with similar magnitudes [Chinh et al., 2017]. Since Can Tho has the highest urban / rural area ratio compared to the other delta provinces, it is likely that agriculture losses have an equal or higher share in flood damages compared to urban losses in the other provinces of the delta.

3.4.4 Rice cropping flood risk

For the current land use, the *EAD* for rice cropping in the whole delta amounts to USD 4.5 *million* (see Fig. 3.10b), with an average crop risk of USD 1.0–4.6 for each unit of land *[ha]* (see Fig. 3.11a). The highest risk was calculated for the provinces located in the deep-submergence region (DSR), except for Kien Giang, where the *EAD* was very low.

An expansion of areas with triple rice cropping in An Giang and Dong Thap, as defined in the expansion development scenario, would increase the exposure to flooding. Figure 3.10 shows that this expansion of AWC would triple the *EAD* to above USD 15.0 *million*. The expansion of triple rice cropping also means that the current low-dyke system must

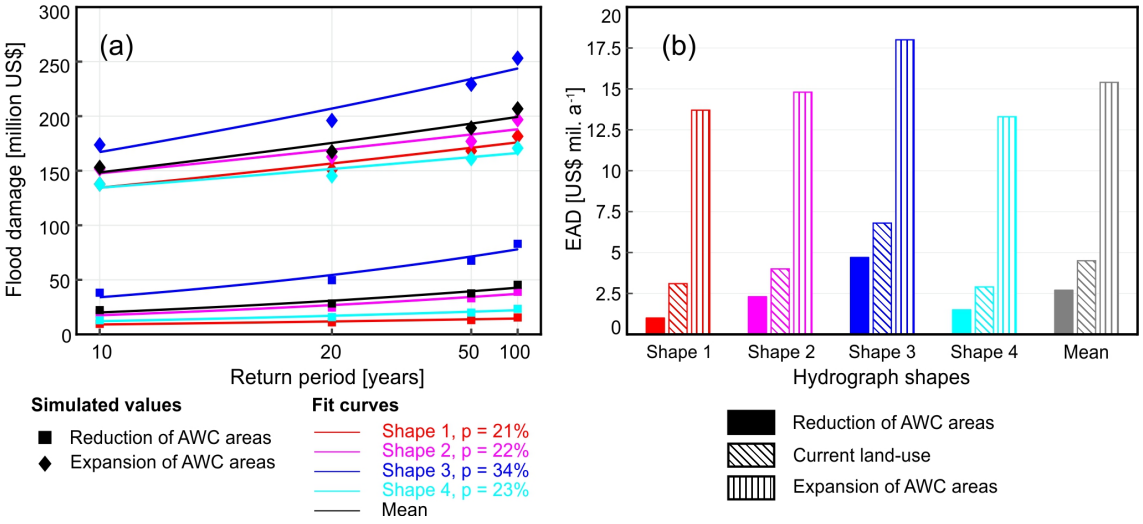

Figure 3.10: (a) Total flood damage for different return periods corresponding to two land-use scenarios. (b) Average crop risk as specific loss for each hydrograph shape.

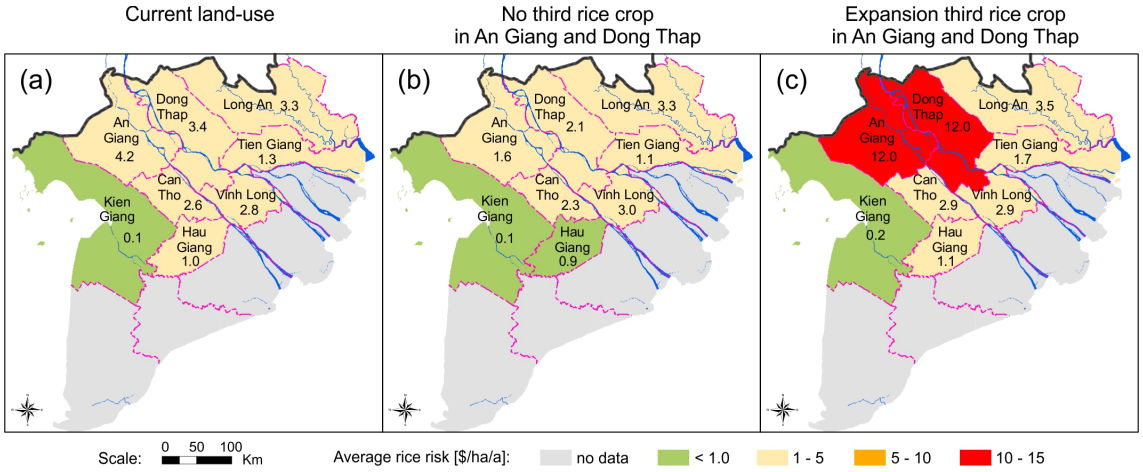

Figure 3.11: Flood risk for rice crops in the Vietnamese Mekong Delta. Specific loss is calculated in USD/ha/a for three land-use scenarios: (a) current land use, (b) no autumn–winter crop (AWC) in An Giang and Dong Thap, and (c) expansion of the AWC in these two provinces.

be raised to a higher design level in order to support the cultivation of AWC during September-November. This, in turn, would lead to higher inundation hazards and risks in downstream provinces [Triet et al., 2017]. Figure 3.11c shows both effects: a substantial increase in *EAD* in Dong Thap and An Giang, and a slight increase in *EAD* in the downstream provinces resulting from a higher-inundation hazard caused by the high-dyke development.

The second development scenario, i.e. introducing floodwater to the paddy fields after the SAC and no cultivation of AWC in An Giang and Dong Thap , resulted in smaller D and *EAD* values, as expected. Abandoning AWC cultivation would result in an *EAD* decrease of about 40% (Fig. 3.10b). The majority of these changes in both scenarios stems from changes in An Giang and Dong Thap. The other provinces account for 5 –15% of the

changes in EAD only.

The full flood control measures (high dykes) supporting the expansion of AWC areas in An Giang and Dong Thap after the flood in 2000 have been continuously debated. Triet et al. [2017] revealed that the change from low-dyke to high-dyke systems in this upstream part of the delta increased the inundation hazard in downstream areas, e.g. by an increase of 9–13 cm in $AMWL$ at Can Tho and My Thuan. Howie [2005] and Käkönen [2008] challenged the claim that farmers could have greater benefit by being able to add another harvest to the cropping system, because of more investment cost for mineral fertilizers to counter the losses of natural fertilization by deposited sediment [Manh et al., 2014], together with negative social and environmental consequences. The profitability of triple rice farming was reported to reduce from initially 57% to 6% after 15 years compared to double rice counterparts due to higher production costs [Tran et al., 2018a]. These arguments and findings might make the expansion of AWC less attractive.

On the other hand, rice cultivation areas in the southern part of the delta are likely to decrease due to increased salinity intrusion following higher sea levels [Smajgl et al., 2015, Hak et al., 2016] and land subsidence [Erban et al., 2014, Minderhoud et al., 2017]. Expansion of AWC in the northern part of the delta is an option for countering such losses and ensuring food security. Our results could support an evaluation of the costs and benefits of further high-dyke development and triple rice cropping expansion and thus provide important information for future flood management and landuse planning in the delta. Additionally, the damage and risks maps can serve as a basis for flood management. They could support the agricultural insurance, initiated in 2011 by the decision of the Prime Minister of Vietnam. In this programme the insurance premium depends on the rice yield only, and the spatial pattern of the flood hazard is not considered [GOV, 2011].

3.4.5 Uncertainties, limitation and future research directions

One of the major sources of uncertainties in our estimation of D and EAD is associated with the inundation maps. The process of interpolating from 1-D water levels to 2-D inundation raster inherits uncertainties from the hydraulic model and from the DEM used for interpolation [Brandt, 2016]. A full 2-D modelling approach might enhance the quality of flood inundation mapping, but this comes at a cost: the setup of a full 2-D hydraulic model on that scale is challenging because of the high density of man-made channels and hydraulic infrastructure, which need to be implemented in the model with high accuracy to substantially improve the simulations. Additionally, model runtime becomes critical in detailed large-scale 2-D hydraulic simulations within a risk assessment requiring a large number of model simulations. Large-scale approaches building on coarse-resolution modelling with sub-grid parameterization [Sampson et al., 2015] still cannot provide sufficient

accuracy to properly map the hydraulic dynamics in such a complex system with flat topography, where details matter a lot. However, refining this approach in high resolution, including all relevant hydraulic structures, and implementation in a highly parallelized environment (e.g. on GPUs) could provide a viable path for reducing the uncertainties in hydraulic modelling of the MD.

Another uncertainty source is the land-use maps used to quantify flood exposure of rice crops. The land-use raster was produced using satellite data from 2014; thus it is somewhat outdated considering the dynamics of agricultural land-use change in the MD. The area of triple-season rice has very likely increased from 2014 to the present. An updated and higher-resolution land-use data set would certainly provide more up-to-date results.

Another uncertainty source is the limited number of return periods used to calculate *EAD*. Ward et al. [2011] showed that the number and choice of the selected return periods can introduce a significant bias in the *EAD* estimates. They also pointed out the importance of considering damages to frequently occurring low damage floods, in line with the findings of Merz et al. [2009]. However, as the agricultural system in the MD is well adapted to frequently occurring floods (in fact these floods are the basis for the current practice of paddy rice cropping), this effect is likely not as important as in the European studies listed above.

Our work does not consider flood damage to other agriculture crops (e.g. orchard farms) or land-use types (e.g. shrimp farms). Although these production types are smaller than rice cropping in terms of area, they generate much higher economic value per cultivation unit. Therefore, it is highly recommended to include these crops in future studies on agricultural flood risk in the VMD. To facilitate such assessments, efforts need to be made to collect data on crop and aquaculture type and area, plantation calendar, and their vulnerability to inundation. Such risk assessments could then be used for scenario planning by varying land-use types and cropping patterns or changing boundary conditions by climate change and upstream developments. In addition, dedicated efforts for validation and development of crop damage curves for the VMD based on recorded flood damages at the plot scale would increase the credibility of the presented risk analysis. Our study is validated against large scale, aggregated damage data only, and it is open to ensuring that small-scale variations, which could be important for local adaptation measures, are represented sufficiently well.

3.5 Conclusion

A top-down approach to estimate flood damages and risks to rice cropping in the flood-prone areas of the Vietnamese Mekong Delta (VMD) is presented. The work was motivated

by recent publications stating that extreme floods in the Mekong are likely to occur more frequently in the 21st century [Delgado et al., 2010, Hirabayashi et al., 2013], but also by the perceived need to shift flood management towards a risk-based approach. The presented quantification of flood risks to rice crops, the predominant land use in the region, is the first step in this direction, as a large-scale flood risk assessment has not been implemented to date. This work is thus the very first publication on a large-scale flood risk assessment for the agricultural sector in the VMD.

The results showed that the timing of the floods, the high tides and the cropping calendar are crucial factors for agricultural crop damage. Although the cropping calendars are adapted to the general flood dynamics in the different areas of the MD, large damages might still occur in the case of extreme events. A reliable seasonal forecast of the annual floods would thus be very helpful for a risk-based adaptive flood management of agricultural production. The study suggests that flood mitigation measures by the government and farmers, e.g. shifting of the cropping calendar and construction of dykes and sluice gates, before and after the historical flood in 2000 have greatly reduced potential agricultural flood damage.

The risk indicators, expected annual damage (EAD), and average crop risk per province can serve as the basis on which to develop spatially explicit flood management and mitigation plans for the delta. The crop risk maps, corresponding to two land-use change scenarios which are frequently used in the public and academic discussion, could be used as input for a cost–benefit analysis to evaluate the alternative of enlargement of the third rice crop in the two northern provinces.

Based on our findings, the following suggestions can be made to support flood management in the region: *(1)* appropriate maintenance is necessary for the flood control systems, with a strong emphasis on the low-dyke systems providing protection against the early flood wave before September. *(2)* The rice cropping scheme referred to as "ba nam tam vu", meaning eight rice crops every 3 years, should be reviewed. According to this scheme, sluice gates will be opened to allow floodwater to inundate the compartments in order to replenish the natural fertilization with deposited sediment at least once every 3 consecutive years. However, the study of Manh et al. [2014] revealed that during low flood years the estimated deposited sediment in the VMD was ∼14 times smaller than in years of extreme floods. Thus, opening flood compartments during low flood year might result in little sediment deposition in paddy fields. We propose to open the flood compartments protected with high dykes in An Giang and Dong Thap during extreme events (i.e. larger than a 10-year return period). However, for a proper implementation of such a scheme, a reliable seasonal forecasts of the expected floods are required. Our estimation of flood damage (D) can be used as reference for developing such management plans based on a thorough cost–benefit analysis including a quantitative consideration of the benefits of

natural fertilization vs. mineral fertilizers. *(3)* The current pilot programme on agriculture insurance should be revised, at least for rice cropping in the VMD. Insurance premiums are preferably calculated based on the average rice yield per province. Using our spatially explicit results would include the actual flood hazard of the insured area. However, the damages should be updated to current economic values, as the values of 2011 were used.

Finally, our inundation hazard maps can be used to quantify flood damages and risks to other agricultural crops and land use in the MD if appropriate land-use maps and damage models are available. In a similar manner changes in flood hazard and risk inflicted by impacts of climate change, sea level rise, the pronounced deltaic land subsidence, landuse changes, and upstream hydropower development can be quantified systematically. These issues will be addressed in future work.

Chapter 4 Future projections of flood dynamics in the Vietnamese Mekong Delta

Abstract

The annual flood pulse of the Mekong River is crucial to sustain agriculture production, nutrition, and the livelihood of millions of people living in the Vietnamese part of the Mekong Delta (VMD). However, climate change impacts on precipitation, temperature and sea-level combined with land subsidence, upstream hydropower development, and water infrastructures (i.e. high-dykes construction) are altering the hydrological regime of the VMD. This study investigates future changes in flood hazard and agricultural production caused by these different scales of human-induced stresses. A quasi- two-dimensional (quasi-2D) hydrodynamic model was used to simulate eight scenarios representing the individual and compound impacts of these drivers for a baseline (1971-2000) and future (2036-2065) period. The scenarios map the most likely future pathway of climate change (RCP 4.5) combined with the best available Mekong upstream hydropower development, and land subsidence scenarios as well as the current delta development plan. We found that sea-level rise and land subsidence would cause the highest changes in flood hazard and damage to rice crop, followed by hydropower and climate change impacts. Expansion of high-dyke areas in two northernmost delta provinces (An Giang and Dong Thap) would have the smallest impact. The combination of all modelled drivers is projected to increase delta inundation extent by 20%, accompanied with prolonging submergence of 1–2 months, and 2–3 times increase in annual flood damage to rice crops in the flood-prone areas of the VMD. These findings of likely increasing risk of tidal induced flood hazard and damage call for well-planned adaptation and mitigation measures, both structural and non-structural.

Published as: Triet, N. V. K., Dung, N. V., Hoang, L. P., Duy, N. L., Tran, D. D., Anh, T. T., Kummu, M., Merz, B., and Apel, H.: Future projections of flood dynamics in the Vietnamese Mekong Delta, Science of The Total Environment, 742, 140596, https://doi.org/10.1016/j.scitotenv.2020.140596, 2020.

4.1 Introduction

World river deltas comprise less than 1% of the Earth's landmass, but they are home for over 500 million inhabitants [Ericson et al., 2006]. Further, many deltas are the key source of regional and even global nutrition due to their rich ecological systems (e.g. fishery), and fertile soils supporting food production. Yet their residents face imminent threats of floods, losses of landmass, pollution, and saline water intrusion. These threats will become even larger under climate change and development activities [e.g. Hirabayashi et al., 2013, Tessler et al., 2015], and will challenge national to global food security [Nelson et al., 2010, Kummu et al., 2012]. In the light of these outlooks, this study aims to give insights on future flood dynamics under multiple future drivers in the Vietnamese Mekong Delta (VMD), the world's third-largest coastal floodplain, which is essential to the food production and security of Vietnam.

The VMD is home for 18 million people; it contributes over 50% of the country's food production, and over 80% of Vietnam's exported rice [GSO, 2015]. Livelihoods of millions of delta residents depend on the annual flood pulse of the Mekong River. While extreme floods can cause excessive damages and losses (e.g. estimated economic losses from the historical flood in 2000 were USD 250 *million*, and over 450 fatalities [Kreibich et al., 2017]), the annual flood benefits in the Lower Mekong Basin (LMB) are estimated at USD 8–10 *billion* on average [MRC, 2012]. Replenishing soil nutrients, support of the ecological system, provision of sediment to counter deltaic land compaction and erosion are some of the well-acknowledged flood benefits [Manh et al., 2014]. Understanding delta flood dynamics is an important, yet highly challenging task to ensure safety and sustainable development of the region.

The VMD with its extreme low mean elevation $0.8m$ [Minderhoud et al., 2019] is one of the globally most vulnerable deltas to climate change and sea-level rise [Tessler et al., 2015]. Recent climate impact projections revealed an intensification in magnitude [Lauri et al., 2012, Hoang et al., 2018] and frequency of extreme floods (i.e. the 100-year flood) in the Mekong River basin [Hirabayashi et al., 2013]. The Fifth Assessment Report of the Intergovernmental Panel on Climate Change predicted an increase of 17–38 cm in tidal level along the coast of the VMD by mid-century [IPCC, 2014b].

In addition to the climate-related factors, anthropogenic interventions both locally and upstream would likely alter the flood dynamics of the VMD. Locally, the deltaic land subsidence amplifies the rising sea-level; the VMD is rapidly sinking at rates of 1.0–2.5 $cm\ year^{-1}$ because of unsustainable groundwater extraction, which is expected to continue in the future. This will increase the risk in both fluvial and tidal induced floods [Erban et al., 2014, Minderhoud et al., 2017]. Further, the development of local water infrastructures also contributes to the alteration of delta inundation dynamics. The construction of high-

dykes and sluice gates have been the conventional flood management approach in the VMD [Hung et al., 2012, Tri, 2012]. These structures prevent protected areas from being flooded and thus reduce flood hazard within the protected areas; however, they divert the flood hazard to neighbouring, mostly downstream communities [e.g. Triet et al., 2017, Tran et al., 2018b]. Besides, sand mining in the LMB is likely to increase flood risk in the VMD [Hackney et al., 2020].

In upstream part of the Mekong Basin, hydropower development affects the hydrological regime and flood pulse of the Mekong [Lauri et al., 2012, Räsänen et al., 2017, Hecht et al., 2019]. The Mekong River Commission (MRC) estimates the basin's active reservoir storage in 2025 would reach 86.8 km^3, about 19% of the mean annual flow of the Mekong [MRC, 2015b]. Note that the estimation from MRC does not include data of the existing and planned dam in China; with the active reservoir storage from the existing dams amounts to 23.0 km^3 [Räsänen et al., 2017]. Besides altering the flow regime of the Mekong as reported in Räsänen et al. [2017], there are concerns about serious impacts on ecosystems [Ziv et al., 2012, Arias et al., 2014], on sediment dynamics [Kummu et al., 2010, Manh et al., 2015, Kondolf et al., 2018], and on the livelihoods of millions of delta inhabitants [Pearse-Smith, 2012].

Although impacts of individual drivers to the VMD have been studied [e.g. Le et al., 2007, Van, 2009, Van et al., 2012, Triet et al., 2017, Dang et al., 2018, Tran et al., 2018b], the compound impacts of all drivers on flood hazard have not been quantified. Moreover, the compound impacts in terms of damage to agriculture crops have not been assessed yet. Dang et al. [2018] investigated changes in the hydrological regime driven by hydropower development, land subsidence, sea-level rise, and local water infrastructure development in the VMD; the authors, however, neither considered climate change nor the cumulative impacts of all drivers. Van et al. [2012], in turn, studied the delta inundation regime in response to climate change using the projected future Mekong streamflow from Hoanh et al. [2010]; arguably this dataset is highly uncertain, because only a single Global Circulation Model (GCM) was used (taken from Lauri et al. [2012]). To fill this knowledge gap, in this study we aim to provide future projections of flood dynamics in the VMD driven by (i) climate change impacts on precipitation and temperature along the Mekong, (ii) sea-level rise plus deltaic land subsidence (so-called effective sea-level rise), (iii) upstream hydropower development, and (iv) development of local water infrastructures. We consider both the individual and cumulative impacts in a set of model simulations of flood dynamics in the Mekong Delta, using state-of-the-art hydrodynamic model MIKE 11. Besides, our study provides an estimation on changes in flood damage to rice cultivation, the predominant land-use type in the region.

4.2 Regional setting

The Vietnamese Mekong Delta (VMD) covers a land area of around 40,000 km^2 in the southernmost tip of Vietnam between 8.5–11.5°N and 104.5–106.8°E. On average, annually 475 $km^3$of the Mekong flow routes through the VMD between June and November, submerging 35–50% of the delta with inundation depths up to 4.0 m for 2–5 $months$ [Toan, 2014]. This flood-prone area of the VMD is commonly distinguished into deep and shallow submergence regions based on inundation depth, i.e. above/less than 1.5 m (right panel of Fig. 4.1. A dense network of natural and man-made channels intersects the delta and separates it into thousands of compartments enclosed by channels. Dykes, sluice gates and pumps are added to protect the compartments against floods or saline water intrusion. There are two types of dykes which are referred to as "low-dyke" and "high-dyke". Low-dykes often have crest levels 1.5–4.0 m $a.m.s.l.$, retaining floodwater from the first flood peak until about mid-August to support the double season rice crop cultivation per year. High-dykes have crest level at 4.0–6.0 m $a.m.s.l.$ on average; therefore, floodplains protected with high-dykes can be cut off from the natural inundation regime, enabling the cultivation of a third rice crop during the flood season. The operation of sluice gates, and pumping stations control the water flow in and out of these compartments [Hung et al., 2012]. Hence, the floodplain processes in the VMD are a result of a complex hydrodynamic interaction of fluvial dynamics, tidal influence, and operation of delta water infrastructures.

4.3 Methodology

4.3.1 Flood propagation model

The presented work modelled the Mekong Delta flood dynamics with the MIKE 11 software developed by the Danish Hydraulic Institute (DHI) (https://www.mikepoweredbydhi.com/). The model structure was initially developed and calibrated by Dung et al. [2011], and have since been continually updated and applied to evaluate flood hazard and damage [Triet et al., 2017, 2018], and sedimentation dynamics [Manh et al., 2014, 2015]. The calibration and validation of this flood propagation model covered a wide spectrum of flood events, including high flood events (e.g. in 2000, 2011), a normal flood event as occurred in 2009, and a low flood year as in 2010 [Triet et al., 2017]. Figure 2.4 (Chapter 2) exemplifies the calibration results for the two recent extreme floods in 2000 and 2011. The model set up, calibration, and validation are described in detail in the cited references.

We adopted the latest model setup of [Triet et al., 2017]. The model domain covers an area of 55,000 km^2 of the Mekong floodplain downstream of Kratie in Cambodia,

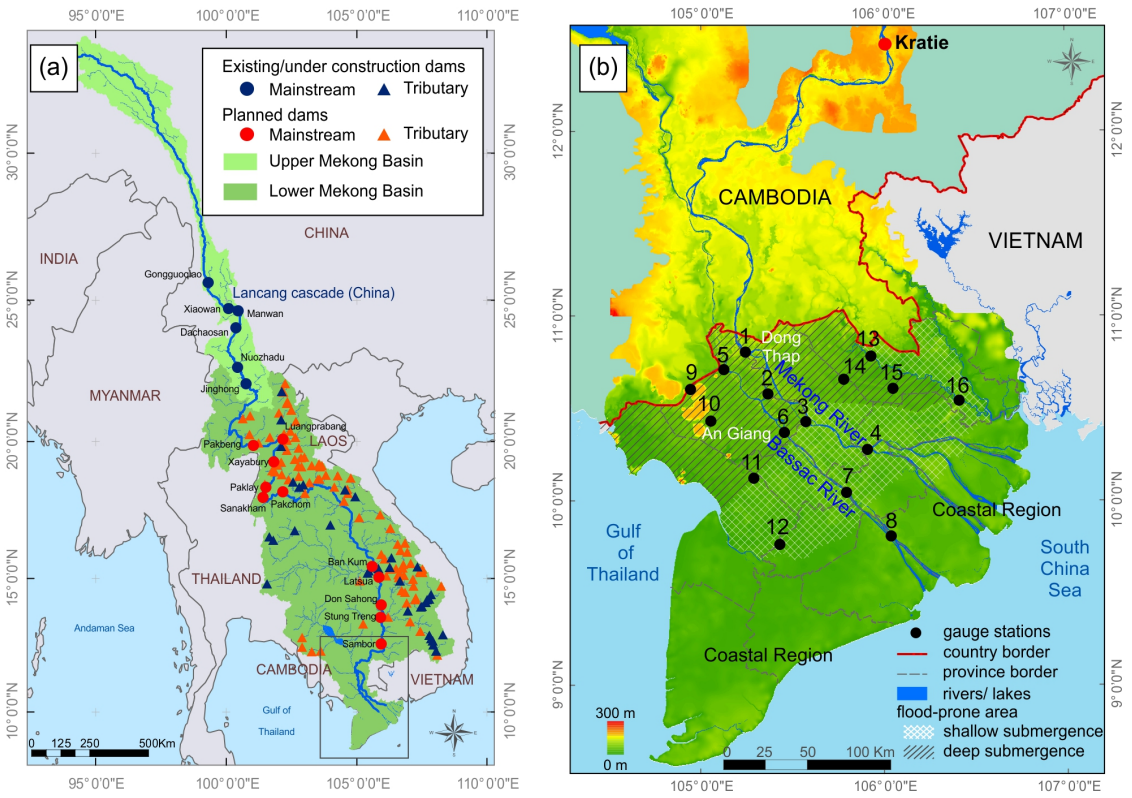

Figure 4.1: Mekong River Basin and location of hydropower projects [Hoang et al., 2018]. (b) The Mekong Delta from Kratie (red dot) to the sea and location of hydrological stations, the Vietnamese Mekong Delta, and its flood-prone, deep and shallow, regions.

including the Tonle Sap lake system (Fig. 4.2 b). Triet et al. [2017] model floodplain inundation process within the one-dimensional modelling software MIKE 11 using virtual branches with wide cross-sections extracted from a digital elevation model (DEM). The dykes enclosing the floodplain compartments are introduced in the model structure as broad crest weirs, with crest levels reflecting dyke height (Fig. 4.2 c). Other flood control structures, e.g. weirs, dams, are also incorporated whenever information is available. The model network comprises 4,000 channels and 2,500 control structures. A complete simulation of one flood event of six months (1 June–30 November) requires 2–3 *hours* on a local PC.

4.3.2 Simulation scenarios

We set up eight scenarios (summarized in Table 4.1 to assess possible changes in flood hazard driven by (1) hydropower dam development in the entire Mekong Basin, (2) changes in flood control infrastructure in the VMD, (3) river flow influenced by climate change, (4) sea-level rise and deltaic land subsidence, i.e. "effective sea-level rise". We first modelled impacts of individual drivers, followed by their cumulative impacts. In each scenario, flood hazard was quantified using the quasi-2D model, which was driven by a 30-year flow series at Kratie. As the focus of the study is on flood hazard and damage, only the flood season

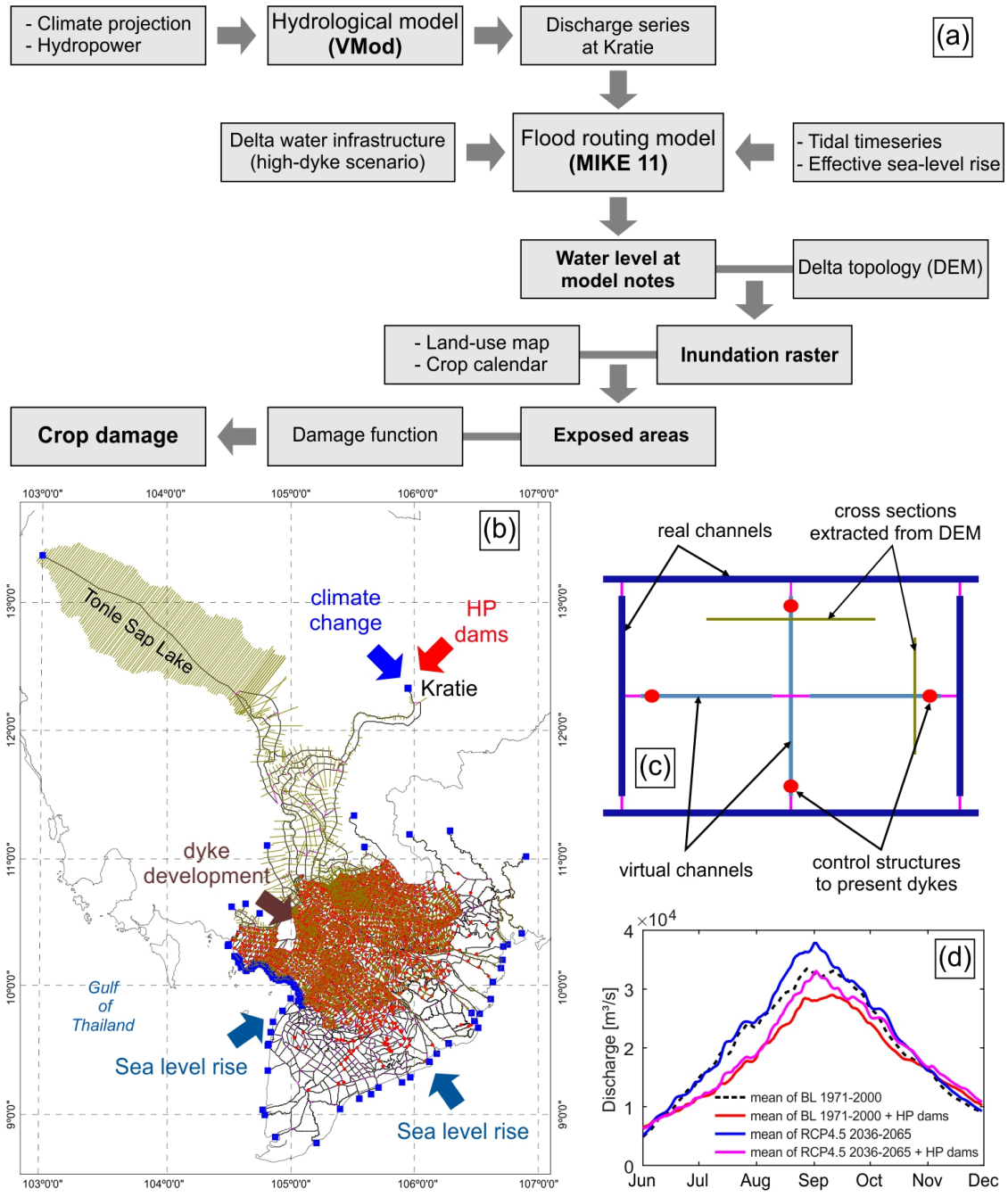

Figure 4.2: (a) Flowchart for the applied methodology to estimate changes in flood dynamics in the VMD. (b) Channel network of the large-scale quasi-2D flood propagation model, and locations where the different drivers affect as considered in the model. (c) Scheme illustrating the modelling of 2-D floodplain inundation and dyke system in the 1D modelling package MIKE 11. (d) Mean baseline and projected future discharge series at Kratie, based on data of Hoang et al. [2018] and calculated as the mean of the 30-year daily discharge of the baseline and future periods.

from June to November was simulated for each year in the 30-year period.

Baseline (BL): the *BL* scenario used the 1971-2000 discharge series at Kratie as the upstream boundary condition, matching the baseline period of Hoang et al. [2018]. Because

the complete timeseries of tidal levels for this period were not available, the average hourly tidal levels of the period 1971-2000 were used as downstream boundary condition. The dyke system as surveyed in 2009 and 2010 was implemented in the hydrodynamic model representing the present state of infrastructure development.

Hydropower development (S1-HP): the flow series at Kratie was simulated as consequences of all hydropower dams on the baseline flow (i.e. period 1971-2000 + all planned dams realized).

Floodplain restoration (S2-FR) and *High-dyke expansion (S3-DE)*: these two scenarios represent changes in local water infrastructure according to two development plans for the VMD proposed in Deltares [2013] in the Mekong Delta plan. *S2-FR* aims at enhancing flood storage capacity, as floodwater is stored in a large number of floodplain compartments protected by high-dykes in An Giang and Dong Thap provinces (Fig. 4.1 b) during high flood phase, i.e. September–October, in order to reduce the flood hazard downstream. On the contrary, *S3-DE* assumes expansion of high-dyke protected floodplains in these two provinces to support the expansion of triple rice crop cultivation, following the "Food Production Scenario".

Climate change (S4-CC): the discharge of the period 2036-2065 as projected by the MPI-ESM-LR (MPI) global simulation model under the Representative Concentration Pathway 4.5 (RCP 4.5) scenario was used as upstream boundary at Kratie.

Sea-level rise (S5-SLR): this scenario investigates future changes in delta inundation under impacts of sea-level rise and deltaic land subsidence. Manh et al. [2015] suggested that the tidal level might increase 22–63 *cm* in the 2050s as consequence of effective sea-level rise. We used the mean of the suggested range (+43 *cm*) as change in the downstream boundary of the quasi-2D model.

Business as Usual (S6-BAU): cumulative impacts of all drivers were examined in the *S6-BAU* scenario. This simulation considered the projected discharge of Kratie in 2036-2065, including all planned hydropower dams. The downstream boundary condition of the hydrodynamic model incorporated future effective sea-level rise, and delta infrastructure was modelled as in *S3-DE*.

Sustainable development (S7-SD): this scenario explores the possibility of countering the effects of climate change and effective sea-level rise on flood hazard with sustainable development measures. The planned hydropower development was excluded, because it is a non-sustainable development causing a series of problems on delta sediment equilibrium, river bank erosion, flood dynamics [Kondolf et al., 2014, Anthony et al., 2015, Pokhrel et al., 2018a,b, Hecht et al., 2019, Nhan and Cao, 2019]. *S7-SD* is the combination of the scenarios *S2-FR*, *S4-CC* and *S5-SLR*.

Table 4.1: Scenarios used to investigate the impacts of climate change, hydropower development, sea-level rise and subsidence, and delta water infrastructure on flood dynamics in the VMD.

Name	Scenario description	Climate change	Hydro-power	Tidal level	Dyke system
BL	Simulated baseline conditions (1971-2000) + dyke system in VMD as survey data of 2009-2010	N[a]	N	N	N
S1-HP	Hydropower Development: Baseline conditions plus the impacts of hydropower development	N	Y	N	N
S2-FR	Floodplain Restoration: Baseline condition plus open high-dyke compartments in two delta provinces: An Giang and Dong Thap to provide flood storage	N	N	N	Y(1)[b]
S3-DE	Dyke Expansion (DE): Baseline condition plus the expansion of high-dyke compartments in An Giang and Dong Thap to maximize food production	N	N	N	Y(2)[c]
S4-CC	Climate Change: Climate change scenario from MPI-ESM-LR (2036-2065) and RCP4.5	Y	N	N	N
S5-SLR	Effective Sea Level Rise: Baseline + impacts of sea-level rise and land subsidence	N	N	Y + 43 cm	N
S6-BAU	Business as Usual: cumulative impacts of all drivers CC, HP dams, SLR, and expansion of high-dyke compartments	Y	Y	Y + 43 cm	Y(2)
S7-SD	Sustainable Development: cumulative impacts of CC + SLR, no further dams being built, and high-dyke flood compartments opened providing flood storage	Y	N	Y + 43 cm	Y(1)

[a] *No (N) / Yes (Y)*

[b] *Y(1): open high-dyke compartments in the delta provinces An Giang and Dong Thap to provide flood storage.*

[c] *Y(2): expand high-dyke compartments in An Giang and Dong Thap to maximize cultivation of triple rice crop in these provinces.*

4.4 Data

4.4.1 Upstream boundary condition of the hydrodynamic model

The upstream boundary of the hydrodynamic model is the gauge station Kratie in Cambodia (Fig. 4.1). The hydrodynamic model is driven by simulated daily discharge series of the Mekong River given in Hoang et al. [2018]. The authors used the distributed, grid-based hydrological model VMod to simulate hydrology and flow dynamics of the Mekong River. The VMod model is grid-based, with varying cell sizes ranging from hundred metres up to several kilometres. For each time step and grid cell, the model first computes the climate forcing from the input meteorological data, followed by the computation of the vertical soil water balance. The runoff from each grid cell is routed through the entire river network to obtain discharge at the gauge Kratie, which is the terminus of the VMod model [Lauri et al., 2012].

Hoang et al. [2018] developed a VMod application covering the entire Mekong River Basin at 5×5 km spatial resolution, and simulated historical Mekong River flow using the WATCH climate data set (http://www.eu-watch.org/) and the APHRODITE precipitation data set (http://www.chikyu.ac.jp/precip/old/index.html). The future Mekong flow was simulated using five GCMs, two emission scenarios (RCP 4.5 and RCP 8.5), and two basin development scenarios, comprised of hydropower dams development and irrigation expansion. Model calibration and validation were performed using observed discharge

series at seven monitoring gauges in the Mekong mainstream from the most upstream at Chiang Sean to most downstream at Kratie. The model performed well against the observations, Nash-Sutcliffe efficiency coefficient of 0.67 for daily discharge, on average, for calibration (1981-1990) and validation (1991-2000). Räsänen et al. [2017] verified that the VMod model is capable of reproducing the flow alteration in the Lower Mekong Basin (LMB) resulting from the hydropower development in the Upper Mekong Basin (UMB). For a detailed description of the modelling setup, calibration, and validation of the VMod model, the readers are referred to [Lauri et al., 2012, Hoang et al., 2016, 2018].

Due to the large number of scenarios, given the different drivers and their combinations (see section 4.3.2), and the required simulation time, not all future scenarios of Hoang et al. [2018] were used to drive the hydrodynamic model. Out of the five GCMs, the MPI-ESM-LR (MPI) model was selected, because it is representative of the mean future hydrology of the Mekong predicted by VMod using all five GCMs (cf. to Fig. 4 in Hoang et al. [2016]). Furthermore, only the RCP 4.5 climate scenario was used, based on the argument of Wang et al. [2017], that global temperature is unlikely to increase above 2.6°C by the end of the century due to the limited supply of fossil fuels. The RCP 4.5 closely matches this argument, as it assumes a peak in greenhouse gas emissions around 2040 with a subsequent decline, which is associated with a projected increase in global mean temperature of 1.1–2.6°C by the end of the 21^{st} century [IPCC, 2014b]. The impacts of irrigation expansion in the LMB were not considered in our assessments due to the minor alteration of the flood season flow at Kratie (less than 3% as depicted in Fig. 2 of Hoang et al. [2018]).

4.4.2 Tidal level, elevation, land-use and other relevant data

Hourly tidal level records from ten national tidal gauges along the coast of the VMD were obtained from the Southern Regional Hydro-Meteorology Center of Vietnam (SHRMC). These data served as lower boundary conditions for the hydraulic model. Locations, dimensions, and operation schemes of flood control structures in the VMD were acquired from the provincial Departments of Agriculture and Rural Development (DARDs). For the model setup and the derivation of inundation raster maps, a high-resolution (5×5 m) lidar-based DEM of the VMD acquired from the Ministry of Environment and Natural Resources of Vietnam (MONRE) was used. LiDAR data was collected and processed between 2009 and 2010. Land-use data of the VMD was provided by the German Aerospace Centre (DLR). Leinenkugel et al. [2013] derived land-use map using the Moderate Resolution Imaging Spectroradiometer (MODIS) instrument aboard the Terra and Aqua satellites. The authors combined different MODIS products were combined to provide cloud free composites for the period 2001-2011, calculated the enhanced vegetation index (EVI), and performed the land-use classification. Triet et al. [2018] reclassified this original product

to two raster images representing the summer-autumn crop, and autumn-winter crop to support flood damage calculation (cf. to Fig.3 in Triet et al. [2018]).

4.5 Results

4.5.1 4.5.1 Future projections of flood hazard and impacts of each driver

Average changes

The average annual maximum water level (*AMWL*) and date of occurrence of *AMWL* (*DO*) at 16 investigated gauges, computed as the mean of 30 flood events, are compared against the baseline simulation. The two-sided t-test is applied to mark the gauges and scenarios with significant changes in mean *AMWL*s or *DO*s (Table 4.2 and 4.3).

Table 4.2: Simulated annual maximum water level (AMWL) at main hydrological gauges in the VMD corresponding to the eight scenarios, computed as average of the 30-yr baseline and future periods. Statistically significant ($p<0.05$) changes compared to the baseline are marked in bold. The numbers in brackets present the changes compared to the baseline. [Unit: meter].

Station name	Modelling scenarios							
	BL	*S1-HP*	*S2-FR*	*S3-DE*	*S4-CC*	*S5-SLR*	*S6-BAU*	*S7-SD*
Tan Chau [1][a]	3.41	**3.03** (–0.38)	3.39 (–0.02)	3.43 (0.02)	3.60 (0.19)	3.55 (0.14)	3.40 (–0.01)	**3.69** (0.28)
Vam Nao [2]	2.55	**2.31** (–0.24)	2.53 (–0.02)	2.56 (0.01)	2.67 (0.12)	**2.76** (0.21)	2.67 (0.12)	**2.84** (0.29)
Cao Lanh [3]	1.96	**1.86** (–0.10)	1.96	1.97 (0.01)	2.02 (0.06)	**2.29** (0.33)	**2.26** (0.30)	**2.33** (0.37)
My Thuan [4]	1.66	**1.64** (–0.02)	1.66	1.66	**1.69** (0.03)	**2.05** (0.39)	**2.06** (0.40)	**2.08** (0.42)
Chau Doc [5]	3.16	**2.77** (–0.39)	3.12 (–0.04)	3.17 (0.01)	3.34 (0.18)	3.30 (0.14)	3.14 (–0.02)	**3.42** (0.26)
Long Xuyen [6]	2.06	**1.96** (–0.10)	2.06	2.07 (0.01)	2.12 (0.06)	**2.37** (0.31)	**2.34** (0.28)	**2.41** (0.35)
Can Tho [7]	1.77	**1.73** (–0.04)	1.77	1.77	1.80 (0.03)	**2.14** (0.37)	**2.13** (0.36)	**2.17** (0.40)
Dai Ngai [8]	1.82	**1.81** (–0.01)	1.82	1.82	1.84 (0.02)	**2.25** (0.43)	**2.25** (0.43)	**2.26** (0.44)
Xuan To [9]	3.06	**2.62** (–0.44)	3.02 (–0.04)	3.07 (0.01)	3.28 (0.22)	3.21 (0.15)	3.03 (–0.03)	**3.35** (0.29)
Tri Ton [10]	1.86	**1.58** (–0.28)	1.85 (–0.01)	1.87 (0.01)	1.95 (0.09)	**2.04** (0.18)	1.94 (0.08)	**2.13** (0.27)
Tan Hiep [11]	1.16	**1.05** (–0.11)	1.16	1.16	1.20 (0.04)	**1.39** (0.23)	**1.36** (0.20)	**1.44** (0.28)
Vi Thanh [12]	0.74	0.73 (–0.01)	0.74	0.74	0.75 (0.01)	**1.15** (0.41)	**1.15** (0.41)	**1.16** (0.42)
Moc Hoa [13]	1.75	**1.51** (–0.24)	1.75	1.77 (0.02)	1.86 (0.11)	**1.97** (0.22)	1.86 (0.11)	**2.06** (0.31)
Hung Thanh [14]	1.99	**1.76** (–0.23)	1.99	2.02 (0.03)	2.11 (0.12)	**2.18** (0.19)	2.09 (0.10)	**2.27** (0.28)
Kien Binh [15]	1.20	**1.09** (–0.11)	1.19 (–0.01)	1.20	1.25 (0.05)	**1.49** (0.29)	**1.46** (0.26)	**1.54** (0.34)
Tan An [16]	1.24	**1.23** (–0.01)	1.24	1.24	1.26 (0.02)	**1.63** (0.39)	**1.63** (0.39)	**1.65** (0.41)

[a] *The numbers next to the station names denote their location (Fig. 4.1, right panel).*

Changes in average *AMWL*s are statistically significant in four scenarios, driven by (i) hydropower development (*S1-HP*) by –1 to –44 *cm*, (ii) effective sea-level rise (*S5-SLR*) by 19–43 *cm*, or (iii) a combination of these (*S6-BAU* and *S7-SD*) by 26–44 *cm*. The climate change (*S4-CC*) scenario projects an increase in mean *AMWL*s by 1–15 *cm* with the most substantial increases at gauges in the northern part of the VMD. However, these changes are not statistically significant at $p=0.05$. For the scenarios *S2-FR* and *S3-DE* with fewer or more high-dyke flood compartments in the VMD, respectively, minor changes

Table 4.3: Simulated shifts in date of occurrence of annual maximum water level (DO) at main hydrological gauges in the VMD. The DOs are computed as computed as the mean of the 30-yr baseline and future periods [Unit: day].

Station name	Modelling scenarios							
	BL	*S1-HP*	*S2-FR*	*S3-DE*	*S4-CC*	*S5-SLR*	*S6-BAU*	*S7-SD*
Tan Chau [1][a]	Sep. 22	+3	0 [b]	0	+1	+3	+6	+3
Vam Nao [2]	Sep. 29	+6	+1	0	–2	+2	**+9**	+1
Cao Lanh [3]	Oct. 11	**+10** [c]	+1	–2	–1	+7	**+12**	+4
My Thuan [4]	Oct. 31	**+17**	0	0	+2	**+8**	**+14**	+5
Chau Doc [5]	Sep. 26	+2	0	–2	–2	0	+4	+1
Long Xuyen [6]	Oct. 09	+6	0	–2	0	+1	+10	+2
Can Tho [7]	Oct. 23	**+11**	–1	–2	–1	–1	**+9**	+2
Dai Ngai [8]	Oct. 29	+1	0	0	0	0	+2	+1
Xuan To [9]	Sep. 27	+2	0	–2	–1	0	+2	+1
Tri Ton [10]	Sep. 30	+3	0	–1	+2	+2	+7	+5
Tan Hiep [11]	Oct. 07	**+8**	+3	0	+2	**+8**	**+14**	+9
Vi Thanh [12]	Nov. 03	**+13**	0	0	0	**+9**	**+16**	+5
Moc Hoa [13]	Oct. 05	–1	0	0	+2	+3	+5	+3
Hung Thanh [14]	Oct. 07	+1	+1	–2	+2	0	+6	+3
Kien Binh [15]	Oct. 14	0	–1	–1	–1	+3	+15	+6
Tan An [16]	Nov. 01	**+20**	+1	–1	+2	**+13**	**+17**	+7

[a] *The numbers next to the station names denote their location (Fig. 4.1, right panel).*

[b] *No difference in the DO compared to baseline.*

[c] *Statistically significant ($p < 0.05$) changes compared to the baseline are marked in bold.*

in mean *AMWL*s in the range of 1–5 *cm* are obtained. For the mean *DO*s, all but three scenarios project an insignificant shift. Similar to changes in mean *AMWL*s, significant alteration in mean *DO*s are modelled in the scenarios *S1-HP*, *S5-SLR* and *S6-BAU*, with a smaller spatial distribution compared to changes in modelled *AMWL*s. The impact is limited to a few gauges in the middle region of the delta (e.g. Can Tho, My Thuan) delaying the occurrence of the *AMWL*s by 10–20 *days* (Table 4.3).

Figure 4.3 summarises the modelled flood extent of the 30 flood events for the eight scenarios. The most significant increases in flood extent are found in the scenarios simulating the impacts of effective sea-level rise, i.e. *S5-SLR*, *S6-BAU*, and *S7-SD*. Mean flood extents increase by 35%, 28% and 43%, respectively, in comparison to the baseline scenario with 22,500 km^2 mean extent. *S2-FR* and *S4-CC* (floodplain restoration and climate change) project only slightly larger flood extent of 3%, while hydropower development (*S1-HP*) and expansion of high-dyke flood compartments (*S3-DE*) reduce the flooded area by 7% and 3%, respectively.

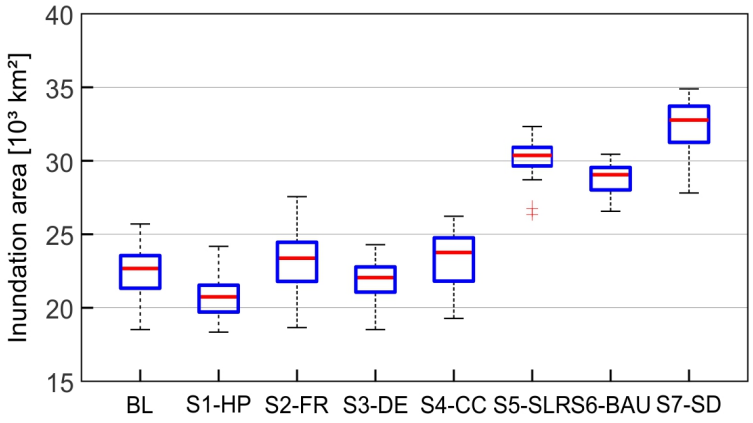

Figure 4.3: Boxplot of the simulated maximum inundation extent for 30 flood events for the eight scenarios.

Changes for a dry, normal and wet year

Impact of hydropower development: The hydropower development scenario shows considerable effects on the flood hydraulics in the Mekong Delta for the dry, normal and wet year. The hydropower dams reduce the flood volume at Kratie during the rising and high flood phase (July-September) 7% in the dry year, and by 15% in the normal and wet years. Compared to the baseline, hydropower development causes a decrease in *AMWL*s of 14% at maximum in a wet year, and up to 27% in a normal or dry year. Eight of the 16 gauges show a decrease in *AMWL*s of more than 5% in the dry year. In the normal and wet years, this decrease in *AMWL*s is observed at even 12 stations (Fig. 4.4 a-c). The largest decreases are found in the northern part of the VMD, where *AMWL*s reduce by 30–70 *cm* (13–30%) at Chau Doc at the Vietnam-Cambodia border. The magnitude of changes sharply decreases –7 to –16 *cm* (4–8%) at Long Xuyen about 60 *km* downstream of Chau Doc, and below –6 *cm* (–5%) at Can Tho in the middle of the delta. Inundation extent also decreases by 8% in the normal year (in relation to 23,000 km^2 or 57% of the delta area), by 5% in the wet year (in relation to 24,500 km^2, 61%), and by 1% in the dry year (in relation to 19,000 km^2, 47%) (Fig. 4.5 a-c). Hydropower dams also shorten the inundation duration. The inundation duration of more than three months in the baseline scenario decreases by 3% in the normal year, and 5% the wet year (Fig. 4.6 and Table B4 in the Appendix B). For the dry year, no changes are modelled.

Impact of local water infrastructure: The local water infrastructure scenarios, floodplain restoration *S2-FR* and expansion of high-dyke compartments *S3-DE*, cause relative minor changes. Both scenarios show no changes in *AMWL*s compared to the baseline in the dry year (Fig. 4.4 d-g). Small decreases of less than 5% (1–5 *cm*) in *AMWL*s are modelled for *S2-FR* in the normal and wet years (Fig. 4.4 e-f). A similar magnitude, but opposite sign is projected for *S3-DE* (Fig. 4.4 h-i). Flood extent alters by ±1.5 % in the normal

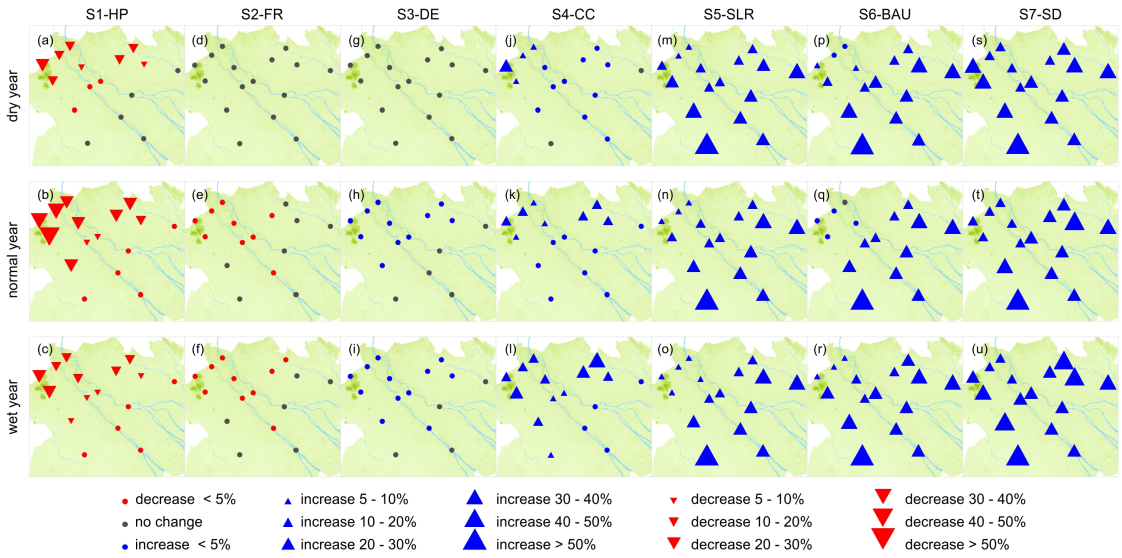

Figure 4.4: Changes in annual maximum water level at main gauges in the VMD relative to the baseline (BL) corresponding to a dry, normal and wet years. See Tables B1 to B3 in the Appendix B for absolute changes.

year, and by ±3% in the wet year; positive changes are computed for *S2-FR*, and negative changes for *S3-DE*. Changes in inundation depth (above 0.5 *m*) and inundation duration (above 2 months) occur at the high-dyke flood compartments which are opened to intake floodwater in *S2-FR* runs (blue pixels in Fig. 4.5 d-f), or at low-dyke compartments converted to high-dykes in *S3-DE* (red pixels in Fig. 4.5 g-i). The effects are thus rather limited and confined to the areas where the changes in water infrastructure were defined (deep submergence areas in the northern part of the VMD). The impacts on downstream areas in terms of *AMWL*s, flood extent and duration are small (below 2 *cm* in *AMWL*).

Impact of climate change: For the climate change scenarios *S4-CC*, the spatial patterns of changes are similar to the impacts of hydropower development, i.e. confined to the border of Vietnam and Cambodia and the centre of the VMD. Compared to the baseline, climate change increases the *AMWL*s by 20–35 *cm* (10–15%) at Chau Doc, 3–15 *cm* (2–8%) at Long Xuyen, and 2–7 *cm* (less than 5%) at Can Tho, with higher changes computed in the wet year (Fig. 4.4 j-l and Table B1-B3 in the Appendix B). Flood extent increases by 1%, 3% and 7% in the dry year, normal year and wet year, respectively (Fig. 4.6 and Table B4 in the Appendix B); and inundation depth increases by 10–40 *cm* (Fig. 4.5 j-l). The impacts of climate change on delta flood hazard approximately offset the changes caused by hydropower development (*S1-HP*) except for the normal year, particularly the inundation depths. For inundation duration, the area inundated for more than two months increases by 1% in the dry and normal years, and by 9% in the wet year (Fig. 4.6 and Table B4 in Appendix B).

Impact of effective sea-level rise: The largest changes in *AMWL*s are obtained in the *S5-SLR* scenario, showing the impacts of effective sea-level rise (sea-level rise plus deltaic

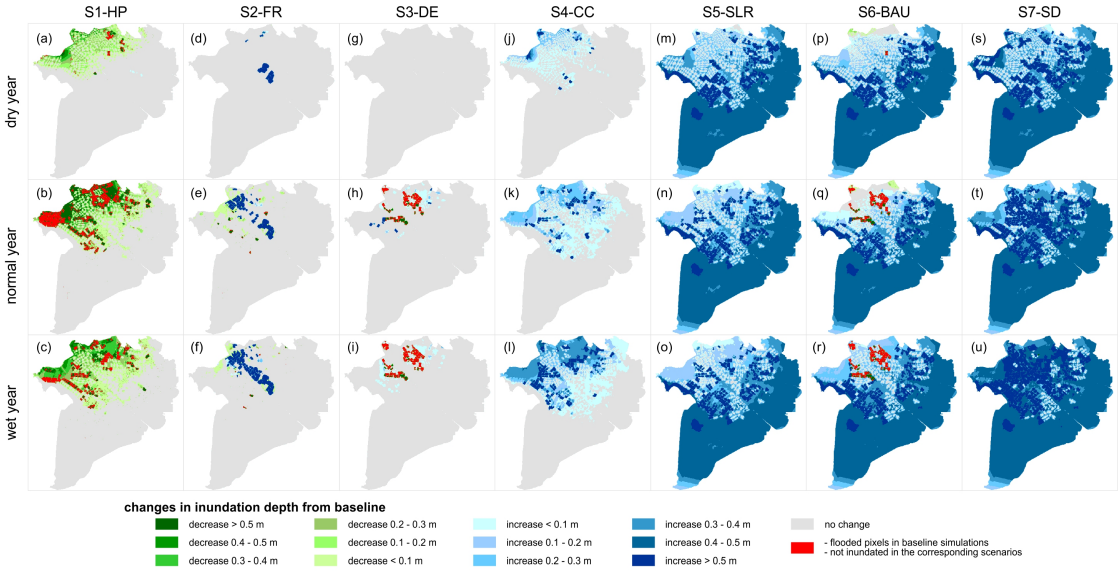

Figure 4.5: Changes in inundation extent and depth relative to the baseline (BL) corresponding to a dry, normal and wet years.

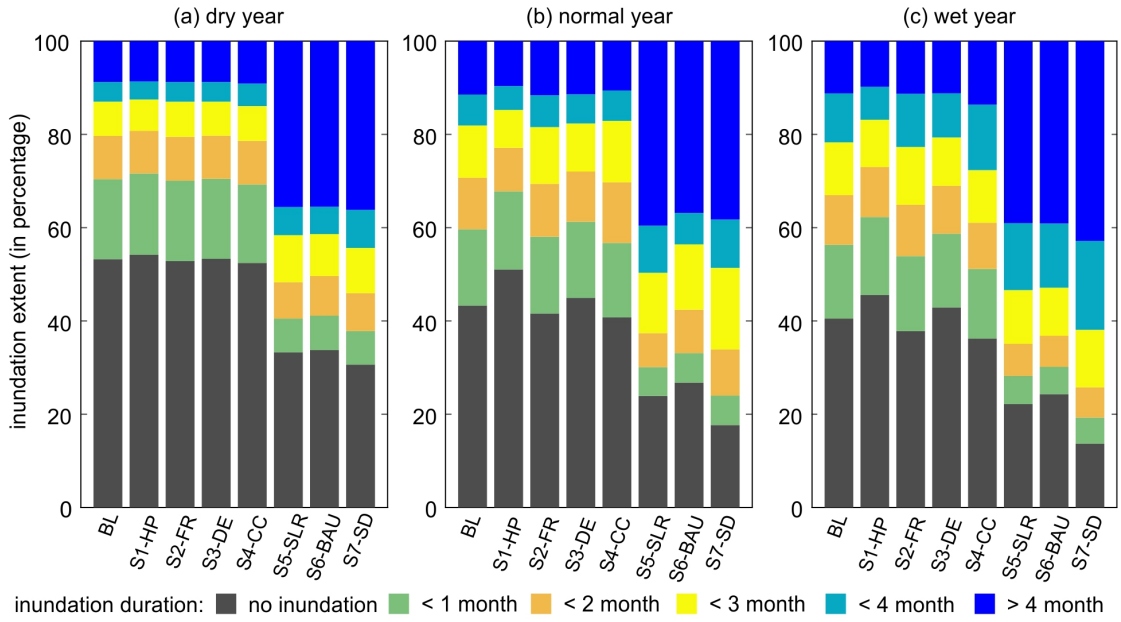

Figure 4.6: Inundated extent differentiated according to duration (number of months flooded) by the different scenarios in dry year (a), normal year (b), and wet year (c). See Table B4 in the Appendix B for tabulated data.

land subsidence). The *AMWL*s increased by 13–40 *cm* (5–60%). Increases are found even at gauges in the deep submergence area of the VMD, with an increase of 13 *cm* (6%) in the normal and wet years, and 22 *cm* (10%) in the dry year in Chau Doc. However, the largest change in *AMWL*s is modelled in the middle and coastal regions of the delta (Fig. 4.4 m-o). For example, at Can Tho *AMWL*s increase by 20–25% for *S5-SLR*, five times higher than the projected change due to hydropower development (*S1-HP*) or climate change (*S4-CC*). In addition to increasing *AMWL*s in the main channels, sea-level rise

led to submergence of additional flood compartments. Therefore, the inundation extent increases by 19–21%, from 47%, 56% and 60% of delta land area computed for the baseline to 67%, 76% and 81% for dry, normal and wet years, respectively (Fig. 4.6). Inundation depth increases by 0.1–0.5 m (Fig. 4.5 m-o), together with a significant shift from short (less than one month) to longer inundation periods (above three months) (Fig. 4.6 and Table B4 in Appendix B).

Cumulative impact of climate change, hydropower, sea-level rise, and delta infrastructure: The cumulative impact of multiple drivers is examined in two scenarios, namely the business-as-usual (*S6-BAU*), and the sustainable-development (*S7-SD*) scenarios. *S6-BAU* is a combination of four drivers: *S1-HP* (hydropower development), *S3-DE* (dyke expansion), *S4-CC* (climate change), and *S5-SLR* (effective sea-level rise). In this scenario, the hydropower development partially compensates the higher *AMWL*s caused by the other drivers, most notably at gauges in the northern part of the delta. At Chau Doc, an increase in *AMWL* by 10 *cm* is simulated for *S6-BAU* for the dry year, and 17 *cm* for the wet year, which is about half of the simulated change for *S4-CC* and *S5-SLR* (20–35 *cm*)(Fig. 4.4).

Due to the comparatively high impact of hydropower development on *AMWL*s in normal years (about the same magnitude as for wet years), *AMWL* at Chau Doc changes by only 2 *cm* in *S6-BAU* in a normal year. From the centre of the delta to the coastal region, an increase of 30–40 *cm* (15–25%) relative to the baseline is simulated (Fig. 4.4 p-r); this range is similar to the *S5-SLR* scenario, i.e. effective sea-level rise alone. The inundated area of *S6-BAU* is marginally smaller (1–3%) than the inundated area simulated in *S5-SLR* (Fig. 4.6 and Table B4 in Appendix B). This is mainly a combined effect of the similar impact of effective sea-level rise on inundation in the central and coastal parts of the delta in *S5-SLR* and *S6-BAU*, and the blocking of floodplain inundation in the deep submergence zone by the development of high dyke compartments just as in *S3-DE* (Fig. 4.5 p-r).

Contrary to *S6-BAU*, the *S7-SD* scenario results in overall increases in *AMWL*s, flood extent, flood depth and duration relative to the baseline (Fig. 4.4 s-u, Fig. 4.5 s-u, and Fig. 4.6). In this scenario, about 70% and 90% of the VMD land area are inundated in the dry and wet year, respectively. The simulated flood extent increases by 22% in the dry year, 25% in the normal year and 26% in the wet year. The *AMWL*s at all gauges increase by 30–40 *cm* (Fig. 4.4 s-u). Moreover, the regions inundated longer than three months increase by 30% in the dry and normal years, and up to 40% in the wet year (Fig. 4.6).

4.5.2 Impacts of flood hazard changes on agriculture damages

Figure 4.7 summarises exposed areas (EA) and estimated damage (*ED*) of paddy rice plantation for the eight scenarios (see Table B5 of the Appendix B for tabulated data). The calculation of *EA* and *ED* is limited to the flood-prone area of the VMD (marked in Fig. 4.1). The expansion of high-dyke compartments in *S3-DE* and *S6-BAU* allows the cultivation of one extra rice crop per year, by changing the cropping system from double to triple season rice. For the baseline, the inundated rice farming areas (*EA*) in the dry, normal and wet years amount to 2,500, 11,000 and 60,500 *ha*, respectively; and the *ED* is computed to 2.0, 9.0 and 54.0 USD *million*.

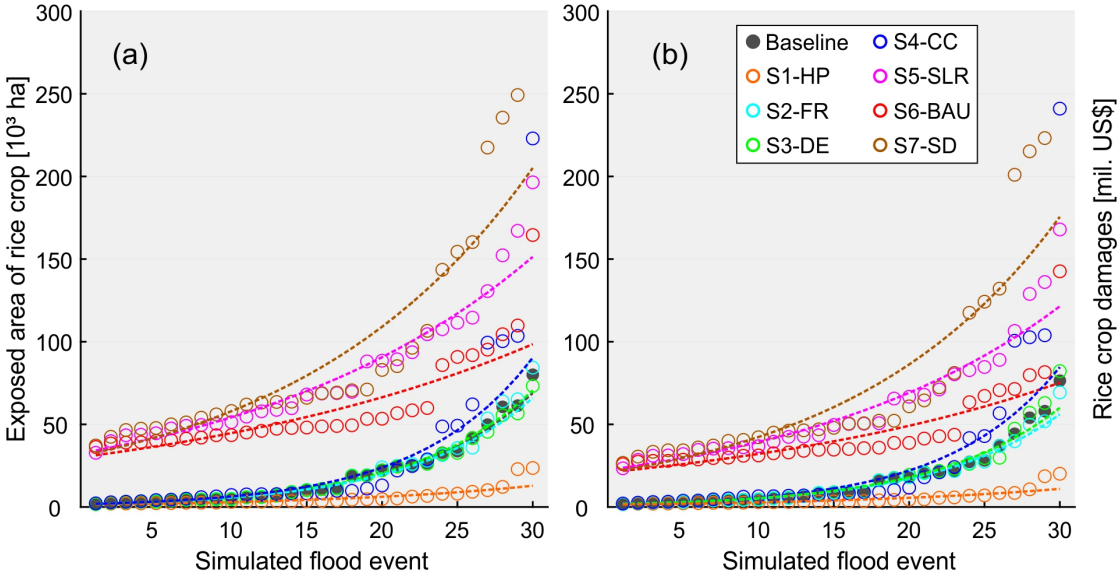

Figure 4.7: Exposed areas (EA) (a) and flood damage (ED) (b) to rice crop for 240 flood events differentiated in the eight scenarios.

S1-HP (hydropower development) and *S2-FR* (floodplain restoration) simulate a decrease in *EA* and *ED*. For *S1-HP*, *EA* is reduced by 17%, 66% and 88% in dry, normal and wet years; this translates into a reduction in *ED* of 19%, 66% and 63%. For *S2-FR*, *EA* and *ED* are reduced by 7% in the wet year only. All other scenarios project an increase in *EA* and *ED*. Similar to *S2-FR*, changes in *EA* and *ED* are found only for the wet year for *S3-DE*, with 64,000 *ha* and USD 57.0 *million* (an increase of 5% relative to the baseline). The climate change scenario (*S4-CC*) projects an increase of *EA* by 38%, 3% and 71% in dry, normal and wet years, respectively; these values are equivalent to an increase of 33%, 11% and 90% in *ED*. Much larger increases of *EA* and *ED* are obtained for the remaining scenarios *S5-SLR*, *S6-BAU* and *S7-SD*, amounting to 15–18 times the baseline *EA* in the dry year (39,000–46,500 *ha*), 5–7 times in the normal year (49,000–70,500 *ha*), and 2–4 times in the wet year (110,000–249,000 *ha*). The corresponding changes in *ED* are computed as 12–14 times (USD 28.0–33.0 *million*), 4–6 times (USD 36.0–52.0 *million*), and 2–4 times (USD 82.0–223.0 *million*) for the dry, normal and wet years.

4.6 Discussion

4.6.1 Future projections of delta flood dynamics

Our scenario simulations revealed an increase in flood hazard and affected agricultural area in the VMD by 2036-2065 as the result of the cumulative impacts of climate change, anthropogenic development and effective sea-level rise. We estimated an increase of flood extent by 20–27% compared to the baseline period 1971-2000 under climate change and effective sea-level rise (*S6-BAU*, *S7-SD*: RCP 4.5, plus 43 *cm* in tidal level). A large share of the additional inundated areas shift from non-flooded, or short period inundation (less than one month) to longer duration inundation (3–4 *months*, Fig. 4.6). Our results demonstrate the dominant impact of sea-level rise and land subsidence on future delta inundation (shown in Fig. 4.5 m-o, and in Fig. 4.6 [e.g. Le et al., 2007, Van et al., 2012, Toan, 2014, Dang et al., 2018]), with climate change acting as a second-order effect (Fig. 4.6 j-l). This statement holds true for many other world coastal deltas, e.g. Ganges-Brahmaputra, Irrawaddy [Auerbach et al., 2015, Tessler et al., 2015]. In line with the expansion of long duration inundation areas, the estimated flood damage to agricultural areas (*ED*) increased by USD 25–170 *million* relative to the baseline (Fig. 4.7 b). The estimation of damage to agricultural areas was limited to the flood-prone areas, amounting to about 50% of the delta land area, and to paddy rice cultivation, as damage models for other crops are lacking [Triet et al., 2018]. Thus, the overall flood damage to delta agriculture production will be significantly higher. Even though these crops, e.g. orchard farms, shrimp ponds, are not comparable to paddy rice in terms of plantation area, their economic values are considerably higher.

The modelled results suggest hydropower development in the Mekong Basin (*S1-HP*) is likely to mitigate the increasing climate change impacts on inundation in the flood-prone area (Fig. 4.1 b) of the VMD. However, this area already experiences deep and long inundation, and agriculture and society are well adapted to this annual flood pulse [Howie, 2012]. Therefore, flood mitigating benefit of hydropower dams is unlikely to compensate for their suggested negative impacts. The scenario examining only the impacts of hydropower dams (*S1-HP*) suggests that in normal flood events part of the delta flood-prone region will not be flooded any more; distressing livelihoods of local residents. More important, hydropower dams substantially reduce sediment load to the Mekong Delta [Kummu et al., 2010, Kondolf et al., 2014], and sedimentation in the delta [Anthony et al., 2015, Manh et al., 2015], thus exacerbating coastal erosion, deltaic land subsidence, riverbank collapse [Van Binh et al., 2019]; and subsequently increasing floodplain inundation.

The floodplain restoration scenario *S2-FR* analysed the impact of the high-dyke system in the VMD, constructed mainly after the disastrous flood in 2000. Our simulations confirmed

the previous studies of Triet et al. [2017] and Dang et al. [2018]: high-dyke development shifted flood hazard to neighbouring areas and caused higher water levels locally. However, the impacts of high-dyke development are less severe than changes caused by the other drivers. Note that *S2-FR* did not consider removing the entire the dyke system in the northern provinces of the VMD An Giang and Dong Thap (Fig. 4.1 b), but assumed an opening of the sluice gates at high-dyke compartments after 31 August (harvest time of the second crop) in order to store floodwater during the high flood phase. From a hydraulic point of view, the high-dyke compartments operate almost as low-dyke compartments in this case, but still offer flood protection for the population living on the high-dyke. It is argued in Tran et al. [2018b] that complete removal of all dyke systems in these two provinces could reduce the flood hazard in the centre and coastal regions of the VMD. We have not explored this scenario, because complete removal of the current dyke system in the VMD is unrealistic. Many delta inhabitants settle on high-dykes after moving from the floodplains to the elevated areas for flood protection [Reis, 2007]. Resettlement of almost the whole population in the deep submergence zone and the demolishing of thousands of kilometres of dykes is not feasible.

On the contrary, the controlled flooding of high-dyke compartments during extreme floods (*S2-FR*) has multiple benefits: (i) use as an emergency flood management option to lower the flood hazard for the central part of the delta including its economic hub Can Tho; a reduced water level of a few centimetres can have a very beneficial effect on flooding in the low terrain of the VMD [Apel et al., 2016], (ii) reduced damage to rice crop (Fig. 4.7), and (iii) controlled replenishment of sediment and nutrients to flooded compartments [Manh et al., 2014]. However, this operation scheme requires a reliable flood forecast by July-early August, i.e. prior to the plantation of the third rice crop during the flood season, in order to reduce economic damages to farmers, whose land is flooded in case of opening the sluice gates. It should also be noted that the reduction in flood water levels is low in the range of 1–5 cm.

The small changes in *AMWL*s and inundation extent by an expansion of the high-dyke system in *S3-DE* can be attributed to the fact that in the baseline runs the high-dyke system already covered two-third of An Giang and one-half of Dong Thap provinces (Fig. 4.1 b). Although the flood extent and agriculture damage in *S3-DE* are comparable to the baseline, the further expansion of high-dykes and the associated introduction of a third rice crop in these newly protected floodplain compartments led to a potential increase in *EA* and *ED* of rice cropping areas. Which can be imminent in case of dyke breach or extreme floods exceeding the design level of the high-dykes. In addition, a high-dyke expansion would result in higher channel flow velocities, thus exacerbating the risk of channel erosion [Kondolf et al., 2018]. Even more important, separating floodplains and channels would reduce floodplain sedimentation delivered by the floods, resulting in higher costs for rice

cultivation and reduced crop yield. Tran et al. [2018a] suggested that after 10–15 *years* the benefit for farmers from cultivation an extra crop is likely to be zero compared to growing only two rice crops due to the increase production costs. Reducing floodplain sedimentation would also further increase the effective sea-level rise and exposure of rice crops to inundation [Manh et al., 2015].

From a flood management point of view, the major concern for the future is the increase in inundation duration. Most of the newly or prolonged submerged areas in scenarios *S5-SLR*, *S6-BAU*, and *S7-SD* are located in the coastal region of the VMD. In these regions, the waterworks for flood control are less developed compared to the northern provinces. The shift in inundation duration from 1–2 to 3–4 *months* means that either the agriculture system in these coastal provinces has to change to match the new emerging condition (e.g. alter cropping calendar or land-use), or substantial infrastructure investments are required to maintain agricultural production (e.g. new dyke systems, embankments, sluice gates, pumping stations). The results thus stress the necessity to develop a flood adaptation and management plan for VMD focussing on tidal backwater induced inundation hazard. The issue has been already observed in many major cities of the VMD, including the largest city Can Tho [Takagi et al., 2014]. These control structures are also required to address the higher saline intrusion in the dry season associated with higher tidal levels [Toan, 2014, Smajgl et al., 2015].

4.6.2 Uncertainties, limitations and directions of future studies

Our results are subject to limitations and uncertainties related to (i) the limited number of scenarios for climate change projections for the Mekong river runoff, for the effective sea-level rise, and for the hydropower development in the basin, and (ii) the structure and parameterization of the hydrological and hydrodynamic models. Hoang et al. [2018] generated ten projections of Mekong streamflow using five GCMs in combination with two emission scenarios (RCP 4.5 and RCP 8.5). The range of the projected streamflow narrowed for these projections compared to earlier studies [e.g. Lauri et al., 2012]. Due to the computer runtime of the hydraulic model, we used only one projection (RCP 4.5, with MPI global circulation model). However, because the MPI-RCP4.5 scenario resembles the ensemble mean of streamflow of Hoang et al. [2018], the simulated changes in flood hazard and potential damages can be regarded as the most likely projection. A similar argument holds for the selected effective sea-level rise scenario, which represents the mean value of the suggested range in Manh et al. [2015]. Our scenarios thus represent the most likely future pathways under current knowledge without addressing the uncertainty associated with the future climate and sea-level rise development [Manh et al., 2015].

We also acknowledge the uncertainty in the scale of hydropower development in the

Mekong Basin. Our analysis considered rather the extreme case of all planned dams to be built and operated. The prospect of all these dams to be constructed and operated for power generation purpose only by 2036-2065 is subject to political and economic development, thus the flood buffering capacity of hydropower development might be considerably smaller.

Another source of uncertainties stems from the hydrological model VMod to simulate streamflow in the Mekong Basin. The model has been extensively updated and calibrated by Hoang et al. [2018], achieving good performance on simulated discharge. However, the model performance with regard to flood volume is not yet defined. It could be argued that a good performance for daily flow should yield acceptable performance for flood volume, but we suggest to determine the model performance also for flood volume as the second parameter in a multi-objective calibration.

The flood propagation model contains some model structure limitations. The model network for the coastal regions is less comprehensive compared to other parts of the delta (e.g. the flood-prone area). Limited data availability resulted in a rather coarse channel network for this part of the model domain. The same holds true for water infrastructures like dykes and sluice gates. Further, monitoring data (water level, discharge series) for model calibration are mainly available for the main rivers. This results in some unquantifiable uncertainty in the discharge and water level simulations in the more remote areas. The model setup for the Cambodian part of the delta is based on a coarser DEM compared to the VMD, and also the information on the channel network and bathymetry are likely outdated. The Cambodian delta has witnessed quite some structural changes in the last decade and is expected to continuously change in the future following the country's socio-economic development [Kondolf et al., 2018]. This might have an impact on the propagation of the Mekong flood pulse to the VMD. Further uncertainty may stem from the transformation of 1-D water levels to 2-D inundation maps, influencing the flood-affected area. A detailed discussion on the limitations of this top-down approach on flood damage and risk to rice crop in the VMD can be found in Triet et al. [2018]. Despite these limitations of the flood propagation model, a number of studies using the same or modified model versions [e.g. Manh et al., 2015, Triet et al., 2017, Dang et al., 2018, Tran et al., 2018b] demonstrated that it provides valid results, particularly on the large, delta-wide scale of this application.

4.7 Conclusions

We implemented a comprehensive set of hydrodynamic modelling scenarios to quantify future projections of flood hazard and potential damage to rice cropping in the Vietnamese Mekong Delta (VMD) under climate change and anthropogenic stresses, namely

hydropower dam development in the Mekong Basin, and high-dyke extension in the VMD. Results from our assessment suggest the combination of sea-level rise and land subsidence dominates the increase in future delta flood hazard and damage to rice cultivation, and hydropower development could counteract the changes in delta inundation dynamics driven by climate change. High-dyke development in the VMD has the smallest and locally confined impact on flood hazard. This can be, however, utilized for emergency flood management, because also small reductions in water levels can make a difference in inundation in this low-lying terrain. Opening of high-dyke compartments has immediate effect on flood propagation in the delta providing that a reliable flood forecast is available.

The assumptions and limitations of the study do not influence the main insights, that mitigation actions are urgently required reduce land subsidence in the delta, which is actually outpacing climate change induced sea-level rise [Minderhoud et al., 2017]. A better control and reduction of groundwater abstraction would be the first and immediate step in this direction. Furthermore, long term strategic planning of flood management should have a particular focus on tidal influenced flood regions of the delta, and should encompass hard measures like flood protection infrastructure, but also non-structural one as changes in land use, cropping calendar combined with a reliable early flood forecast.

Chapter 5 Main findings and conclusion

5.1 Main findings

This thesis aimed to gain further insights into the present and future flood hazard, damage and risk in the Vietnamese Mekong Delta by addressing two main research objectives:

- How does the high- and low-dyke flood protection systems affect the inundation dynamics and thus the flood hazard and risk to rice production in the Mekong delta?
- How do climate change and anthropogenic interventions in the Mekong delta and basin alter the flood hazard and risk in the delta in future?

These overarching research objectives resulted in five research questions, analysed and discussed in the three chapters of this thesis (Chapter 2-4). The following paragraphs summarize the answers to these research questions.

1. Has high-dyke development in the VMD shifted flood hazard downstream?

To answer this question, historical data of flood volume, flood peak (water level, discharge), and duration at five hydrological gauges were analysed for the gradual trends with the Mann-Kendall test, and step changes with the Pettitt test. The locations of these gauges were selected to explicitly detect flood trends up- and down- stream of the high-dyke development areas. A Monte Carlo (MC) uncertainty experiment was added to assess the robustness of the detected trends against hypothetical measurement errors.

The analyses revealed strong and robust increasing trends of peak water levels and duration downstream of the high-dyke areas with a step change in 2000/2001, i.e. immediately after the disastrous flood which initiated the high-dyke development. These changes were in contrast to the negative trends detected at stations upstream (Section 2.3.1 and 2.3.2). This spatially different behaviour of detected trends supported the claims that high-dyke development has shifted flood hazard downstream.

2. What explains the higher flood levels observed at many gauges during the high flood in 2011 compared to the century flood in 2000?

The question was addressed with hydraulic simulations of the two recent extreme floods in 2000 and 2011. First, the hydrodynamic model was refined and updated with data from the newly available DEM and field survey of dyke system in 2009-2010. A set of scenarios

were developed, in which the boundaries conditions, i.e. dykes settings, flood hydrograph and tidal level, of the two events 2000 and 2011 were interchanged (Table 2.3).

The simulations confirmed that the high-dyke implemented in the northern provinces of the VMD after the historical flood in 2000 has shifted flood hazard to downstream and neighbouring regions. High-dykes accounted for a change in flood level by 3–13 *cm*, which is equivalent to 23–94% of the observed changes between 2000 and 2011. However, high-dyke was not the main and only cause for the higher flood level observed in 2011. Here, the flood hydrograph had the highest contribution in the northern part of the delta, while the tidal level had 2–3 times higher influence than high-dyke from the centre of the delta to the coast.

Hydraulic simulations, for the very first time, provided numerical evidence that the concurrence of fluvial flood peaks and spring tides substantially amplify the flood level in the central and coastal regions compared to the fluvial flood alone.

3. What is the expected annual flood damage to rice cultivation in the VMD with the current dyke system?

A top-down approach was developed to estimate flood damage and risk to rice cropping in the flood-prone areas of the VMD. The methodology was chosen for its ability to overcome data limitation. Probabilistic flood hazard maps of the delta were generated using bivariate extreme value statistics of the Mekong discharge, synthetic flood hydrographs, and a large-scale hydraulic model. Based on these hazard maps, rice crop damages were estimated using published damage function, while explicitly considering the temporal occurrence of floods, the cropping calendar, rice phenology and harvest times based on a time series of enhanced vegetation index (EVI) maps derived from MODIS satellite data.

The analysis of flood events showed that the events had identical magnitude (i.e. flood peak and volume) but differed in timing (i.e. hydrograph shape). This causes significant differences in flood damage. Flood damage was highest if inundation started already in mid-August to mid-September. Such an early flood with $p = 0.1$ (10-year flood) causes similar economic losses as a 100-year event with a flood peak in October (Section 3.4.3).

The estimated flood damage to rice cultivation in the flood prone region varied from USD 25.0 to 115 *million* (0.02–0.1% of the total GDP of Vietnam in 2011) corresponding to the 10-year and the 100-year floods. Estimated damage from the 100-year flood was less than 50% of the reported damage from the 50-year flood in 2000. This comparison explicitly highlights the effectiveness of the flood control structures, including both low- and high-dyke, that have been developed in the delta in the recent decades after the flood in 2000.

The overall flood risk to rice crops was estimated at an expected annual damage of USD 4.5 *million* , translated to USD 1.0–5.0 *per hectare* of rice. The highest risk was calculated for the provinces located in the deep-submergence region with an exception in Kien Giang, where the expected annual damage was very low.

4. How does expansion of high-dyke area, or conversion of high- to low-dyke affect the flood damage and risk?

In order to get insights into this heavily debated question among the administrative bodies and the general public in the Mekong delta, the synthetic hazard scenarios developed for the research question 3 were run with two modified versions of the hydraulic model. In one version the extension of the high dykes was simulated; while in the second version large parts of the existing high dykes were converted into low dykes in the model. For both setups the lower boundary conditions were set to those observed in 2011. The scenarios were evaluated as for the research question 3 in order to quantify then changes in flood exposure, flood damage and flood risk.

Under the high-dyke expansion scenario the flood damage rose to USD 140 and 250 *million* for 10-year and 100-year floods respectively. The expected annual flood damage increased 3 times compared to the current state. The average crop risk tripled in the two delta provinces where new high-dyke areas were implemented, because of the additionally planted crop. For the other provinces, an increase in average crop risk by 10–15% was calculated as high-dyke development shifted flood hazard to neighbouring and downstream areas.

In the opposite scenario, the conversion from high- to low-dykes and the cease of the cultivation of the third crop reduced the expected annual flood damage by 40%. The average crop risk reduced by 40–65% in the most affected provinces Dong Thap and An Giang, and by 5–10% to the other downstream regions relative to the current state (Section 3.3.4).

5. What are the future projections of delta flood hazard and agricultural damage?

Future projections of delta flood hazard and damage were quantified using the updated hydraulic model (Chapter 2), the damage estimation concept (Chapter 3) and a set of eight (8) scenarios for simulating the impact of different drivers. These scenarios denoted the individual and compound impacts of (1) hydropower dam development, (2) flood control infrastructure in the VMD, (3) the impact of climate change on Mekong river flow, and (4) sea-level rise and deltaic land subsidence (Sec. 4.3.2).

The resulting hydraulic simulations projected an increase of flood extent by 20–27% for the period 2036-2065 compared to the baseline period 1971-2000 under cumulative impacts of climate change, sea-level rise and deltaic land subsidence. A large share of the additional inundated areas shifted from non- or short inundation (less than one month) to long inundation (3–4 months). The estimated flood damage to rice cultivation increased by USD 29.3 *million* (12 times), 50.0 *million* (6 times) and 185.0 *million* (3 times) in dry, normal and wet years compared to the baseline.

Among the individual drivers, sea-level rise and land subsidence caused the highest changes in flood hazard and damage to rice crop, followed by hydropower and climate change impacts. It was estimated that delta inundation extent increases by 19–21% under impact of sea-level rise and land subsidence. Subsequently, even in a dry year flood damage was projected to increase to USD 28.5 *million* compared to the baseline estimation of USD 2.4 *million* . The losses were further amplified in larger flood, i.e. USD 40–82.0 *million* in normal and wet years compared to USD 9.3–54.0 *million* estimated for the baseline period.

The hydraulic simulations suggested that in extreme floods the hydropower dams in the Mekong Basin could substantially offset the increasing flood hazard and agriculture losses caused by a changed hydrological regime of the Mekong under climate change. However, the operation of these dams would disrupt the annual flood pulse of the low and normal floods in the delta (Fig. 4.5 b). The disruption of inundation in combination with other adverse consequences of hydropower dams (e.g. sediment trapping) imposes a major challenge for rice cultivation in the VMD in the coming decades.

5.2 Discussions

During the analysis of the current state and future prospects of flood dynamics in the delta, many aspects emerged which require discussion in a broader context. The following subsections discuss the main objectives of this thesis: *high-dyke development, future projection of delta flood dynamics*, and *the flood damage/risk assessment concept* developed to quantify flood damage and risk to paddy rice cultivation.

5.2.1 High-dyke development

The analysis in this thesis reveals that high-dyke compartments can and should be used as flood retention areas in extreme floods. Opening of high-dyke compartments will have immediate effect on flood propagation in this low-lying terrain, minimizing flood losses downstream, including the delta major socio-economic hub, i.e. Can Tho city. Two features are required to realize this measure. First, a reliable flood forecast by August-and

latest early September is important to inform farmers to stop planting the third crop. Furthermore, a compensation for their income loss is a prerequisite criterion for the acceptance of this measure. Second, the measure requires good governance, and coordination to ensure coordination and consistency in operating the sluice gates of the high-dyke compartments. Therefore, a regional flood/ water management board is highly recommended in this context, because the issue goes beyond the administrative border of local communes and provinces.

For the hot debate of the high-dyke system should be further extended to increase the agricultural production, or if it should be converted to mainly low- dykes, this thesis could not provide a decisive answer, but information for an evidence-based discussion of the pros and cons of these development strategies. This discussion has to consider not only the flood risk aspects dealt within this thesis, but also other environmental and economic impacts of these measures. This includes the replenishment of nutrients and sanitisation of the flood plains by the annual inundation and thus the reduction of production costs for the next coming crop [Manh et al., 2014]. The declining fertility of the soils without annual flooding is also expected to reduce the economic benefit of the third crop within 10-15 years [e.g. Tran et al., 2018a]. Considering these findings and those of this thesis, the cropping schedules as proposed in the first Mekong delta development plan (2 rice plus vegetable or 2 rice plus aquaculture), are thus considered as most sustainable [Deltares, 2013].

However, the increasing impact of higher sea levels combined with land subsidence on flood risk as shown in this thesis also means, that salt water intrusion and agricultural droughts occur more often. This puts the rice production of the coastal areas of the delta at high risk [Toan, 2014, Smajgl et al., 2015]. Therefore agricultural production in this region should shift to more salinity resistant cropping strategies, i.e. shift to the hybrid rice plus shrimp farming or salinity resistant vegetable cropping [GOV, 2017]. But the reduction of rice production, the staple food of Vietnam, in the coastal regions might also require an expansion of the third rice crop in the deep submergence region of the delta in order to assure the country food security by 2030-2050. Therefore, further studies are necessary to provide the concrete answer to the future direction of high-dyke flood control measure. These studies should cover cost-benefit assessment including sensitivity analysis of the market price of rice and other agricultural crops to be planted, as well as a thorough estimation of the food requirements in future and the assessment of the productivity of saline resistant rice varieties and the alternative cropping options in the coastal regions.

5.2.2 Future projection of delta flood dynamics

Tidal inundation is the major issue in the VMD in the coming decades, especially in the central and coastal regions of the delta. It is undisputed that the VMD is sinking mainly as a consequence of excessive ground water abstraction in the last 25 years. In many places, estimated sinking rate outpaces sea-level rise level by 10–15 times [Erban et al., 2014, Minderhoud et al., 2017]. The open but important question is how fast this process will continue in future in order to design appropriate management plans. Technical solutions, like protecting the entire delta with coastal dykes and close estuaries with tidal gates is, however, neither technically nor economically feasible providing the scale of the delta and high compaction rate in its coastal region [Minderhoud et al., 2019]. Blocking sediment flux from the Mekong to the sea might even foster shoreline erosion [Anthony et al., 2015], and cause a deeper incision of the river channels [Jordan et al., 2020, Thi Kim et al., 2020], thus exacerbating the existing problems of tidal flooding and salinity intrusion. Therefore, better control and reduction of groundwater abstraction is the first and urgent step to mitigate land subsidence. This should be augmented by construction of water treatment plans (using surface water) providing fresh water for domestic use, and shift in land-use to brackish/saline crops in the coastal region [Smajgl et al., 2015]. Besides, engineering solutions are required to protect drainage systems in major delta cities, e.g. Can Tho and Rach Gia, during high tidal phase, where the natural and man-made canals are often the drainage points of these aging sewer collecting systems [Huong and Pathirana, 2013].

For the floods stemming from the Mekong river flow, a disruption of inundation in normal years and a higher variability of inundation dynamics in extreme wet year were projected. Missing of floodplain inundation in normal years was modelled in Chapter 4 of this thesis, and is corroborated by modelled hydrological alterations of the Mekong flood pulse in other studies [e.g. Räsänen et al., 2012, 2017, Pokhrel et al., 2018b] and the trend analyses in Chapter 2 and in [Delgado et al., 2010, Hirabayashi et al., 2013]. The disruption of floodplain inundation, together with the reduction of river sediments and floodplain sedimentation constitutes a serious hazard to agriculture production in the delta in the coming decades.

The hydraulic simulations in Chapter 4 suggested hydropower dams could mitigate flood hazard and damage. This finding is associated with high uncertainties, depending on how dams to be operated in these extreme events. Besides, the extreme dam development scenario (all dams planned are built) would reduce sedimentation in the delta by 40–90% [Manh et al., 2015]. Next to the problems for floodplain nutrient delivery, this increases the river bank and bed erosion as well as the probability of structural failure of flood protection measures. The excessive sand-mining in the region further aggravates this

problem [Hackney et al., 2020].

5.2.3 Flood damage and risk assessment

The concept for quantifying flood risk resulted in a large-scale quantification of flood damage and risk to rice cultivation, which had not been available for the VMD before. Furthermore, the concept can be easily transferred to quantify flood losses to other agriculture crops, and to other riverine deltas, e.g. Ganges-Brahmaputra due to its generic approach. It has to be noted, however, that due to its large spatial scale the risk assessment cannot be used for very local flood management plans. It is rather meant to provide a quantitative basis for large scale, i.e. regional flood risk management planning.

One of the major challenges in this study is the lack of recorded damage data to validate the results of the study. Survey data from governmental agencies contain few information, as it is limited to exposed areas and roughly estimated economic losses. Other risk factors, e.g. inundation depth, duration and flow velocity, are not yet documented. Limitations of funds for data acquisition, and the usually long delay between the event and the compilation of the data are the main constrains. In addition, the data is often scattered among different authorities at different administrative levels and, in many cases, not publicly available. Therefore there is a strong need for a regional and public flood damage database similar to the HOWAS 21 in Germany [Kellermann et al., 2020]. The database would support reducing uncertainty of the top-down damage assessment concept, and developing of data-driven models for flood risk assessment. In this context, a platform incorporating official data from authorities as well as "soft" data collected by citizen science through smart-phone apps [Goodchild and Glennon, 2010] is the ideal solution. Smart-phone apps where people can document main risk factors, e.g. flood depths and duration, complement to the post event survey well [e.g. Barz et al., 2018]. This approach is favoured over telephone (land-line) interviews, because of the high mobile connection rate in Vietnam with over 50% of the adults having a smart-phone [Silver et al., 2019], compared to the rather low land-line telephone coverage. Another possibility is taking advantage of unnamed aerial vehicles (UAVs) footage to improve inundation mappings as demonstrated in Appeaning Addo et al. [2018].

The presented thesis opens the door for a data driven and quantitative flood risk management in the Mekong Delta, as it provides a probabilistic flood risk assessment with a particular focus on rice cropping for the delta for the first time. The results can be used for a regional flood management planning, that includes both hard technical measures like dyke construction, but also soft measures as adaptation of cropping patterns and the control of groundwater abstraction. Because of the identification of the most important drivers for flood risk and future changes in different regions of the delta, management

plans tailored to target the most pressing issues, and the design of the most cost effective measures can be developed. In order to improve the robustness of such plans, the uncertainties in the risk assessment were discussed and recommendations for a reduction of these uncertainties were given. The most important uncertainty stems from the lack of damage data to validate the damage estimation, and thus a concerted effort for a combined data collection from authorities and citizens is recommended.

5.3 Research outlooks

The results presented in this research helped to gain further insights into the current state and future projections on flood dynamics in the Mekong Delta. However, there are still considerable limitations and uncertainties linked to, i.e. the hydraulic model, climate projection of the Mekong river flow, and flood damage estimation concept. Some important recommendations are proposed to improve the results presented in this thesis, and to support the new master plan for the VMD following the Resolution 120 issued by the Government of Vietnam.

Refine and update the quasi-2D flood model: The model post-update shows improvement in capturing flood level and inundation extent; however, its performance in the coastal area is not as good as the flood-prone region due to limited data for model set up and calibration. Therefore, a dedicated field survey on bathymetric data, dyke elevation, sluice gates in this region would significantly improve the large-scale hydraulic model. The recommendation is also valid to the floodplain part in Cambodia. Besides, it is suggested to test the full 2D approach in future research given a substantial improvement in computation capacity and the high-resolution DEM.

Quantify flood damage to other land-use types: It is recommended to address flood damage assessment to other agriculture crops in the future studies. To facilitate the assessment, efforts need to be made to collect data land-use, plantation calendar, and their vulnerability to inundation.

Improve the projected flow of the Mekong: It is advised to include the flood volume in addition to discharge series to the calibration, validation process of the hydrological model for the Mekong. Equally important is the constant update of the hydrological model with information on hydropower projects and climate change projection.

Combine flood and drought risk assessment: A comprehensive study evaluating agricultural damage and risk to flood and saline water intrusion is strongly proposed to support the new regional plan of the VMD.

Flood forecast: A good and reliable flood forecast by August-September will facilitate

the decision makers and farmers to develop flood preparedness and response measures mitigating damages and economic losses.

5.4 Concluding remarks

The assumptions and limitations of the study do not influence the main insights:

First, high-dyke compartments can and should be utilized for emergency flood management in extreme events. Also, proper maintenance of dykes and flood defence structure is required to reduce the risk of structure failure, dyke breach during extreme floods (as perceived in 2011).

Second, mitigation actions are urgently required to reduce land subsidence in the delta, which is actually outpacing climate change induced sea-level rise. A better control and reduction of groundwater abstraction would be the first and immediate step in this direction.

Lastly, long term strategic planning of flood management should have a particular focus on tidal influenced flood regions of the delta, and should encompass hard measures like flood protection infrastructure, but also non-structural one as changes in land use, cropping calendar.

Appendix

Appendix A–Supplement to Chapter 2

Table A1: List of gauged data used in this study, name of station, its location, type of data and purpose of usage.

No.	Name of station	Geographical location			Data		
		latitude	*longitude*	*located at*	*data*	*type of data*	*used in*
1	Kratie	12.260°N	105.984°E	Mekong river (CFP)	H&Q[1]	daily	trend& boundary
2	Kampong Cham	11.932°N	105.336°E	Mekong river (CFP)	H	daily	calibration
3	Prekdam	11.815°N	104.807°E	Tonlesap river (CFP)	H	daily	calibration
4	Phnom Penh port	11.583°N	104.924°E	Tonlesap river (CFP)	H	daily	calibration
5	Neakluong	11.260°N	105.280°E	Mekong river (CFP)	H	daily	calibration
6	Khokhel	12.255°N	105.030°E	Bassac river (CFP)	H	daily	calibration
7	Tan Chau	10.805°N	105.235°E	Mekong river (VMD)	H&Q	daily/hourly	trend& calibration
8	Chau Doc	10.709°N	105.125°E	Bassac river (VMD)	H&Q	daily/hourly	trend& calibration
9	Vam Nao	10.567°N	105.350°E	Vam Nao river (VMD)	H&Q	hourly	calibration
10	Long Xuyen	10.393°N	105.435°E	Bassac river (VMD)	H	hourly	calibration
11	Cao Lanh	10.417°N	105.644°E	Mekong river (VMD)	H	hourly	calibration
12	Can Tho	10.041°N	105.799°E	Bassac river (VMD)	H	hourly	trend& calibration
12	My Thuan	10.278°N	105.910°E	Mekong river (VMD)	H	hourly	trend & calibration
14	Hung Thanh	10.659°N	105.779°E	Phuoc Xuyen canal (VMD)	H	hourly	calibration
15	Moc Hoa	10.777°N	105.935°E	Vaico river (VMD)	H	hourly	calibration
16	Kien Binh	10.617°N	106.050°E	Kenh 12 canal (VMD)	H	hourly	calibration
17	Xuan To	10.606°N	104.944°E	Vinh Te canal (VMD)	H	hourly	calibration
18	Tri Ton	10.436°N	105.056°E	Tri Ton canal (VMD)	H	hourly	calibration
19	Tan Hiep	10.118°N	105.285°E	Cai San canal (VMD)	H	hourly	calibration
20	Vi Thanh	9.784°N	105.467°E	Xa No canal (VMD)	H	hourly	calibration
21	Vung Tau	10.333°N	107.067°E	South China Sea	H	hourly	model boundary
22	Vam Kenh	10.270°N	106.740°E	Mekong estuary	H	hourly	model boundary
23	Binh Dai	10.197°N	106.711°E	Mekong estuary	H	hourly	model boundary
24	An Thuan	9.976°N	106.605°E	Mekong estuary	H	hourly	model boundary
25	Ben Trai	9.881°N	106.529°E	Mekong estuary	H	hourly	model boundary
26	My Thanh	9.425°N	106.171°E	Bassac estuary	H	hourly	model boundary
27	Ganh Hao	9.031°N	105.419°E	Ganh Hao estuary	H	hourly	model boundary
28	Song Doc	9.041°N	104.833°E	Song Doc river (VMD)	H	hourly	model boundary
29	Xeo Ro	9.865°N	105.111°E	Cai Lon river (VMD)	H	hourly	model boundary
30	Rach Gia	10.012°N	105.084°E	Gulf of Thailand	H	hourly	model boundary

[1] *H - water stage data, Q - discharge data*

Table A2: Changes in inundation area as percentage of provincial area between the two model setups (with / without high-dyke system). The numbers are the mean of the two model setups as given in Table 2.4.

Province	No high-dyke *(scenarios S1 and S3)*			With high-dyke *(scenarios S2 and S4)*			Changes		
	shallow inundation	deep inundation	total inundation area	shallow inundation	deep inundation	total inundation area	shallow inundation	deep inundation	total inundation area
An Giang	5.4	73.1	78.5	3.0	43.8	46.8	-2.4	-29.2	- 31.7
Dong Thap	13.1	59.4	72.5	5.7	48.1	53.8	-7.4	-11.4	-18.7
Long An	37.9	36.3	74.2	39.3	38.1	77.4	1.4	1.8	3.2
Kien Giang	33.2	22.5	55.7	31.9	23.8	55.7	-1.3	1.3	0.0
Can Tho	37.3	34.8	72.1	30.7	41.4	72.1	-6.6	6.6	0.0
Vinh Long	51.7	35.7	87.4	39.6	48.0	87.7	-12.0	12.3	0.3
Hau Giang	42.1	21.6	63.7	43.5	24.5	68.0	1.5	2.9	4.4
Tien Giang	41.9	14.7	56.6	41.5	18.0	59.5	-0.3	3.3	2.9
Ben Tre	51.3	29.0	80.3	52.0	29.4	81.4	0.6	0.5	1.1

Appendix B–Supplement to Chapter 4

Table B 1: Changes in simulated annual maximum water level (AMWL) for the dry year.

Station name	AMWL at *BL* [in *m*]	Changes in modelled AMWL compared to control runs (in *cm*)						
		S1-HP	*S2-FR*	*S3-DE*	*S4-CC*	*S5-SLR*	*S6-BAU*	*S7-SD*
Tan Chau [1]	2.52	–33	0	0	23	22	12	40
Vam Nao [2]	2.01	–17	0	0	9	28	20	36
Cao Lanh [3]	1.70	–1	0	0	4	34	37	39
My Thuan [4]	1.55	0	0	0	0	40	43	41
Chau Doc [5]	2.27	–31	0	0	21	22	10	40
Long Xuyen [6]	1.80	–7	0	0	3	32	29	35
Can Tho [7]	1.62	0	0	0	2	39	41	41
Dai Ngai [8]	1.77	0	0	0	0	42	43	43
Xuan To [9]	1.91	–52	0	0	40	34	14	59
Tri Ton [10]	1.24	–21	0	0	8	32	22	38
Tan Hiep [11]	0.88	–3	0	0	4	32	33	35
Vi Thanh [12]	0.69	0	0	0	0	42	43	42
Moc Hoa [13]	1.31	–14	0	0	4	25	20	28
Hung Thanh [14]	1.52	–18	0	0	7	21	16	28
Kien Binh [15]	1.00	–7	0	0	0	30	31	32
Tan An [16]	1.20	0	0	0	0	39	40	39

Table B 2: Changes in simulated annual maximum water level (AMWL) for the normal year.

Station name	AMWL at *BL* [in *m*]	Changes in modelled AMWL compared to control runs (in *cm*)						
		S1-HP	*S2-FR*	*S3-DE*	*S4-CC*	*S5-SLR*	*S6-BAU*	*S7-SD*
Tan Chau [1]	3.47	–66	–3	2	21	14	0	29
Vam Nao [2]	2.60	–45	–2	2	12	21	9	27
Cao Lanh [3]	1.96	–12	–1	2	8	32	33	40
My Thuan [4]	1.66	–3	0	0	7	38	40	45
Chau Doc [5]	3.21	–69	–5	1	24	14	2	31
Long Xuyen [6]	2.08	–16	–1	1	4	31	27	35
Can Tho [7]	1.77	–6	–1	0	6	37	38	42
Dai Ngai [8]	1.82	–1	0	0	3	43	44	45
Xuan To [9]	3.14	–74	–5	1	28	14	1	33
Tri Ton [10]	1.92	–53	–3	2	8	14	5	24
Tan Hiep [11]	1.18	–18	0	1	4	21	20	28
Vi Thanh [12]	0.74	–1	0	0	2	40	41	42
Moc Hoa [13]	1.75	–36	0	3	16	21	15	36
Hung Thanh [14]	2.00	–38	–1	4	21	18	16	34
Kien Binh [15]	1.17	–13	0	1	12	31	33	42
Tan An [16]	1.24	–2	0	0	5	38	39	43

Table B 3: Changes in simulated annual maximum water level (AMWL) for the normal year.

Station name	AMWL at *BL* [in *m*]	Changes in modelled AMWL compared to control runs (in *cm*)						
		S1-HP	*S2-FR*	*S3-DE*	*S4-CC*	*S5-SLR*	*S6-BAU*	*S7-SD*
Tan Chau[1]	3.67	–42	–3	2	33	13	17	40
Vam Nao [2]	2.73	–28	–2	2	26	20	25	40
Cao Lanh [3]	2.04	–9	–1	1	16	33	39	44
My Thuan [4]	1.72	–4	0	0	6	39	42	45
Chau Doc [5]	3.41	–43	–4	2	35	13	17	41
Long Xuyen [6]	2.15	–10	–1	1	15	29	36	41
Can Tho [7]	1.84	–6	–1	0	7	35	39	43
Dai Ngai [8]	1.85	–1	0	0	3	42	44	45
Xuan To [9]	3.38	–48	–6	1	35	12	15	39
Tri Ton [10]	2.03	–28	–2	4	30	11	26	47
Tan Hiep [11]	1.22	–8	0	1	16	23	30	37
Vi Thanh [12]	0.76	–1	0	1	4	41	43	44
Moc Hoa [13]	1.88	–26	–1	3	40	23	34	56
Hung Thanh [14]	2.16	–29	–1	2	32	16	25	45
Kien Binh [15]	1.25	–10	0	0	15	31	36	44
Tan An [16]	1.27	–3	0	0	5	38	40	44

Table B 4: Changes in simulated maximum inundation extent and duration according to different scenarios.

	Baseline inundation	**Changes from control runs (in percentage)**						
	% of delta area	*S1-HP*	*S2-FR*	*S3-DE*	*S4-CC*	*S5-SLR*	*S6-BAU*	*S7-SD*
Dry year								
No inundation	53.2	1.0	–0.4	0.1	–0.8	–20.0	–19.5	–22.6
<1 month	17.2	0.3	0.1	0.0	–0.3	–9.9	–9.8	–10.0
<2 month	9.3	–0.1	0.1	0.0	0.1	–1.5	–0.8	–1.2
<3 month	7.3	–0.6	0.2	–0.1	0.1	2.7	1.6	2.4
<4 month	4.2	–0.3	0.0	0.0	0.6	1.8	1.6	3.9
>4 month	8.8	–0.1	0.0	0.0	0.3	26.8	26.8	27.4
Normal year								
No inundation	43.3	7.7	–1.7	1.6	–2.5	–19.4	–16.5	–25.6
<1 month	16.3	0.4	0.1	0.0	–0.4	–10.2	–10.0	–10.0
<2 month	11.1	–1.7	0.3	–0.3	1.9	–3.8	–1.7	–1.2
<3 month	11.2	–3.1	1.0	–0.9	2.0	1.7	2.8	6.3
<4 month	6.6	–1.5	0.2	–0.4	–0.1	3.5	0.1	3.7
>4 month	11.5	–1.8	0.1	–0.1	–0.9	28.1	25.4	26.8
Wet year								
No inundation	40.5	5.1	–5.5	–0.4	–7.1	–21.1	–19.0	–29.6
<1 month	15.8	0.9	–0.3	–0.5	–1.4	–10.3	–10.5	–10.8
<2 month	10.6	0.1	0.0	–0.8	–1.2	–4.2	–4.4	–4.6
<3 month	11.3	–1.2	1.2	–0.8	0.1	0.3	–0.9	1.1
<4 month	10.5	–3.4	4.8	2.8	7.4	7.7	7.1	12.4
>4 month	11.2	–1.4	–0.2	–0.3	2.2	27.6	27.6	31.4

Table B 5: Exposed areas of rice crop, and estimated damages.

Simulated event	Exposed areas (*thousand hectares*)								Estimated damages (USD *million*)							
	BL	*S1-HP*	*S2-FR*	*S3-DE*	*S4-CC*	*S5-SLR*	*S6-BAU*	*S7-SD*	*BL*	*S1-HP*	*S2-FR*	*S3-DE*	*S4-CC*	*S5-SLR*	*S6-BAU*	*S7-SD*
1	5.9	4.7	5.9	5.9	7.8	54.7	47.4	63.5	5.2	4.4	5.2	5.3	6.8	39.5	34.0	46.2
2	10.9	3.1	10.9	10.9	9.8	68.7	53.3	71.1	9.3	2.9	9.3	9.3	9.0	50.2	38.8	52.2
3	24.1	3.7	24.9	24.9	7.6	111.5	43.5	62.0	20.4	3.4	21.0	21.0	6.5	82.8	31.2	45.0
4	26.6	9.2	26.1	28.0	8.3	93.6	46.1	66.1	22.0	8.5	21.7	23.1	7.0	71.1	33.0	47.9
5	1.7	4.7	1.7	1.7	5.9	32.8	43.4	56.0	1.8	4.3	1.8	1.8	5.2	23.4	31.0	40.6
6	22.5	1.8	22.2	24.0	7.2	88.5	41.3	58.1	18.2	1.8	18.0	19.4	6.2	66.7	29.6	42.2
7	2.5	3.6	2.5	2.5	99.5	39.9	104.5	235.6	2.4	3.4	2.4	2.4	100.6	28.5	79.8	215.2
8	33.8	2.1	32.7	35.6	2.8	107.6	38.4	42.5	28.2	2.0	27.4	29.6	2.6	84.7	27.4	30.5
9	6.0	8.1	6.0	6.2	9.8	58.8	48.1	68.9	5.4	6.8	5.4	5.6	8.9	42.6	34.7	50.5
10	3.9	3.2	3.9	4.1	62.1	49.1	95.2	160.3	3.7	2.9	3.7	3.8	56.7	35.3	71.4	132.1
11	3.2	2.6	3.2	3.5	4.2	43.4	39.0	50.0	2.9	2.5	2.9	3.1	3.8	31.0	27.9	36.0
12	2.9	2.1	2.9	3.1	8.2	43.7	53.4	69.3	2.7	2.0	2.7	2.9	7.8	31.2	38.8	50.7
13	19.0	2.2	19.0	19.2	49.2	59.7	85.9	154.4	17.4	2.1	17.4	17.6	41.7	43.4	63.4	124.2
14	8.7	3.2	9.1	8.7	100.3	68.9	91.9	217.5	8.3	3.0	8.6	8.3	103.9	50.4	70.7	201.0
15	4.7	4.4	4.7	4.9	7.7	47.5	48.8	63.2	4.3	4.0	4.4	4.6	7.5	34.5	35.1	46.4
16	60.6	2.3	56.6	63.9	4.4	167.1	42.0	47.4	54.0	2.2	49.8	57.0	3.9	136.1	29.9	34.3
17	18.8	12.2	18.9	19.0	103.5	88.1	109.8	249.3	16.1	10.1	16.1	16.2	102.7	65.6	81.6	223.2
18	32.8	6.3	32.1	35.9	24.8	114.6	56.8	96.3	27.3	5.6	26.7	29.8	21.0	89.0	41.4	72.4
19	4.6	10.2	4.6	4.9	13.1	49.6	59.9	82.9	4.2	8.5	4.2	4.4	11.7	35.6	43.7	60.9
20	24.9	2.6	24.5	26.1	11.2	89.4	49.0	70.6	20.8	2.5	20.5	21.8	10.3	67.9	35.9	52.2
21	11.2	5.2	11.2	11.4	22.1	69.7	49.4	85.2	9.2	4.6	9.2	9.4	18.0	50.7	35.6	64.5
22	10.1	3.4	10.2	10.3	2.2	68.0	36.3	37.2	8.7	3.3	8.7	8.9	2.1	49.6	25.9	26.7
23	61.3	3.5	55.5	65.2	3.2	152.3	40.0	47.8	58.0	3.3	51.9	62.9	3.0	128.9	28.6	34.3
24	4.5	22.9	4.5	4.5	28.8	50.3	58.5	106.6	4.1	18.6	4.1	4.1	24.2	36.1	42.8	81.1
25	4.3	2.4	4.3	4.5	5.0	51.3	40.4	51.2	4.0	2.3	4.0	4.1	4.6	36.8	28.8	37.2
26	49.8	2.7	45.5	53.5	6.4	130.6	45.1	54.0	44.3	2.6	39.8	47.4	6.5	106.5	32.5	40.0
27	6.8	8.0	6.9	7.0	223.0	57.9	164.5	425.2	6.4	7.0	6.5	6.7	241.0	42.4	142.6	423.2
28	80.0	4.0	73.2	84.3	48.7	196.4	90.8	143.5	76.4	3.6	69.3	82.2	42.9	167.9	67.2	117.5
29	42.1	23.6	41.6	31.4	8.6	104.6	47.8	63.7	37.4	20.1	36.9	26.1	8.3	80.3	34.6	47.0
30	3.1	6.7	3.1	3.2	3.5	44.6	39.2	46.6	3.0	5.8	3.0	3.1	3.2	32.0	27.9	33.4
Mean	*19.7*	*5.8*	*18.9*	*20.3*	*30.1*	*80.1*	*60.3*	*101.5*	*17.5*	*5.2*	*16.8*	*18.1*	*29.3*	*61.4*	*44.9*	*83.6*

The numbers marked in blue, green and red represent dry, normal, and wet years respectively (quantile 5%, 50% and 95% of the annual flood volume at Kratie)

Bibliography

M. B. Abbott and F. Ionescu. On the numerical computation of nearly horizontal flows. *Journal of Hydraulic Research*, 5(2):97–117, 1967.

E. J. Anthony, G. Brunier, M. Besset, M. Goichot, P. Dussouillez, and V. L. Nguyen. Linking rapid erosion of the mekong river delta to human activities. *Scientific reports*, 5:srep14745, 2015.

H. Apel, O. M. Trepat, N. N. Hung, D. T. Chinh, B. Merz, and N. V. Dung. Combined fluvial and pluvial urban flood hazard analysis: concept development and application to can tho city, mekong delta, vietnam. *Natural Hazards and Earth System Sciences*, 16(4):941–961, 2016.

K. Appeaning Addo, P.-N. Jayson-Quashigah, S. N. A. Codjoe, and F. Martey. Drone as a tool for coastal flood monitoring in the volta delta, ghana. *Geoenvironmental Disasters*, 5(1):17, 2018.

M. E. Arias, T. A. Cochrane, M. Kummu, H. Lauri, G. W. Holtgrieve, J. Koponen, and T. Piman. Impacts of hydropower and climate change on drivers of ecological productivity of southeast asia's most important wetland. *Ecological modelling*, 272: 252–263, 2014.

G. Aronica, P. Bates, and M. Horritt. Assessing the uncertainty in distributed model predictions using observed binary pattern information within glue. *Hydrological Processes*, 16(10):2001–2016, 2002.

L. W. Auerbach, S. L. Goodbred Jr, D. R. Mondal, C. A. Wilson, K. R. Ahmed, K. Roy, M. S. Steckler, C. Small, J. M. Gilligan, and B. A. Ackerly. Flood risk of natural and embanked landscapes on the ganges–brahmaputra tidal delta plain. *Nature Climate Change*, 5(2):153–157, 2015.

B. Barz, K. Schröter, M. Münch, B. Yang, A. Unger, D. Dransch, and J. Denzler. Enhancing flood impact analysis using interactive retrieval of social media images. *Archives of Data Science, Series A (Online First)*, 5(1):A06,–21, 2018.

A. Bouvet and N. Le Toan, Thuy Lam Dao. Monitoring of the rice cropping system in the mekong delta using envisat/asar dual polarization data. *IEEE Transactions on Geoscience and Remote Sensing*, 47:10, 2009.

A. Bouvet and T. Le Toan. Use of envisat/asar wide-swath data for timely rice fields mapping in the mekong river delta. *Remote Sensing of Environment*, 115(4):1090–1101, 2011.

S. A. Brandt. Modeling and visualizing uncertainties of flood boundary delineation: algorithm for slope and dem resolution dependencies of 1d hydraulic models. *Stochastic Environmental Research and Risk Assessment*, 30(6):1677–1690, 2016.

D. Chinh, N. Dung, A. Gain, and H. Kreibich. Flood loss models and risk analysis for private households in can tho city, vietnam. *Water*, 9(5):313, 2017.

D. T. Chinh, P. Bubeck, N. V. Dung, and H. Kreibich. The 2011 flood event in the mekong delta: preparedness, response, damage and recovery of private households and small businesses. *Disasters*, 40(4):753–778, 2016.

T. D. Dang, T. A. Cochrane, M. E. Arias, P. D. T. Van, and T. T. de Vries. Hydrological alterations from water infrastructure development in the mekong floodplains. *Hydrological Processes*, 30(21):3824–3838, 2016.

T. D. Dang, T. A. Cochrane, M. E. Arias, and V. P. D. Tri. Future hydrological alterations in the mekong delta under the impact of water resources development, land subsidence and sea level rise. *Journal of Hydrology: Regional Studies*, 15:119–133, 2018.

J. Delgado, H. Apel, and B. Merz. Flood trends and variability in the mekong river. *Hydrology and Earth System Sciences*, 14(3):407–418, 2010.

Deltares. Mekong delta plan, long-term vision and strategy for a safe, prosperous and sustainable delta, 2013.

Q. Dinh, S. Balica, I. Popescu, and A. Jonoski. Climate change impact on flood hazard, vulnerability and risk of the long xuyen quadrangle in the mekong delta. *International Journal of River Basin Management*, 10(1):103–120, 2012.

N. Dung, H. Apel, and T. Thang. Floods in the mekong delta: a future perspective. In *EGU General Assembly Conference Abstracts*, volume 11, page 13470, 2009.

N. V. Dung, B. Merz, A. Bárdossy, T. D. Thang, and H. Apel. Multi-objective automatic calibration of hydrodynamic models utilizing inundation maps and gauge data. *Hydrology and Earth System Sciences*, 15(4):1339–1354, 2011.

N. V. Dung, B. Merz, A. Bárdossy, and H. Apel. Handling uncertainty in bivariate quantile estimation–an application to flood hazard analysis in the mekong delta. *Journal of Hydrology*, 527:704–717, 2015.

D. Dutta, S. Herath, and K. Musiake. A mathematical model for flood loss estimation. *Journal of hydrology*, 277(1):24–49, 2003.

D. A. Edmonds, R. L. Caldwell, E. S. Brondizio, and S. M. O. Siani. Coastal flooding will disproportionately impact people on river deltas. *Nature Communications*, 11(1):4741, 2020.

L. E. Erban, S. M. Gorelick, and H. A. Zebker. Groundwater extraction, land subsidence, and sea-level rise in the mekong delta, vietnam. *Environmental Research Letters*, 9(8): 084010, 2014.

J. P. Ericson, C. J. Vörösmarty, S. L. Dingman, L. G. Ward, and M. Meybeck. Effective sea-level rise and deltas: Causes of change and human dimension implications. *Global and Planetary Change*, 50(1):63–82, 2006.

S. Förster, B. Kuhlmann, K. E. Lindenschmidt, and A. Bronstert. Assessing flood risk for a rural detention area. *Natural Hazards and Earth System Sciences*, 8(2):311–322, 2008.

K. Fu and D. He. Analysis and prediction of sediment trapping efficiencies of the reservoirs in the mainstream of the lancang river. *Chinese Science Bulletin*, 52(2):134–140, 2007.

K. Fu, D. He, and X. Lu. Sedimentation in the manwan reservoir in the upper mekong and its downstream impacts. *Quaternary International*, 186(1):91–99, 2008.

Y. Fujihara, K. Hoshikawa, H. Fujii, A. Kotera, T. Nagano, and S. Yokoyama. Analysis and attribution of trends in water levels in the vietnamese mekong delta. *Hydrological Processes*, 30(6):835–845, 2016.

M. F. Goodchild and J. A. Glennon. Crowdsourcing geographic information for disaster response: a research frontier. *International Journal of Digital Earth*, 3(3):231–241, 2010.

GOV. The government of viet nam, decision no. 99/ttg on water resources, infrastructure and rural development plan for the vietnamese mekong delta during the period 1996 - 2000 (in vietnamese), 1996.

GOV. The government of viet nam, decision no. 315/ttg on pilot programme for agriculture insurance in vietnam (in vietnamese), 2011.

GOV. The government of viet nam, resolution no. 120/nq-cp. nghi quyet ve phat trien ben vung dong bang song cuu long thich ung voi bien doi khi hau (in vietnamese), 2017.

GSO. Statistical handbook of vietnam 2015. Technical report, General statistics office of Viet Nam, 2015.

H. Gupta, S.-J. Kao, and M. Dai. The role of mega dams in reducing sediment fluxes: A case study of large asian rivers. *Journal of Hydrology*, 464:447–458, 2012.

C. R. Hackney, S. E. Darby, D. R. Parsons, J. Leyland, J. L. Best, R. Aalto, A. P. Nicholas, and R. C. Houseago. River bank instability from unsustainable sand mining in the lower mekong river. *Nature Sustainability*, 2020.

D. Hak, K. Nadaoka, L. Patrick Bernado, V. Le Phu, N. Hong Quan, T. Quang Toan, N. Hieu Trung, D. Van Ni, and V. Pham Dang Tri. Spatio-temporal variations of sea level around the mekong delta: their causes and consequences on the coastal environment. *Hydrological Research Letters*, 10(2):60–66, 2016.

J. Hall, B. Arheimer, M. Borga, R. Brázdil, P. Claps, A. Kiss, T. Kjeldsen, J. Kriauciuniene, Z. Kundzewicz, and M. Lang. Understanding flood regime changes in europe: A state of the art assessment. *Hydrology and Earth System Sciences*, 18(7):2735–2772, 2014.

T. Hashimoto. *Environmental Issues and Recent Infrastructure Development in the Mekong Delta: review, analysis and recommendations with particular reference to large-scale water control projects and the development of coastal areas.* Australian Mekong Resource Centre, 2001.

J. S. Hecht, G. Lacombe, M. E. Arias, T. D. Dang, and T. Piman. Hydropower dams of the mekong river basin: A review of their hydrological impacts. *Journal of Hydrology*, 568:285–300, 2019.

Y. Hirabayashi, R. Mahendran, S. Koirala, L. Konoshima, D. Yamazaki, S. Watanabe, H. Kim, and S. Kanae. Global flood risk under climate change. *Nature Climate Change*, 3:816, 2013.

L. P. Hoang, H. Lauri, M. Kummu, J. Koponen, M. T. Van Vliet, I. Supit, R. Leemans, P. Kabat, and F. Ludwig. Mekong river flow and hydrological extremes under climate change. *Hydrology and Earth System Sciences*, 20(7):3027–3041, 2016.

L. P. Hoang, M. T. H. van Vliet, M. Kummu, H. Lauri, J. Koponen, I. Supit, R. Leemans, P. Kabat, and F. Ludwig. The mekong's future flows under multiple drivers how climate change, hydropower developments and irrigation expansions drive hydrological changes. *Science of The Total Environment*, 2018.

C. T. Hoanh, K. Jirayoot, G. Lacombe, and V. Srinetr. Impacts of climate change and development on mekong flow regimes. first assessment-2009. Technical report, 2010.

T. N. Hoi. Research on scientific and technological solutions on building dike system for sustainable development in the mekong delta, southern institute of water resour. res., ho chi minh city (in vietnamese). Technical report, 2005.

C. Howie. High dykes in the mekong delta in vietnam bring social gains and environmental pains. *Aquaculture News*, 32(1):15–17, 2005.

C. Howie. Dike building and agricultural transformation in the mekong delta, vietnam: dilemmas in water management, 2012.

A. Huete, K. Didan, T. Miura, E. P. Rodriguez, X. Gao, and L. G. Ferreira. Overview of the radiometric and biophysical performance of the modis vegetation indices. *Remote Sensing of Environment*, 83(1):195–213, 2002.

N. N. Hung, J. M. Delgado, V. K. Tri, L. M. Hung, B. Merz, A. Bárdossy, and H. Apel. Floodplain hydrology of the mekong delta, vietnam. *Hydrological Processes*, 26(5):674–686, 2012.

H. Huong and A. Pathirana. Urbanization and climate change impacts on future urban flooding in can tho city, vietnam. *Hydrology and Earth System Sciences*, 17(1):379–394, 2013.

H. Huu Nguyen, P. Dargusch, P. Moss, and D. B. Tran. A review of the drivers of 200 years of wetland degradation in the mekong delta of vietnam. *Regional Environmental Change*, 16(8):2303–2315, 2016.

IPCC. Climate change 2013: The physical science basis. (technical summary). Technical report, Intergov. Panel Clim. Chang., 2014a.

IPCC. Climate change 2014: Synthesis report. contribution of working groups i, ii and iii to the fifth assessment report of the intergovernmental panel on climate change, 2014b.

C. Jordan, J. Visscher, N. Viet Dung, H. Apel, and T. Schlurmann. Impacts of human activity and global changes on future morphodynamics within the tien river, vietnamese mekong delta. *Water*, 12(8):2204, 2020.

P. Kellermann, K. Schröter, A. H. Thieken, S. N. Haubrock, and H. Kreibich. The object-specific flood damage database howas 21. *Nat. Hazards Earth Syst. Sci.*, 20(9):2503–2519, 2020.

M. Kendall. *Rank Correlation Methods*. Charles Griffin, London, UK, 1975.

N. D. Khang, A. Kotera, T. Sakamoto, and M. Yokozawa. Sensitivity of salinity intrusion to sea level rise and river flow change in vietnamese mekong delta - impacts on potential irrigation water. *Proceedings of annual meeting of the Society of Agricultural Meteorology of Japan*, isam08:158–158, 2008.

M. Käkönen. Mekong delta at the crossroads: more control or adaptation? *AMBIO: A Journal of the Human Environment*, 37(3):205–212, 2008.

S. Klaus, H. Kreibich, B. Merz, B. Kuhlmann, and K. Schröter. Large-scale, seasonal flood risk analysis for agricultural crops in germany. *Environmental Earth Sciences*, 75(18): 1289, 2016.

G. M. Kondolf, Z. K. Rubin, and J. T. Minear. Dams on the mekong: Cumulative sediment starvation. *Water Resources Research*, 50(6):5158–5169, 2014.

G. M. Kondolf, R. J. Schmitt, P. Carling, S. Darby, M. Arias, S. Bizzi, A. Castelletti, T. A. Cochrane, S. Gibson, and M. Kummu. Changing sediment budget of the mekong: Cumulative threats and management strategies for a large river basin. *Science of The Total Environment*, 625:114–134, 2018.

A. Kotera, K. D. Nguyen, T. Sakamoto, T. Iizumi, and M. Yokozawa. A modeling approach for assessing rice cropping cycle affected by flooding, salinity intrusion, and monsoon rains in the mekong delta, vietnam. *Paddy and Water Environment*, 12(3):343–354, 2014.

A. Kotera, Y. Uneno, and T. Nagano. Quasi-real-time satellite monitoring for assessing agronomic flood damage, 28-30 January, 2018 2015.

A. Kotera, T. Nagano, P. Hanittinan, and S. Koontanakulvong. Assessing the degree of flood damage to rice crops in the chao phraya delta, thailand, using modis satellite imaging. *Paddy and water environment*, 14(1):271–280, 2016.

H. Kreibich, G. Di Baldassarre, S. Vorogushyn, J. C. J. H. Aerts, H. Apel, G. T. Aronica, K. Arnbjerg-Nielsen, L. M. Bouwer, P. Bubeck, T. Caloiero, D. T. Chinh, M. Cortès, A. K. Gain, V. Giampá, C. Kuhlicke, Z. W. Kundzewicz, M. C. Llasat, J. Mård, P. Matczak, M. Mazzoleni, D. Molinari, N. V. Dung, O. Petrucci, K. Schröter, K. Slager, A. H. Thieken, P. J. Ward, and B. Merz. Adaptation to flood risk: Results of international paired flood event studies. *Earth's Future*, 5(10):953–965, 2017.

C. Kuenzer, H. Guo, J. Huth, P. Leinenkugel, X. Li, and S. Dech. Flood mapping and flood dynamics of the mekong delta: Envisat-asar-wsm based time series analyses. *Remote Sensing*, 5(2):687–715, 2013.

M. Kummu and O. Varis. Sediment-related impacts due to upstream reservoir trapping, the lower mekong river. *Geomorphology*, 85(3):275–293, 2007.

M. Kummu, X. Lu, J. Wang, and O. Varis. Basin-wide sediment trapping efficiency of emerging reservoirs along the mekong. *Geomorphology*, 119(3):181–197, 2010.

M. Kummu, H. de Moel, M. Porkka, S. Siebert, O. Varis, and P. J. Ward. Lost food, wasted resources: Global food supply chain losses and their impacts on freshwater, cropland, and fertiliser use. *Science of The Total Environment*, 438:477–489, 2012.

H. Lauri, H. de Moel, P. J. Ward, T. A. Räsänen, M. Keskinen, and M. Kummu. Future changes in mekong river hydrology: impact of climate change and reservoir operation on discharge. *Hydrology and Earth System Sciences*, 16(12):4603–4619, 2012.

T. N. Le, A. K. Bregt, G. E. van Halsema, P. J. G. J. Hellegers, and L.-D. Nguyen. Interplay between land-use dynamics and changes in hydrological regime in the vietnamese mekong delta. *Land Use Policy*, 73:269–280, 2018.

T. V. H. Le, H. N. Nguyen, E. Wolanski, T. C. Tran, and S. Haruyama. The combined impact on the flooding in vietnam's mekong river delta of local man-made structures, sea level rise, and dams upstream in the river catchment. *Estuarine, Coastal and Shelf Science*, 71(1–2):110–116, 2007.

P. Leinenkugel, C. Kuenzer, N. Oppelt, and S. Dech. Characterisation of land surface phenology and land cover based on moderate resolution satellite data in cloud prone areas — a novel product for the mekong basin. *Remote Sensing of Environment*, 136: 180–198, 2013.

D. P. Loucks. Developed river deltas: are they sustainable? *Environmental Research Letters*, 14(11):113004, 2019.

N. Manh, B. Merz, and H. Apel. Sedimentation monitoring including uncertainty analysis in complex floodplains: a case study in the mekong delta. *Hydrology and Earth System Sciences*, 17(8):3039–3057, 2013.

N. V. Manh, N. V. Dung, N. N. Hung, B. Merz, and H. Apel. Large-scale suspended sediment transport and sediment deposition in the mekong delta. *Hydrology and Earth System Sciences*, 18(8):3033–3053, 2014.

N. V. Manh, N. V. Dung, N. N. Hung, M. Kummu, B. Merz, and H. Apel. Future sediment dynamics in the mekong delta floodplains: Impacts of hydropower development, climate change and sea level rise. *Global and Planetary Change*, 127:22–33, 2015.

H. Mann. Non-parametric tests against trend. *Econometrica 13*, pages 245–259, 1945.

B. Merz, F. Elmer, and A. H. Thieken. Significance of high probability/low damage versus low probability/high damage flood events. *Natural Hazards and Earth System Sciences*, 9(3):1033–1046, 2009.

B. Merz, H. Kreibich, R. Schwarze, and A. Thieken. Review article" assessment of economic flood damage". *Natural Hazards and Earth System Sciences*, 10(8):1697–1724, 2010.

P. S. J. Minderhoud, G. Erkens, V. H. Pham, V. T. Bui, L. Erban, H. Kooi, and E. Stouthamer. Impacts of 25 years of groundwater extraction on subsidence in the mekong delta, vietnam. *Environ Res Lett*, 12(6):064006, 2017.

P. S. J. Minderhoud, L. Coumou, G. Erkens, H. Middelkoop, and E. Stouthamer. Mekong delta much lower than previously assumed in sea-level rise impact assessments. *Nature Communications*, 10(1):3847, 2019.

MRC. Flood damages, benefits and flood risk in focal areas, mekong river commission. Technical report, December 2009 2009.

MRC. Flood situation report 2011, mrc technical paper no. 36, mekong river commission. Technical report, November 2011 2011.

MRC. The impact and management of floods and droughts in the lower mekong basin and the implications of possible climate change, mekong river commission. Technical report, March 2012 2012.

MRC. Annual mekong flood report 2011, mekong river commission, 72 pages. Technical report, 2015a.

MRC. Mekong dam database, mekong river commision, 2015b.

MunichRE. Flood risks: underestimated natural hazards, 2020.

G. C. Nelson, M. W. Rosegrant, A. Palazzo, I. Gray, C. Ingersoll, R. Robertson, S. Tokgoz, T. Zhu, T. B. Sulser, and C. Ringler. *Food security, farming, and climate change to 2050: scenarios, results, policy options*, volume 172. Intl Food Policy Res Inst, 2010.

D. B. Nguyen, K. Clauss, S. M. Cao, V. Naeimi, C. Kuenzer, and W. Wagner. Mapping rice seasonality in the mekong delta with multi-year envisat asar wsm data. *Remote Sensing*, 7(12):15868–15893, 2015.

N. H. Nhan and N. B. Cao. Chapter 19 - damming the mekong: Impacts in vietnam and solutions. In E. Wolanski, J. W. Day, M. Elliott, and R. Ramachandran, editors, *Coasts and Estuaries*, pages 321–340. Elsevier, 2019.

S. W. D. Pearse-Smith. The impact of continued mekong basin hydropower development on local livelihoods. 2012.

E. Penning-Rowsell, T. Wilson, and F. H. R. Centre. *The benefits of flood and coastal defence: techniques and data for 2003*. Middlesex University, 2003.

A. N. Pettitt. A non-parametric approach to the change-point problem. *Journal of the Royal Statistical Society. Series C (Applied Statistics)*, 28(2):126–135, 1979.

Y. Pokhrel, M. Burbano, J. Roush, H. Kang, V. Sridhar, and W. D. Hyndman. A review of the integrated effects of changing climate, land use, and dams on mekong river hydrology. *Water*, 10(3), 2018a.

Y. Pokhrel, S. Shin, Z. Lin, D. Yamazaki, and J. Qi. Potential disruption of flood dynamics in the lower mekong river basin due to upstream flow regulation. *Scientific Reports*, 8 (1):17767, 2018b.

N. Reis. Flood management and development planning. the allocation of risk in the mekong delta, vietnam, 2007.

T. A. Räsänen, J. Koponen, H. Lauri, and M. Kummu. Downstream hydrological impacts of hydropower development in the upper mekong basin. *Water Resources Management*, 26(12):3495–3513, 2012.

T. A. Räsänen, P. Someth, H. Lauri, J. Koponen, J. Sarkkula, and M. Kummu. Observed river discharge changes due to hydropower operations in the upper mekong basin. *Journal of Hydrology*, 545:28–41, 2017.

T. Sakamoto, N. Van Nguyen, A. Kotera, H. Ohno, N. Ishitsuka, and M. Yokozawa. Detecting temporal changes in the extent of annual flooding within the cambodia and the vietnamese mekong delta from modis time-series imagery. *Remote sensing of environment*, 109(3):295–313, 2007.

C. C. Sampson, A. M. Smith, P. D. Bates, J. C. Neal, L. Alfieri, and J. E. Freer. A high-resolution global flood hazard model. *Water Resources Research*, 51(9):7358–7381, 2015.

G. Schumann, P. Matgen, M. E. J. Cutler, A. Black, L. Hoffmann, and L. Pfister. Comparison of remotely sensed water stages from lidar, topographic contours and srtm. *ISPRS Journal of Photogrammetry and Remote Sensing*, 63(3):283–296, 2008.

P. K. Sen. Estimates of the regression coefficient based on kendall's tau. *Journal of the American Statistical Association*, 63(324):1379–1389, 1968.

J. F. Shroder, P. Paron, and G. D. Baldassare. *Hydro-Meteorological Hazards, Risks, and Disasters*. Elvisier, 2014.

L. Silver, A. Smith, C. Johnson, J. Jiang, M. Anderson, and L. Rainie. Mobile connectivity in emerging economies. Technical report, 2019.

SIWRP. Southern institute of water resources planning: Bao cao tong hop quy hoach tong the thuy loi dong bang song cuu long trong dieu kien bien doi khi hau-nuoc bien dang (in vietnamese). Technical report, 2011.

SIWRP. Southern institute of water resources planning: Quy hoach lu dong bang song cuu long den nam 2020, dinh huong 2030 (in vietnamese). Technical report, 2015.

SIWRR. Southern institue of water resources research: Results of dyke survey for 4 provinces located in the flood prone areas of vietnamese mekong delta (in vietnamese). Technical report, 2010.

A. Smajgl, T. Q. Toan, D. K. Nhan, J. Ward, N. H. Trung, L. Q. Tri, V. P. D. Tri, and P. T. Vu. Responding to rising sea levels in the mekong delta. *Nature Climate Change*, 5(2):167–174, 2015.

H. Takagi, T. V. Ty, and N. D. Thao. 12 - investigation on floods in can tho city: Influence of ocean tides and sea level rise for the mekong delta's largest city. In N. D. Thao, H. Takagi, and M. Esteban, editors, *Coastal Disasters and Climate Change in Vietnam*, pages 257–274. Elsevier, Oxford, 2014.

Z. D. Tessler, C. J. Vörösmarty, M. Grossberg, I. Gladkova, H. Aizenman, J. P. M. Syvitski, and E. Foufoula-Georgiou. Profiling risk and sustainability in coastal deltas of the world. *Science*, 349(6248):638–643, 2015.

T. Thi Kim, N. T. M. Huong, N. D. Q. Huy, P. A. Tai, S. Hong, T. M. Quan, N. T. Bay, W.-K. Jeong, and N. K. Phung. Assessment of the impact of sand mining on bottom morphology in the mekong river in an giang province, vietnam, using a hydro-morphological model with gpu computing. *Water*, 12(10):2912, 2020.

D. N. Tinh. 2011 flood lesson leraned in vietnam, 2012.

T. Q. Toan. Climate change and sea level rise in the mekong delta: Flood, tidal inundation, salinity intrusion, and irrigation adaptation methods. In H. T. M. Esteban, Nguyen Danh Thao, editor, *Coastal Disasters and Climate Change in Vietnam*, pages 199–218. Elsevier, Oxford, 2014.

D. D. Tran, G. van Halsema, P. J. G. J. Hellegers, F. Ludwig, and A. Wyatt. Questioning triple rice intensification on the vietnamese mekong delta floodplains: An environmental and economic analysis of current land-use trends and alternatives. *Journal of Environmental Management*, 217:429–441, 2018a.

D. D. Tran, G. van Halsema, P. J. G. J. Hellegers, L. Phi Hoang, T. Quang Tran, M. Kummu, and F. Ludwig. Assessing impacts of dike construction on the flood dynamics of the mekong delta. *Hydrology and Earth System Sciences*, 22(3):1875–1896, 2018b.

V. Tri. Hydrology and hydraulic infrastructure systems in the mekong delta, vietnam. In F. G. Renaud and C. Kuenzer, editors, *The Mekong Delta System*, Springer Environmental Science and Engineering, pages 49–81. Springer Netherlands, 2012.

N. V. K. Triet, N. V. Dung, H. Fujii, M. Kummu, B. Merz, and H. Apel. Has dyke development in the vietnamese mekong delta shifted flood hazard downstream? *Hydrology and Earth System Sciences*, 21(8):3991–4010, 2017.

N. V. K. Triet, N. V. Dung, B. Merz, and H. Apel. Towards risk-based flood management in highly productive paddy rice cultivation - concept development and application to the mekong delta. *Natural Hazards and Earth System Sciences*, 18(11):2859–2876, 2018.

P. D. T. Van, I. Popescu, A. van Griensven, D. P. Solomatine, N. H. Trung, and A. Green. A study of the climate change impacts on fluvial flood propagation in the vietnamese mekong delta. *Natural Hazards and Earth System Sciences*, 16(12):4637–4649, 2012.

T. C. Van. Identification of sea level rise impacts on the mekong delta and orientation of adaptation activities, 2009.

D. Van Binh, S. Kantoush, and T. Sumi. Changes to long-term discharge and sediment loads in the vietnamese mekong delta caused by upstream dams. *Geomorphology*, page 107011, 2019.

J. Wang, L. Feng, X. Tang, Y. Bentley, and M. Höök. The implications of fossil fuel supply constraints on climate change projections: A supply-side analysis. *Futures*, 86:58–72, 2017.

P. J. Ward, H. d. Moel, and J. Aerts. How are flood risk estimates affected by the choice of return-periods? 2011.

R. Wassmann, N. Hien, C. Hoanh, and T. Tuong. Sea level rise affecting the vietnamese mekong delta: Water elevation in the flood season and implications for rice production. *Climatic Change*, 66(1-2):89–107, 2004.

Z. Xue, J. P. Liu, and Q. Ge. Changes in hydrology and sediment delivery of the mekong river in the last 50 years: connection to damming, monsoon, and enso. *Earth Surface Processes and Landforms*, 36(3):296–308, 2011.

G. Ziv, E. Baran, S. Nam, I. Rodríguez-Iturbe, and S. A. Levin. Trading-off fish biodiversity, food security, and hydropower in the mekong river basin. *Proceedings of the National Academy of Sciences*, page 201201423, 2012.